

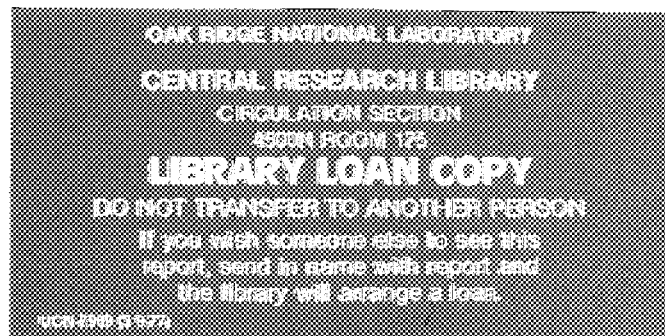


3 4456 0366301 5

ORNL/TM-11917

ornl**OAK RIDGE
NATIONAL
LABORATORY****MARTIN MARIETTA****Analysis of the Spring-1990 Two-
Meter Box Test Bed Experiments
Performed at the Army Pulse
Radiation Facility (APRF)**

J. O. Johnson
J. D. Drischler
J. M. Barnes



MANAGED BY
MARTIN MARIETTA ENERGY SYSTEMS, INC.
FOR THE UNITED STATES
DEPARTMENT OF ENERGY

This report has been reproduced directly from the best available copy.

Available to DCE and DOE contractors from the Office of Scientific and Technical Information, P.O. Box 62, Oak Ridge, TN 37831; prices available from (615) 576-8401, FTS 626-8401.

Available to the public from the National Technical Information Service, U.S. Department of Commerce, 5285 Port Royal Rd., Springfield, VA 22161.

NTIS price codes--Printed Copy: A03 Microfiche A01

This report was prepared as an account of work sponsored by an agency of the United States Government. Neither the United States Government nor any agency thereof, nor any of their employees, makes any warranty, express or implied, or assumes any legal liability or responsibility for the accuracy, completeness, or usefulness of any information, apparatus, product, or process disclosed, or represents that its use would not infringe privately owned rights. Reference herein to any specific commercial product, process, or service by trade name, trademark, manufacturer, or otherwise, does not necessarily constitute or imply its endorsement, recommendation, or favoring by the United States Government or any agency thereof. The views and opinions of authors expressed herein do not necessarily state or reflect those of the United States Government or any agency thereof.

Engineering Physics and Mathematics Division

**ANALYSIS OF THE SPRING-1990 TWO-METER BOX TEST BED EXPERIMENTS
PERFORMED AT THE ARMY PULSE RADIATION FACILITY (APRF)**

J. O. Johnson
J. D. Drischler
J. M. Barnes*

*Computing and Telecommunications Division

DATE PUBLISHED - AUGUST 1992

NOTICE This document contains information of a preliminary nature.
It is subject to revision or correction and therefore does not represent a
final report.

This work is sponsored by the Defense Nuclear Agency
under DNA MIPR #92-524, Work Unit 00001
and DOE Interagency Agreement No 1205-E097-A1

Prepared by
Oak Ridge National Laboratory
Oak Ridge, Tennessee 37831
managed by
MARTIN MARIETTA ENERGY SYSTEMS, INC.
for the
U.S. DEPARTMENT OF ENERGY
under Contract No. DE-AC05 84OR21400



CONTENTS

	<u>Page</u>
LIST OF FIGURES	v
LIST OF TABLES	vii
ACKNOWLEDGEMENTS	xi
EXECUTIVE SUMMARY	xiii
ABSTRACT	xv
1.0 INTRODUCTION	1
2.0 THE TWO-METER BOX TEST BED EXPERIMENTS	2
2.1 The APRF Reactor Source	2
2.2 The Two-Meter Box Test Bed	2
2.3 The RT-200 Anthropomorphic Phantom	2
2.4 Details of the Measurements	3
2.5 Experimental Equipment	3
3.0 MASH CALCULATIONAL TECHNIQUES	5
3.1 Definition of Protection and Reduction Factors	5
3.2 Air-Over-Ground Environment	5
3.3 The Two-Meter Box and Phantom Geometry Models	10
3.4 The Two-Meter Box Calculations	11
4.0 DISCUSSION OF RESULTS	18
4.1 Neutron Dose and Reduction Factors	18
4.2 Gamma-Ray Dose and Reduction Factors	20
5.0 MONTE CARLO STATISTICAL UNCERTAINTY	37
6.0 CONCLUSIONS	38
7.0 RECOMMENDATIONS	41
8.0 REFERENCES	42
APPENDIX A	43
APPENDIX B	48
APPENDIX C	65

LIST OF FIGURES

<u>Page</u>		<u>Page</u>
1.	Isometric View of the Two-Meter Box Test Bed	12
2.	Isometric View of the Combinatorial Geometry Phantom Model Used in the MASH Analysis	13
3.	Isometric View of the MASH Geometry Model of the Combinatorial Geometry Phantom Standing Inside the Two-Meter Box Test Bed	14
C-1.	Sample GIP Input for the MASH Analysis of the APRF Spring 1990 Two-Meter Box Test Bed Experiments	66
C-2.	Sample GRTUNCL Input for the MASH Analysis of the APRF Spring 1990 Two-Meter Box Test Bed Experiments	68
C-3.	Sample DORT Input for the MASH Analysis of the APRF Spring 1990 Two-Meter Box Test Bed Experiments	77
C-4.	Sample VISTA Input for the MASH Analysis of the APRF Spring 1990 Two-Meter Box Test Bed Experiments	80
C-5.	Sample XCHEKER Input for the MASH Analysis of the APRF Spring 1990 Two-Meter Box Test Bed Experiments	81
C-6.	Sample MORSE Input for the MASH Analysis of the Empty Two-Meter Box Used in the APRF Spring 1990 Two-Meter Box Test Bed Experiments	83
C-7.	Sample Geometry Input for the MASH Analysis of the Empty Two-Meter Box Used in the APRF Spring 1990 Two-Meter Box Test Bed Experiments	84
C-8.	Sample MORSE Input for the MASH Analysis of the Combinatorial Geometry Phantom (with BD-100R Detectors) Used in the APRF Spring 1990 Two-Meter Box Test Bed Experiments	87
C-9.	Sample Geometry Input for the MASH Analysis of the Combinatorial Geometry Phantom (with BD-100R Detectors) Used in the APRF Spring 1990 Two-Meter Box Test Bed Experiments	88

C-10. Sample MORSE Input for the MASH Analysis of the Combinatorial Geometry Phantom (with BD-100R Detectors) Standing in the Two-Meter Box Used in the APRF Spring 1990 Two-Meter Box Test Bed Experiments	94
C-11. Sample Geometry Input for the MASH Analysis of the Combinatorial Geometry Phantom (with BD-100R Detectors) Standing in the Two-Meter Box Used in the APRF Spring 1990 Two-Meter Box Test Bed Experiments	96
C-12. Sample DRC Input for the MASH Analysis of the APRF Spring 1990 Two-Meter Box Test Bed Experiments	105

LIST OF TABLES

<u>Table</u>	<u>Page</u>
1. Definitions of Radiation Protection Factors and Reduction Factors	6
2. APRF Reactor Neutron Leakage Spectrum and DABL69 Free-In-Air Tissue Kerma Response Function (Gy-cm ² /n) Used in the MASH Analysis	8
3. APRF Reactor Gamma-Ray Leakage Spectrum and DABL69 Free-In-Air Tissue Kerma Response Function (Gy-cm ² /γ) Used in the MASH Analysis	9
4. Meteorological Data and Air Number Densities Used in the MASH Analysis of the APRF Spring 1990 Two-Meter Box Test Bed Experiments	10
5. Compositions of the Materials Used in the MASH Analysis of the APRF Spring 1990 Two-Meter Box Test Bed Experiments	15
6. MASH Coordinate Positions for the Analysis of the APRF Spring 1990 Two-Meter Box Test Bed Experiments BD-100R Bubble Dosimeter Locations on the RT-200 Humanoid Phantom and Inside the Two-Meter Box	16
7. MASH Geometry Regions and Cross-Section Materials Used in the Analysis of the APRF Spring 1990 Two-Meter Box Test Bed Experiments	17
8. Comparisons of Calculated and BTI/DREO Measured Neutron Dose Averaged Over External, Internal, and All Detector Locations On or Inside the RT-200 Humanoid Phantom at the 400 Meter Test Site at the APRF	23
9. Comparisons of Calculated and BTI/DREO Measured Neutron Reduction Factors Averaged Over External, Internal, and All Detector Locations On or Inside the RT-200 Humanoid Phantom at the 400 Meter Test Site at the APRF	24
10. Comparisons of Calculated and HDL Measured Gamma-Ray Dose Averaged Over External, Internal, and All Detector Locations On or Inside the RT-200 Humanoid Phantom at the 400 Meter Test Site at the APRF	25
11. Comparisons of Calculated and HDL Measured Gamma-Ray Reduction Factors Averaged Over External, Internal, and All Detector Locations On or Inside the RT-200 Humanoid Phantom at the 400 Meter Test Site at the APRF	26

12.	Comparisons of Calculated and APRF Measured Gamma-Ray Dose Averaged Over External, Internal, and All Detector Locations On or Inside the RT-200 Humanoid Phantom at the 400 Meter Test Site at the APRF	27
13.	Comparisons of Calculated and APRF Measured Gamma-Ray Reduction Factors Averaged Over External, Internal, and All Detector Locations On or Inside the RT-200 Humanoid Phantom at the 400 Meter Test Site at the APRF	28
14.	Comparisons of Calculated and BTI Measured Gamma-Ray Dose Averaged Over External, Internal, and All Detector Locations On or Inside the RT-200 Humanoid Phantom at the 400 Meter Test Site at the APRF	29
15.	Comparisons of Calculated and BTI Measured Gamma-Ray Reduction Factors Averaged Over External, Internal, and All Detector Locations On or Inside the RT-200 Humanoid Phantom at the 400 Meter Test Site at the APRF	30
16.	Comparisons of Calculated and DREO Measured Gamma-Ray Dose Averaged Over External, Internal, and All Detector Locations On or Inside the RT-200 Humanoid Phantom at the 400 Meter Test Site at the APRF	31
17.	Comparisons of Calculated and DREO Measured Gamma-Ray Reduction Factors Averaged Over External, Internal, and All Detector Locations On or Inside the RT-200 Humanoid Phantom at the 400 Meter Test Site at the APRF	32
18.	Comparisons of Calculated and ETCA Measured Gamma-Ray Dose Averaged Over External, Internal, and All Detector Locations On or Inside the RT-200 Humanoid Phantom at the 400 Meter Test Site at the APRF	33
19.	Comparisons of Calculated and ETCA Measured Gamma-Ray Reduction Factors Averaged Over External, Internal, and All Detector Locations On or Inside the RT-200 Humanoid Phantom at the 400 Meter Test Site at the APRF	34
20.	Comparisons of Calculated and Average Experimentally Measured Gamma-Ray Dose(Tissue) Averaged Over External, Internal, and All Detector Locations On or Inside the RT-200 Humanoid Phantom at the 400 Meter Test Site at the APRF	35
21.	Comparisons of Calculated and Average Experimentally Measured Gamma-Ray Reduction Factors(Tissue) Averaged Over External, Internal, and All Detector Locations On or Inside the RT-200 Humanoid Phantom at the 400 Meter Test Site at the APRF	36

22. Overall Comparisons of Calculated and Average Experimentally Measured Neutron and Gamma-Ray Dose and Reduction Factors Averaged Over External, Internal, and All Detector Locations On or Inside the RT-200 Humanoid Phantom, and Phantom Orientation Free-Field or Inside the Two-Meter Box, at the 400 Meter Test Site at the APRF	40
A-1. MASH VS. BTI/DREO: Phantom Free-Field Neutron Dose	44
A-2. MASH VS. BTI/DREO: Phantom In 2m Box Neutron Dose	45
A-3. MASH VS. BTI/DREO: Phantom Free-Field Neutron Reduction Factors	46
A-4. MASH VS. BTI/DREO: Phantom In 2m Box Neutron Reduction Factors	47
B-1. MASH VS. HDL: Phantom Free-Field Gamma-Ray Dose	49
B-2. MASH VS. HDL: Phantom In 2m Box Gamma-Ray Dose	50
B-3. MASH VS. HDL: Phantom Free-Field Gamma-Ray Reduction Factors	51
B-4. MASH VS. HDL: Phantom In 2m Box Gamma-Ray Reduction Factors	52
B-5. MASH VS. APRF: Phantom Free-Field Gamma-Ray Dose	53
B-6. MASH VS. APRF: Phantom In 2m Box Gamma-Ray Dose	54
B-7. MASH VS. APRF: Phantom Free-Field Gamma-Ray Reduction Factors	55
B-8. MASH VS. APRF: Phantom In 2m Box Gamma-Ray Reduction Factors	56
B-9. MASH VS. BTI: Phantom Free-Field Gamma-Ray Dose	57
B-10. MASH VS. BTI: Phantom In 2m Box Gamma-Ray Dose	58
B-11. MASH VS. BTI: Phantom Free-Field Gamma-Ray Reduction Factors	59
B-12. MASH VS. BTI: Phantom In 2m Box Gamma-Ray Reduction Factors	60
B-13. MASH VS. DREO: Phantom Free-Field and In 2m Box Gamma-Ray Dose ..	61
B-14. MASH VS. DREO: Phantom Free-Field Gamma-Ray Reduction Factors	62
B-15. MASH VS. DREO: Phantom In 2m Box Gamma-Ray Reduction Factors	63
B-16. MASH VS. ETCA: Phantom Free-Field Gamma-Ray Dose and Reduction Factors	64

ACKNOWLEDGEMENTS

The authors wish to express their gratitude to the Defense Nuclear Agency for continuously supporting and patiently monitoring the development, verification, and validation of the MASH code system. Also, the authors would like to thank Mrs. Sue Shriner for her significant efforts in preparing this manuscript.

EXECUTIVE SUMMARY

This report summarizes the results of a "benchmark" analysis of the Monte Carlo Adjoint Shielding Code system (MASH) against a series of experiments performed at the Army Pulse Radiation Facility (APRF) in Aberdeen Proving Ground, Maryland. This series of experiments was performed during the period from May 7, 1990 through May 18, 1990 and involved experimentalists from APRF, Harry Diamond Laboratories (HDL), the Defence Research Establishment Ottawa, Canada (DREO), Bubble Technology Industries, Canada, (BTI), and the *l'Armement*, France (ETCA). The "benchmark" analysis of MASH is being performed at Oak Ridge National Laboratory (ORNL) and Science Applications International Corporation (SAIC) and is designed to determine the capability of MASH in reproducing the measured neutron and gamma-ray integral and spectral data. This effort is one of the primary objectives of the MASH Verification and Validation Subtask of the Defense Nuclear Agency (DNA) Radiation Environments Program (REP). Results of the "benchmark" analyses were used in the recommendations to the North Atlantic Treaty Organization (NATO) Panel VII Ad Hoc Group of Shielding Experts for replacing the Vehicle Code System (VCS) with MASH as the reference code of choice for future armored vehicle nuclear vulnerability calculations.

The reactor was operated in the steady state mode for all of the measurements and environmental effects due to terrain, meteorological data, and ground moisture were assessed for inclusion in the MASH analysis. Two different detectors were used by the experimentalists to measure the radiation environments in the free-field and inside the two-meter box test bed, including the BD-100R Bubble Dosimeters for neutron measurements and Thermoluminescent Dosimeters (TLDs) for gamma-ray measurements. Integral measurements were made at a distance of 400 meters from the APRF reactor. In particular, free-field environments were measured along with measurements made using the "NATO standard test bed" and the RT-200 humanoid phantom standing in the free-field and inside the test bed at the "NATO standard reference point" at 400 meters. The "NATO standard test bed" is a large cubical steel walled box having interior dimensions of 200 cm x 200 cm x 200 cm and wall thickness (top and sides) of 5.08 cm. The bottom plate is 10.16 cm thick. The top and side wall thicknesses can be increased to 10.16 cm by the addition of 5.08 cm thick steel plates. The two-meter box test bed was chosen because the geometry provides a simplistic assembly for experimental and theoretical (MASH) comparisons of radiation transmission through material types and thicknesses indicative of modern armored vehicles. The RT-200 anthropomorphic phantom approximates the size, height, and weight of the typical U. S. armored vehicle crewman. The RT-200 is 175.0 cm tall, and weighs 74.0 kg. The chest depth and width are 21.4 cm and 33.8 cm respectively, and the head depth and width are 20.8 cm and 14.8 cm. The RT-200 has non-articulating arms and legs as separate solid members and a physical appearance that closely resembles the male human form.

The MASH calculational technique employs a forward discrete ordinates calculation to determine the neutron and gamma-ray flux on a coupling surface surrounding the armored vehicle or shielded structure and an adjoint Monte Carlo calculation to determine the dose importance of the surface flux. MASH then folds the flux together with the dose importance

to yield the desired detector response(s). MASH was specifically designed to calculate the neutron and gamma-ray radiation environments and shielding protection factors of vehicles, structures, trenches, and other shield configurations. Consequently, the two-meter box experiments represent a realistic test problem for verifying the MASH code system. All calculation utilized a P_5 Legendre expansion of the cross sections, the reference DNA DABL69 69 group ($^{46}\text{n}/^{23}\gamma$) cross-section library, and the Kerr fluence-to-dose free-in-air tissue dose conversion factors (from the DABL69 library).

In general, the calculational results show mixed agreement with the measured data reported by the different teams of experimentalist. The neutron dose results indicate MASH consistently calculates more dose than was measured for both the phantom standing in the free-field and the phantom standing inside the two-meter box. The calculation/measurement differences were typically 20% to 30% for the phantom standing in the free-field and 10% to 20% for the phantom standing inside the two-meter box. The neutron reduction factors, however, typically agreed within $\pm 20\%$ for both phantom/box geometry configurations and orientations. With respect to the gamma-ray data, there were individual discrepancies between calculations and measurements however, typical agreement was within $\pm 20\%$. The gamma-ray free-field environment at 400 meters continues to show a discrepancy between calculation and experiment which further manifest itself through the comparisons of the gamma-ray reduction factors. To determine the overall quality of the comparisons between MASH and the measurements, the data (both calculational and experimental) were averaged over detector position (internal and external), response function (Tissue and $\text{CaF}_2\text{-Mn}$), radiation type (neutron and gamma-ray), and phantom orientation (front facing and right side toward reactor). This averaging procedure produced one set of data for the phantom in the free-field, and one set of data for the phantom inside the two-meter box. The results show overall, that the calculations agreed quite well with most of the measured data supplied by the experimental teams. Generally, the agreement was within the $\pm 20\%$ limit deemed acceptable by the DNA.

This was the second concerted effort aimed at benchmarking the MASH code against measurements and again there were some minor problems in the effort. The most significant problem occurred in the reporting of the gamma-ray dose data. The calculational and experimental results must report the same data for a meaningful comparison to be made. For TLD data, all corrections to the data for spectral effects (calibration field versus radiation field), response functions [dose(Tissue) or dose(TLD)], and contributions due to thermal neutrons must be accounted for or removed from both sets of data. This will allow a true "benchmark" comparison of the MASH code system and reduce the sources of discrepancy. The comparisons further indicate multiple teams of experimentalists performing the same set of measurements yield a better indication of the quality of the comparison. By averaging the different sets of experimental data together, the anomalies and inconsistencies associated with any one measurement will not manifest itself in the overall comparison, yet the trends and results consistent in all of the sets of experimental data will remain. To resolve the discrepancy associated with the calculated and measured free-field gamma-ray data, the differences in the spectral data must be successfully addressed and reconciled. To resolve discrepancies with the comparisons on or inside the phantom, future experiments should possibly include the use of a simplified phantom model of known dimensions, simple geometric shapes, and known materials, e.g. a cylindrical water-filled lucite phantom.

ABSTRACT

The capability to accurately assess and predict the effectiveness of radiation shielding materials in vehicles, structures, trenches, and other configurations is of considerable interest to the DoD and the DNA. A research effort involving several institutions has worked towards providing this capability for several years, resulting in the Monte Carlo Adjoint Shielding Code system - MASH. The purpose of this report is to present the results of a "benchmark" analysis of MASH against a set of measurements performed in the Spring of 1990 at the APRF and determine the capability of MASH in reproducing the measured neutron and gamma-ray dose data. In particular, the free-field environment was calculated along with measurements made using the "NATO standard test bed" (i.e. a two-meter box) and the RT-200 anthropomorphic phantom standing in the free-field and inside the two-meter box at the "NATO standard reference point" at 400 meters.

The calculational results show mixed agreement with the measured data reported by the different teams of experimentalist. The neutron dose results indicate MASH consistently calculates more dose than was measured for both the phantom standing in the free-field and the phantom standing inside the two-meter box. The calculation/measurement differences were typically 20% to 30% for the phantom standing in the free-field and 10% to 20% for the phantom standing inside the two-meter box. The neutron reduction factors, however, typically agreed within $\pm 20\%$ for both phantom/box geometry configurations and orientations. With respect to the gamma-ray data, there were individual discrepancies between calculations and measurements however, typical agreement was within $\pm 20\%$. The gamma-ray free-field environment at 400 meters continues to show a discrepancy between calculation and experiment which further manifest itself through the comparisons of the gamma-ray reduction factors.

To determine the overall quality of the comparisons between MASH and the measurements, the data (both calculational and experimental) were averaged over detector position (internal and external), response function (Tissue and CaF₂:Mn), radiation type (neutron and gamma-ray), and phantom orientation (front facing and right side toward reactor). This averaging procedure produced one set of data for the phantom in the free-field, and one set of data for the phantom inside the two-meter box. In general, the calculations agreed quite well with most of the measured data supplied by the experimental teams. The agreement was typically within the $\pm 20\%$ limit deemed as acceptable by the DNA.

1.0 INTRODUCTION

The Monte Carlo Adjoint Shielding Code System - MASH 1.0¹ was used to analyze the first in a series of nuclear radiation shielding experiments performed in the Fall of 1989 at the Army Pulse Radiation Facility (APRF) in Aberdeen Proving Grounds, Maryland. The objective of this effort was to "benchmark" MASH 1.0 against the experiments performed at the APRF and determine the capability of MASH in reproducing the measured neutron and gamma-ray integral and spectral data. The results of this analysis² were used in the recommendations to the North Atlantic Treaty Organization (NATO) Panel VII Ad Hoc Group of Shielding Experts for replacing the Vehicle Code System (VCS)^{3,4} with MASH 1.0 as the reference code of choice for future armored vehicle nuclear vulnerability calculations.

This report summarizes the results of MASH 1.0 calculations designed to model a second set of measurements in this series of nuclear radiation shielding experiments. These experiments were performed in the Spring of 1990 at the APRF and involved measurements obtained by experimentalists from APRF, the Defence Research Establishment Ottawa, Canada (DREO), Bubble Technology Industries, Canada, (BTI), Harry Diamond Laboratories (HDL), and the Etablissement Technique Central de l'Armement, France (ETCA). The experimentalists utilized two passive integral detectors including the BD-100R Bubble Dosimeters for neutron measurements and Thermoluminescent Dosimeters (TLDs) for gamma-ray measurements.

The analysis of the Fall 1989 measurements involved calculating free-field environments at distances of 170 and 400 meters from the APRF reactor along with measurements made using the "NATO standard test bed" (i.e. a two-meter box) at the "NATO standard reference point" at 400 meters. The specific objective of the effort described in this report was to further "benchmark" MASH 1.0 against experiments involving a humanoid phantom and two-meter box, and determine the capability of MASH of reproducing the measured neutron and gamma-ray integral data. In particular, free-field environments at 400 meters were to be calculated along with measurements made using the two-meter box and the RT-200 humanoid phantom standing in the free-field and inside the two-meter box.

MASH is currently being appraised as the "code-of-choice" to replace VCS. However, before it can be fully adopted for use in armored vehicle nuclear vulnerability calculations, the code system must first be verified and validated through comparisons with experimental data. This effort is one of the primary objectives of the Oak Ridge National Laboratory (ORNL) MASH Verification and Validation Subtask of the Defense Nuclear Agency (DNA) Radiation Environments Program (REP).

2.0 THE TWO-METER BOX TEST BED EXPERIMENTS

One of the purposes of the two-meter box test bed experiments was to provide spectral and integral data for use in the verification and validation of MASH. The experimental measurements were conducted at the Army Pulse Radiation Facility (APRF) bare fast reactor at Aberdeen Proving Grounds, Maryland. The verification and validation of MASH is being performed by ORNL and Science Applications International Corporation (SAIC).

2.1 The APRF Reactor Source

The APRF reactor is a bare critical assembly in the form of a right circular cylinder 22.6 cm in diameter and 19.8 cm in height. The reactor is mounted on a transporter and positioned outdoors at a height of 12.7 meters above a borated concrete experiment pad and approximately 14 meters (on the average) above the surrounding terrain to simulate the (low intensity) neutron and gamma-ray radiation environment typical of a tactical nuclear weapon. The neutron emission from the reactor is anisotropic, with the angular distribution peaked in the horizontal (forward) direction.

2.2 The Two-Meter Box Test Bed

The "NATO standard test bed" is a large cubical steel walled box having interior dimensions of 200 cm x 200 cm x 200 cm and wall thickness (top and sides) of 5.08 cm. The bottom plate is 10.16 cm thick. The top and side wall thicknesses can be increased to 10.16 cm by the addition of 5.08 cm thick steel plates. The box contains lift tabs (for movement by crane), drainage holes at the base, a cable access hole at the base on the back side of the box, and two hatches. The hatches are located in the center of the top and back faces of the box and the hatch diameters in the interior box and outside plates are staggered to mitigate radiation streaming paths into the box. The hatches are included for loading and unloading experimental equipment (e.g. detectors, phantoms, etc.) and for simulating open-hatch vehicle experiments. The interior air space volume with dimensions of 200 cm x 200 cm x 200 cm gives the test bed the common name - "the two-meter box."

2.3 The RT-200 Anthropomorphic Phantom

The RT-200 anthropomorphic phantom supplied by the Defence Research Establishment Ottawa, Canada (DREO), approximates a typical U. S. armored vehicle crewman. The RT-200 stands 175.0 cm tall and weighs 74.0 kg. The chest depth and width are 21.4 cm and 33.8 cm respectively, and the head depth and width are 20.8 cm and 14.8 cm. The RT-200 is comprised of a head, neck, and torso (which contains a set of lungs). The

phantom has non-articulating arms and legs as separate solid members and a physical appearance that closely resembles the male human form. The phantom is constructed from a numbered series of one-inch thick slices held together with plastic rods. Four of the slices, two in the mid-head and two in the mid-gut regions, have removable cut-outs to allow for "in-phantom" dosimetry measurements. External dosimetry measurements are made by taping the dosimeters directly to the phantom in the desired location(s), e.g., wrist, chest, belt, etc.

2.4 Details of the Measurements

The reactor was operated in the steady state mode for all of the experiments reported in this document. Power levels and run durations were determined for each experiment by the requirements of the detector system being used to assure sufficient statistical accuracy in the measured results. Meteorological data (air temperature, barometric pressure, and relative humidity) were recorded during the course of the experiments by the Aberdeen Proving Grounds Meteorological Observation Station at Poverty Island and provided to the APRF staff. In addition, the APRF staff made several ground moisture measurements throughout the course of the experiments to record the water content of the soil.

All measurements in the two-meter box test bed and RT-200 phantom were made at a distance of 400 meters from the APRF reactor. The 400 meter test site is referred to as the "NATO standard reference point" and is a sufficient distance for the neutron and gamma-ray spectra to reach equilibrium shapes due to modifications of the reactor source spectrum from interactions in the air and ground. The box was oriented with one face normal to the axis from the reactor to the test site and with the side hatch away from the APRF reactor. In all of the measurements both hatches were closed. The box was always present at the 400 meter test site. The measurements involving the RT-200 phantom were made with the phantom standing in the free-field or inside the two-meter box, either facing the APRF reactor or with the right side towards the reactor. Free-field measurements were obtained by placing the detectors or RT-200 phantom at a distance of 400 meters from the reactor and at a distance from the two-meter box of approximately 10 meters. The in-box measurements were obtained by placing the detectors or RT-200 phantom inside the box with the signal and high voltage cables (if required) passing through the cable port to data acquisition equipment inside the APRF building or to mobile counting laboratories located near the 400 meter site.

2.5 Experimental Equipment

Two different detectors were used by the experimentalists to measure the radiation environments in the free-field and inside the two-meter box test bed, including BD-100R Bubble Dosimeters for neutron measurements and Thermoluminescent Dosimeters (TLDs) for gamma-ray measurements. Both of these detector systems measure integral quantities, and consequently, no spectral measurements were performed.

The BD-100R Bubble Dosimeter is ideally suited for these measurements because it is capable of measuring very low neutron dose (less than one mrem) and is tissue equivalent for neutron energies between 100 keV and 20 MeV. Furthermore, the BD-100R maintains

an isotropic response over its active range, and is capable of immediate on-site data analysis. The experimentalists from BTI (in conjunction with the team from DREO) were the only team performing neutron dose measurements for this series of experiments.

The Thermoluminescent Dosimeter (TLD) measures gamma-ray dose between 10 keV and 20 MeV. The TLD is sensitive to gamma rays but also moderately sensitive to thermal neutrons. Several varieties of TLDs with different shapes, sizes, and shields were used by the experimentalists. All experimentalists participated in the gamma-ray dose measurements and reported results in units of dose (Tissue) except HDL which reported results in units of dose ($\text{CaF}_2:\text{Mn}$). Consequently, HDL provided ORNL analysts with the $\text{CaF}_2:\text{Mn}$ gamma-ray energy sensitive response function (relative to air) for the MASH analysis of the HDL measurements.

The sequence of free-field and in-box neutron and gamma-ray measurements was carefully planned and coordinated by the APRF staff to ensure minimum interference between the different experimentalists and to achieve optimum reactor-detector-box dispositions. The integral power required for the BD-100R neutron dosimeter measurements is significantly less than that required for the TLD measurements. Consequently, the neutron measurements were performed separately from the gamma-ray measurements. The TLD measurements required full day runs (approximately 50 kWh of integrated power) due to the low sensitivity of the TLDs. Therefore, all experimentalists performed the TLD measurements simultaneously to allow for completion of the full experimental schedule.

Kerma values were reported for free-field measurements, free-in-air measurements inside the two-meter box, and measurements external and internal to the RT-200 humanoid phantom standing in the free-field and inside the two-meter box. The experimental data summarized in this report were taken from presentation charts and other documents provided by the different experimentalists.

3.0 MASH CALCULATIONAL TECHNIQUES

The MASH calculational technique employs a GRTUNCL-DORT⁵ forward discrete ordinates calculation to determine the neutron and gamma-ray fluence on a coupling surface surrounding the armored vehicle or shielded structure and a MORSE⁶ adjoint Monte Carlo calculation to determine the dose importance of the surface fluence. MASH then utilizes the Detector Response Code (DRC)¹ to fold the fluence together with the dose importance to yield the desired detector response(s). MASH was specifically designed to calculate the neutron and gamma-ray radiation environments and shielding protection factors of vehicles, structures, trenches, and other shield configurations. Consequently, the two-meter box experiments represent a realistic test problem for verifying the MASH code system.

3.1 Definition of Protection and Reduction Factors

Two quantities that are indicative of the ability of a ground combat vehicle to protect its crew members from penetrating nuclear radiation are protection factors (PFs) and reduction factors (RFs). The protection factors are more useful in the characterization of the vehicle shielding, whereas the reduction factors are more useful for comparisons with experimental data.

The neutron protection factor considers only the incident radiation field due to scattered and unscattered neutrons and secondary gamma radiation arising from (n,γ) reactions in the vehicle. Similarly, the gamma protection factor treats only that incident radiation resulting from gamma rays produced by prompt fission and extra-vehicle (n,γ) reactions (air and ground). Because detector systems are unable to discern the origin of the gamma rays (i.e. source, air secondary gamma ray, vehicle secondary gamma ray, etc.) contributing to the in-vehicle dose, the calculated reduction factors are more easily compared with experimental measurements than the protection factors. The definitions of the parameters and protection factors used in DRC to characterize the effectiveness of the vehicle shields are given in Table 1. It should be noted that the definitions of the protection factors and reduction factors are independent of the response function (i.e. tissue dose, silicon dose, etc.) used in the analysis.

3.2 Air-Over-Ground Environment

The APRF radiation environment was modeled in the GRTUNCL and DORT codes to determine the air-over-ground environment from which the fluence on the coupling surface could be obtained. GRTUNCL calculates the uncollided component of the fluence and DORT calculates the scalar and directional fluences of the collided component. All three components of the fluence are processed through VISTA¹ to obtain the fluence on the coupling surface to be folded in DRC.

Table 1. Definitions of Radiation Protection Factors and Reduction Factors.

TPF = TOTAL PROTECTION FACTOR $TPF = \frac{\text{Free-Field Dose}}{\text{Inside-Vehicle Dose}} = \frac{D_n^{FF} + D_{n\gamma,air}^{FF} + D_\gamma^{FF}}{D_n^{iv} + D_{n\gamma,veh}^{iv} + D_{n\gamma,air}^{iv} + D_\gamma^{iv}}$
NPF = NEUTRON PROTECTION FACTOR $NPF = \frac{\text{Free-Field Neutron Dose}}{\text{Target Dose Summing Direct Neutrons + Vehicle}(n,\gamma)} = \frac{D_n^{FF}}{D_n^{iv} + D_{n\gamma,iv}^{iv}}$
GPF = GAMMA PROTECTION FACTOR $GRF = \frac{\text{Free-Field Gamma Dose, (Direct } \gamma \text{ + Air and Grnd}(n,\gamma)\text{)}}{\text{Target Dose Caused By All Gamma Sources}} = \frac{D_{n\gamma,air}^{FF} + D_{n\gamma,grnd}^{FF} + D_\gamma^{FF}}{D_{n\gamma,veh}^{iv} + D_{n\gamma,air}^{iv} + D_{n\gamma,grnd}^{iv} + D_\gamma^{iv}}$
TRF = TOTAL REDUCTION FACTOR $TRF = \frac{\text{Free-Field Dose}}{\text{Inside-Vehicle Dose}} = \frac{D_n^{FF} + D_{n\gamma,air}^{FF} + D_\gamma^{FF}}{D_n^{iv} + D_{n\gamma,veh}^{iv} + D_{n\gamma,air}^{iv} + D_\gamma^{iv}}$
NRF = NEUTRON REDUCTION FACTOR $NRF = \frac{\text{Free-Field Neutron Dose}}{\text{Target Dose Caused By Direct Neutrons}} = \frac{D_n^{FF}}{D_n^{iv}}$
GRF = GAMMA REDUCTION FACTOR $GRF = \frac{\text{Free-Field Gamma Dose, (Direct } \gamma \text{ + Air and Ground}(n,\gamma)\text{)}}{\text{Target Dose Caused By All Gamma Sources}} = \frac{D_{n\gamma,air}^{FF} + D_{n\gamma,grnd}^{FF} + D_\gamma^{FF}}{D_{n\gamma,veh}^{iv} + D_{n\gamma,air}^{iv} + D_{n\gamma,grnd}^{iv} + D_\gamma^{iv}}$

where

D_n^{FF} - Direct neutron Free-Field Dose	$D_{n\gamma,air}^{FF}$ - Air (n,γ) Free-Field Dose
$D_{n\gamma,grnd}^{FF}$ - Ground (n,γ) Free-Field Dose	D_γ^{FF} - Direct Gamma Free-Field Dose
D_n^{IV} - Direct neutron Inside-Vehicle Dose	$D_{n\gamma,veh}^{IV}$ - Vehicle (n,γ) Inside-Vehicle Dose
$D_{n\gamma,air}^{IV}$ - Air (n,γ) Inside-Vehicle Dose	$D_{n\gamma,grnd}^{IV}$ - Ground (n,γ) Inside-Vehicle Dose
D_γ^{IV} - Direct Gamma Inside-Vehicle Dose	

In early 1989, SAIC performed a detailed analysis of the APRF reactor and produced the energy- and angle-differential leakage spectrum to be used as the source for all transport calculations.⁷ SAIC calculated the neutron leakage from the APRF reactor, integrated over all angles, to yield 1.293×10^{17} neutrons per kWh. Table 2 lists the APRF reactor neutron leakage spectrum (normalized to unity). The APRF gamma-ray leakage spectrum is divided into two components, prompt plus secondary gamma-ray leakage, and delayed gamma-ray leakage. The prompt and secondary gamma-ray leakage spectrum is a function of the reactor model used in the source analysis and is constant in both number of gamma rays per source neutron and spectral shape. The delayed gamma-ray leakage spectrum changes as a function of time after a fission event and therefore varies in both number and spectral shape. SAIC calculated delayed gamma-ray spectra for three different durations of operation; fifteen minutes, one hour, and four hours. For the purposes of the two-meter box test bed experiments, the one hour delayed gamma spectrum was utilized in the MASH analysis. The number of gamma rays per source neutron for the prompt plus secondary, one hour delayed, and total gamma-ray leakage spectra are 0.276, 0.112, and 0.388 respectively. The combined prompt plus secondary and one-hour delayed gamma-ray leakage spectrum (normalized to unity) for the APRF reactor is given in Table 3.

The air-over-ground model utilized 123 radial intervals and 146 axial intervals in a flat topographical r-z model. This mesh modeled a 2000 meter by 2000 meter air environment. Approximately one meter of

Table 2. APRF Reactor Neutron Leakage Spectrum (number of neutrons per energy bin) and DABL69 Free-In-Air Tissue Kerma Response Function (Gy-cm²/n) Used in the MASH Analysis.

Group No.	Upper Energy (eV)	APRF Reactor Leakage	DABL69 Free-In-Air Tissue	Group No.	Upper Energy (eV)	APRF Reactor Leakage	DABL69 Free-In-Air Tissue
1	1.9640+07 ^a	2.78-06	7.365-11	24	8.2085+05	3.50-02	2.059-11
2	1.6905+07	1.09-05	7.046-11	25	7.4274+05	5.35-02	1.937-11
3	1.4918+07	1.26-05	6.859-11	26	6.3927+05	5.04-02	1.791-11
4	1.4191+07	9.28-06	6.745-11	27	5.5023+05	1.05-01	1.638-11
5	1.3840+07	7.15-05	6.616-11	28	3.6883+05	7.33-02	1.301-11
6	1.2523+07	2.88-05	6.381-11	29	2.4724+05	4.78-02	1.026-11
7	1.2214+07	2.16-04	6.355-11	30	1.5764+05	2.18-02	8.065-12
8	1.1052+07	4.68-04	5.988-11	31	1.1109+05	1.86-02	5.634-12
9	1.0000+07	9.04-04	5.763-11	32	5.2475+04	4.38-03	3.592-12
10	9.0484+06	1.63-03	5.515-11	33	3.4307+04	1.55-03	2.592-12
11	8.1873+06	2.67-03	5.464-11	34	2.4788+04	4.48-04	2.130-12
12	7.4082+06	6.83-03	5.127-11	35	2.1875+04	9.36-04	1.476-12
13	6.3763+06	2.13-02	4.709-11	36	1.0595+04	2.53-04	6.284-13
14	4.9658+06	6.07-03	5.578-11	37	3.3546+03	3.84-05	2.199-13
15	4.7237+06	2.24-02	4.436-11	38	1.2341+03	3.46-06	9.259-14
16	4.0657+06	6.40-02	4.194-11	39	5.8495+02	4.90-07	4.481-14
17	3.0119+06	6.70-02	3.573-11	40	2.7536+02	1.17-07	2.073-14
18	2.3852+06	1.07-02	3.325-11	41	1.0130+02	1.94-08	1.037-14
19	2.3096+06	7.85-02	3.211-11	42	2.9023+01	2.51-09	9.324-15
20	1.8268+06	9.20-02	2.912-11	43	1.0677+01	4.74-10	1.359-14
21	1.4227+06	9.83-02	2.634-11	44	3.0590+00	6.92-11	2.285-14
22	1.1080+06	5.42-02	2.525-11	45	1.1253+00	1.21-11	3.727-14
23	9.6164+05	6.00-02	2.225-11	46	4.1399-01	1.94-12	1.291-13
					1.0000-05		

^aRead as 1.9640 x 10⁷

Table 3. APRF Reactor Gamma-Ray Leakage Spectrum (number of gamma-rays per energy bin) and DABL69 Free-In-Air Tissue Kerma Response Function ($\text{Gy}\cdot\text{cm}^2/\gamma$) Used in the MASH Analysis.

Group No.	Upper Energy (eV)	APRF Reactor Leakage	DABL69 Free-In-Air Tissue	Group No.	Upper Energy (eV)	APRF Reactor Leakage	DABL69 Free-In-Air Tissue
1	2.000+07 ^a	4.51-08	4.011-11	13	1.500+06	2.05-01	5.853-12
2	1.400+07	2.23-07	3.176-11	14	1.000+06	1.90-01	4.272-12
3	1.200+07	1.01-05	2.761-11	15	7.000+06	1.73-01	2.964-12
4	1.000+07	3.20-04	2.352-11	16	4.550+05	7.90-02	1.930-12
5	8.000+06	4.67-04	2.051-11	17	3.000+05	6.40-02	1.054-12
6	7.000+06	1.17-03	1.851-11	18	1.500+05	1.17-02	5.296-13
7	6.000+06	4.55-03	1.644-11	19	1.000+05	1.42-03	3.482-13
8	5.000+06	1.17-02	1.433-11	20	7.000+04	5.93-05	3.132-13
9	4.000+06	3.76-02	1.213-11	21	4.500+04	1.57-06	4.846-13
10	3.000+06	3.98-02	1.036-11	22	3.000+04	1.75-07	1.050-12
11	2.500+06	6.76-02	9.027-12	23	2.000+04	6.30-07	3.396-12
12	2.000+06	1.13-01	7.556-12	24	1.000+04		

^aRead as 2.000×10^7

ground was included in the air-over-ground calculations to model ground scattering. The source height was set at 16.143 meters above the air/ground interface and at the center of the radial mesh ($r=0.0$). The air-over-ground model utilized a 240 direction forward biased quadrature, a P_5 Legendre expansion of the cross sections, the reference DNA Defense Applications Broad-group Library (DABL69) 69 group ($46n/23\gamma$) cross-section library,⁸ and three different materials - air, ground, and borated concrete (the reactor pad). Three ground moisture and four air moisture contents were utilized to encompass the full spectrum of ground moisture and meteorological data recorded by APRF. To model the ground moisture conditions, 32%, 39%, and 45% water (by weight) was utilized in the APRF soil compositions. The meteorological data and number densities for the various air compositions used in this analysis are given in Table 4. Six air-over-ground fluence files at the coupling surface were calculated using the GRTUNCL-DORT-VISTA code sequence. Utilizing these six fluence files enabled the ORNL analysts to choose an air-over-ground environment which closely approximated the environmental conditions for a given measurement.

Table 4. Meteorological Data and Air Number Densities Used in the MASH Analysis of the APRF Spring 1990 Two-Meter Box Test Bed Experiments.

Meteorological Data					
Date	Experiment Number	Pressure (mm Hg)	Temperature (K)	Relative Humidity (%)	Density (gm/cm ³)
5/9/90	ss90-124	762.3	297.3	58.0	1.183-03 ^a
5/11/90	ss90-127	758.4	287.2	44.0	1.223-03
5/14/90	ss90-130	764.7	296.5	50.0	1.191-03
5/16/90	ss90-136	760.0	294.6	86.0	1.188-03
Air Number Densities					
Date	Experiment Number	Hydrogen (atoms/barn·cm)	Nitrogen (atoms/barn·cm)	Oxygen (atoms/barn·cm)	Argon (atoms/barn·cm)
5/9/90	ss90-124	8.511-07	3.798-05	1.062-05	2.272-07
5/11/90	ss90-127	3.560-07	3.952-05	1.078-05	2.364-07
5/14/90	ss90-130	7.011-07	3.833-05	1.063-05	2.292-07
5/16/90	ss90-136	1.081-06	3.804-05	1.075-05	2.275-07

^aRead as 1.183×10^{-3} .

3.3 The Two-Meter Box and Phantom Geometry Models

An isometric view of the two-meter box test bed described in Section 2.0 is shown in Figure 1. The two-meter box test bed was chosen for the "NATO standard test bed" because the geometry provides a simplistic vehicle for experimental and analytical (MASH) comparisons of radiation transmission through material types and thicknesses indicative of modern armored vehicles.

The RT-200 anthropomorphic phantom (also described in Section 2.0) is a complex form which does not lend itself easily to modeling using standard combinatorial geometry input currently available in the MASH code system. Consequently, a modified combinatorial geometry phantom model, developed from the original Snyder phantom model,⁹ was used in the MASH analysis. An isometric view of the combinatorial geometry phantom model is shown in Figure 2. The

combinatorial geometry model represents a simplified form of the RT-200 phantom and does not have all the detailed contours which characterize the anthropomorphic RT-200 phantom actually used in the measurements. The simplified phantom model is 174.4 cm tall and weighs approximately 70.0 kg. The chest contains a set of lungs and has a depth and width of 20.0 cm and 34.4 cm, respectively. Likewise, the head depth and width are 20.0 cm and 15.1 cm. Since the gross features, i.e., size, height, weight, physical dimensions, etc., of the combinatorial geometry phantom are similar to those of the RT-200 phantom, it is believed that the differences in the calculational and experimental phantom models will not cause significant errors in the MASH analysis of the measurements.

The two-meter box (Figure 1) and combinatorial geometry phantom (Figure 2) were modeled in the MORSE component of the MASH code system using the GIFT^{10,11} geometry package. Figure 3 depicts an isometric view of the GIFT geometry model of the phantom standing in the two-meter box (facing the reactor). The material compositions for the air, ground, steel, BD-100R neutron dosimeters, and phantom (soft tissue, bone, and lung) are given in Table 5.

There were multiple detector positions utilized in the Spring 1990 experiments. Table 6 lists the positions of the BD-100R bubble dosimeters. The same general locations were used for the TLD measurements. There were multiple dosimeters used in the measurements on and inside the phantom as evidenced in Table 6. A set of preliminary scoping calculations determined significant differences in the calculated neutron doses as a result of including (or excluding) the BD-100R dosimeters in the geometry model. Differences within statistical deviations were generally seen in the calculated gamma-ray doses. However, the BD-100R bubble dosimeter is a volumetric detector and MASH utilizes a point detector for computing the dose. Consequently, the BD-100R detectors were not modeled in the MASH calculations even though they are included in the geometry models. At each detector location (left wrist, front belt, etc.), the MASH analyses utilized a point central to the location of the multiple BD-100R detectors. There are two positions not associated with the phantom relating to measurements made inside the box. The "Center of Box" location corresponds to the location used in the Fall 1989 measurements and was used when the phantom was outside the box. The "Detector on Shelf" location is situated off to one side on a small aluminum table and was used when the phantom was standing inside the box. The Kerr neutron and gamma-ray Free-In-Air (FIA) tissue kerma response functions in the DABL69 cross-section library were utilized in DRC to obtain the dose responses in the free-field and in the two-meter box. Listings of the neutron and gamma-ray FIA tissue kerma response functions are given in Tables 2 and 3 respectively.

3.4 The Two-Meter Box Calculations

The MASH calculations also utilized the reference DNA DABL69 69 group ($46n/23\gamma$) cross-section library. The Monte Carlo (MORSE) calculations for the phantom standing in the free-field generated and tracked 200,000 primary source particles for the external detector locations (belt, wrist, chest, etc.), and 400,000 primary source particles for the internal detector locations (mid-head, and mid-gut). The Monte Carlo (MORSE) calculations for the phantom standing in the two-meter box generated and tracked 500,000 primary source particles for all detector locations (including "Center of Box" and Detector on Shelf" locations). In all MORSE calculations, the primary source particles were sampled over the 69 energy groups. An energy dependent relative importance factor was utilized over the 69 groups to increase the frequency of sampling the adjoint source particles from energy groups which have a significant effect on the

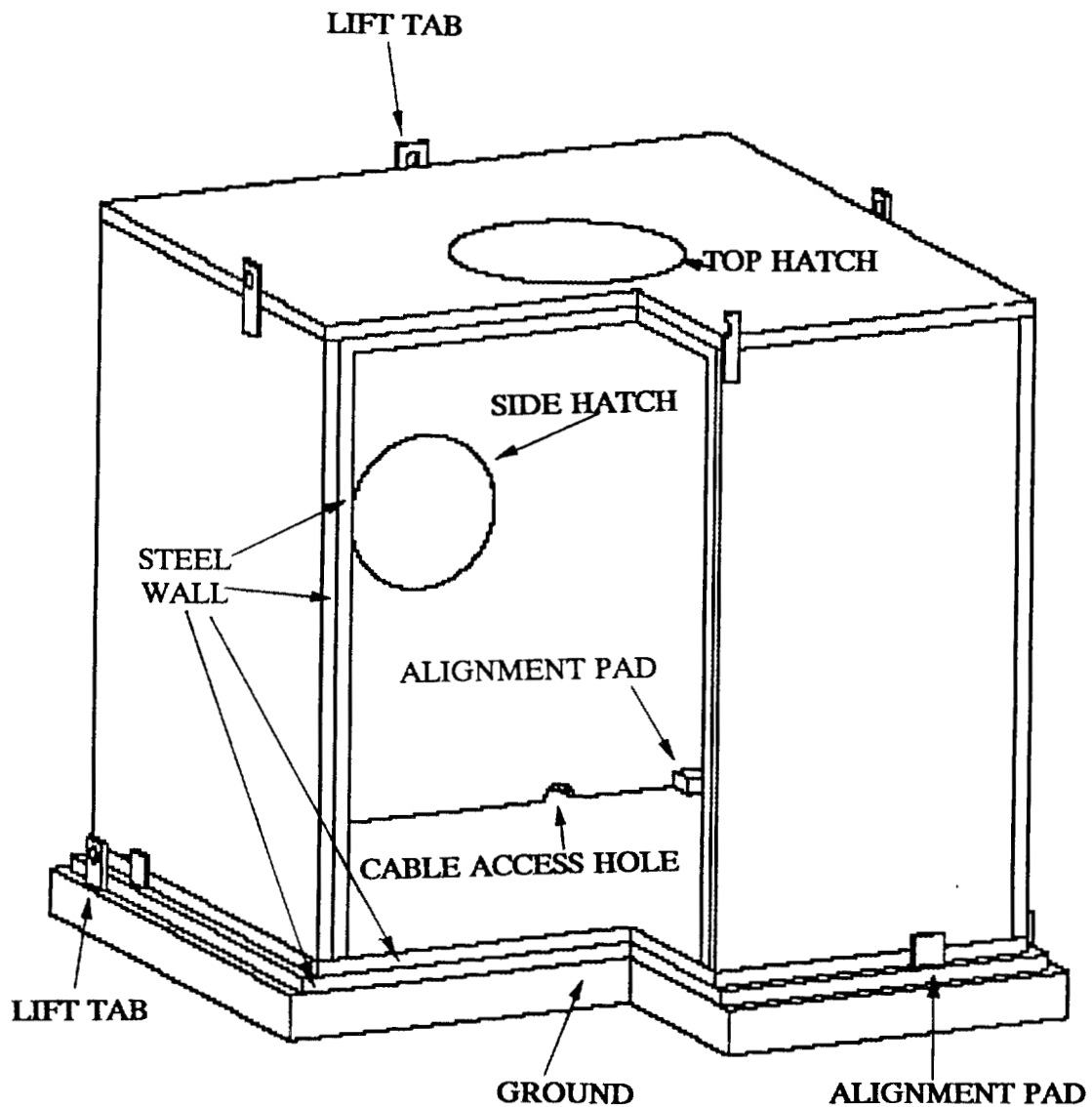


Figure 1. Isometric View of the Two-Meter Box Test Bed.

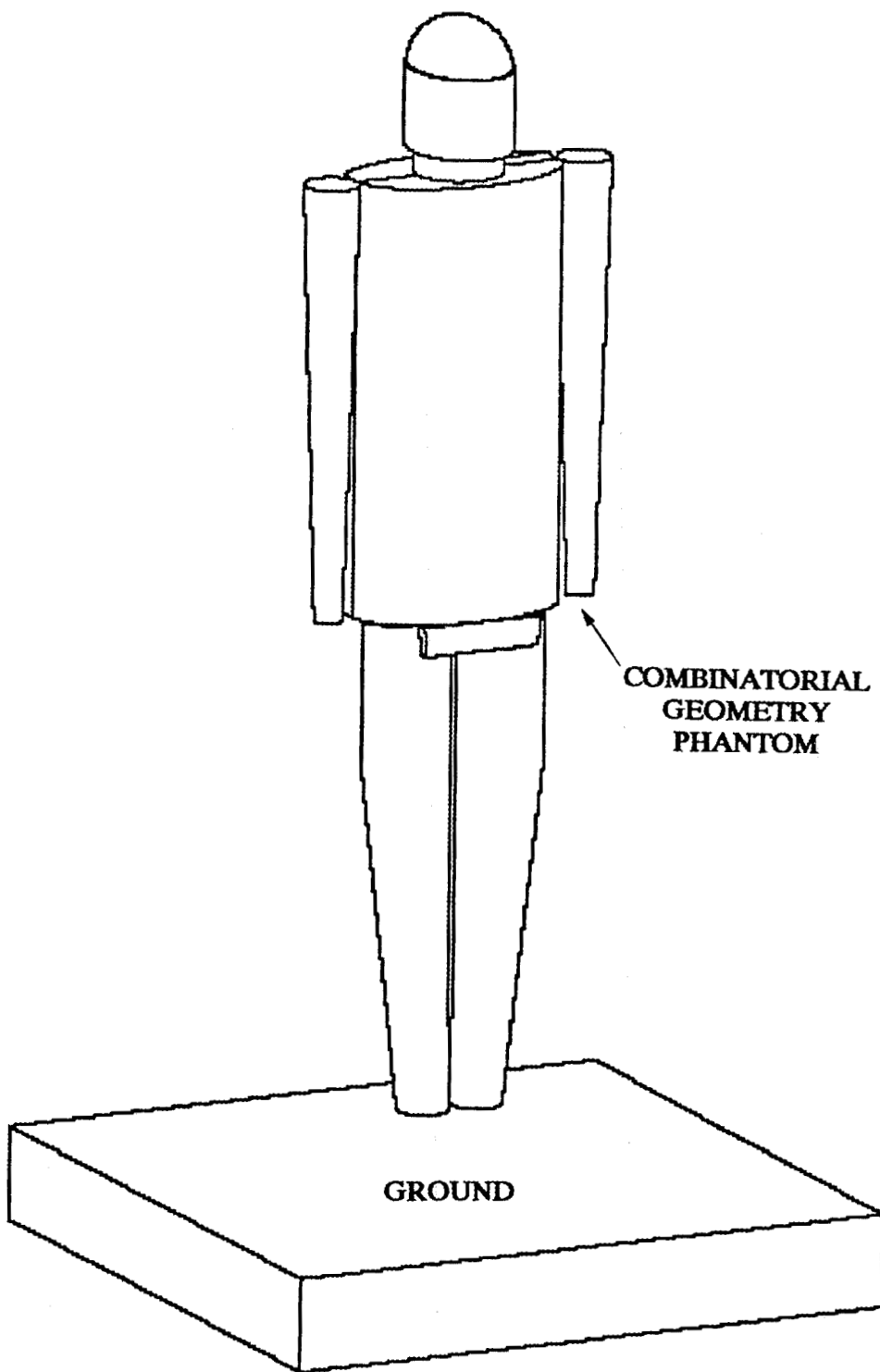


Figure 2. Isometric View of the Combinatorial Geometry Phantom Model Used in the MASH Analysis.

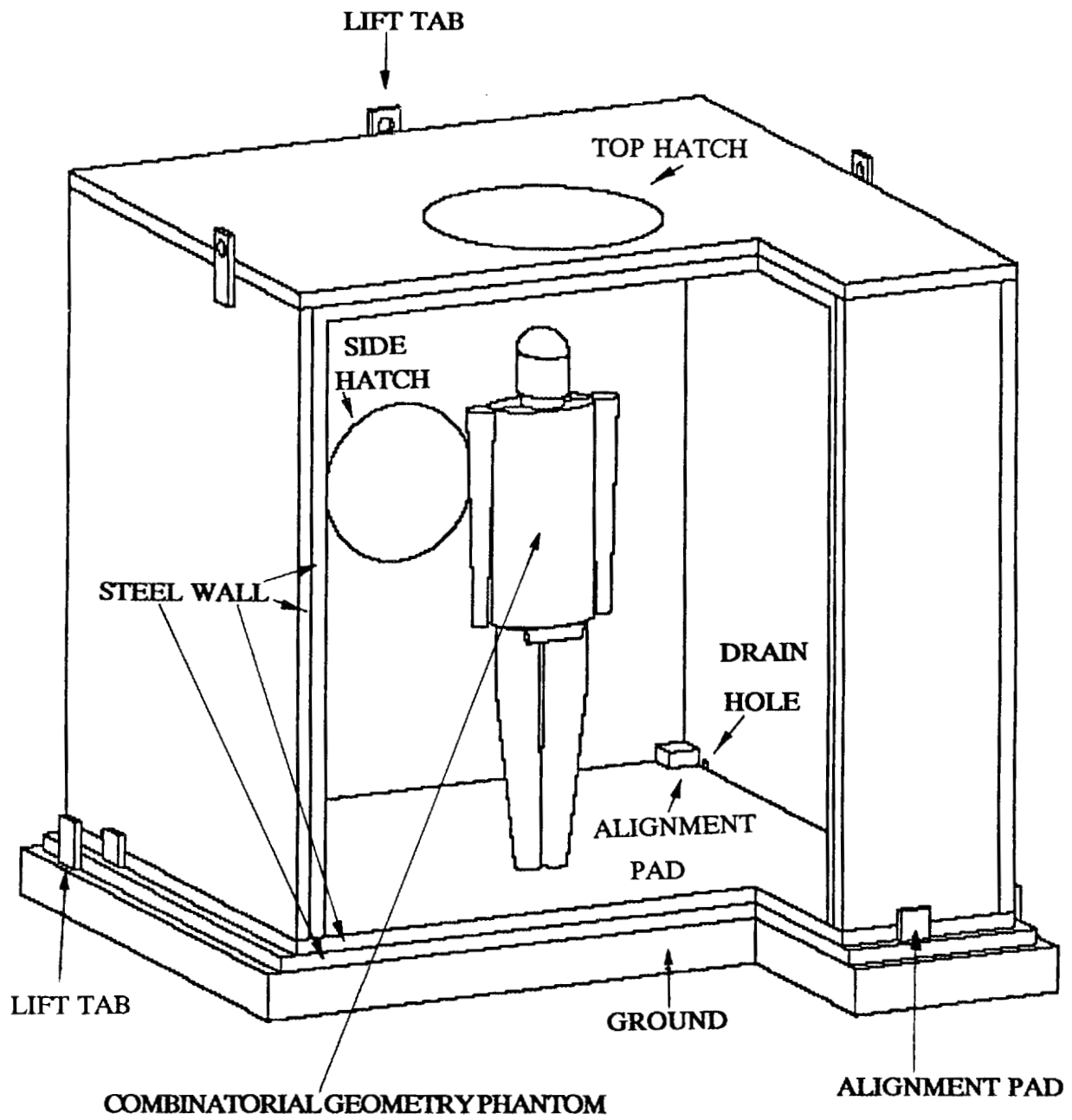


Figure 3. Isometric View of the MASH Geometry Model of the Combinatorial Geometry Phantom Standing Inside the Two-Meter Box Test Bed.

Table 5. Compositions of the Materials Used in the MASH Analysis of the APRF Spring 1990 Two-Meter Box Test Experiments.

Atomic Number	Element	Material Composition (atoms/(barn-cm))								
		APRF Ground	Air	1020 Steel	Plastic Lung	Soft Tissue	Bone	Water	Lexan	5% Borated Polyethylene
1	Hydrogen	4.80-02 ^a	7.01-07		1.65-02	5.88-02	6.14-02	6.69-02	3.98-02	7.13-02
5	Boron-10	8.86-09								4.87-04
5	Boron-11	3.24-08								1.97-03
6	Carbon	3.49-04		8.08-04	1.18-02	3.36-02	1.79-02		4.54-02	3.41-02
7	Nitrogen	4.39-05	3.83-05		1.02-03	1.99-03	1.84-03			
8	Oxygen	4.30-02	1.06-05		3.82-03	7.72-03	2.52-02	3.34-02	8.52-03	3.64-03
11	Sodium	1.32-04				2.32-07	1.20-04			
12	Magnesium	8.43-05					3.88-05			
13	Aluminum	1.27-03			1.31-09	2.29-09				
14	Silicon	8.79-03		4.21-04			6.00-07			
15	Phosphorus			6.11-05			1.39-03			
16	Sulfur	3.34-06		7.38-05			4.55-05			
17	Chlorine	3.27-06			7.13-08	2.35-08	3.40-05			
18	Argon		2.29-07							
19	Potassium	1.89-04					3.30-05			
20	Calcium	2.40-05					2.14-03			
25	Manganese	6.65-06		3.88-04						
26	Iron	2.97-04		8.39-02			1.21-06			
27	Cobalt	2.57-07								
28	Nickel	2.58-07								
29	Copper	4.49-07								
50	Tin	6.76-08								
	$\rho(\text{gm/cm}^3)$	1.75+00	1.19-03	7.86+00	3.90-01	1.03+00	1.40+00	1.00+00	1.20+00	9.40-01
		^a Read as 4.80×10^{-2}								

SI

Table 6. MASH Coordinate Positions for the Analysis of the APRF Spring 1990 Two-Meter Box Test Bed Experiments BD-100R Bubble Dosimeter Locations

Table 6. MASH Coordinate Positions for the Analysis of the APRF Spring 1990 Two-Meter Box Test Bed Experiments BD-100R Bubble Dosimeter Locations on the RT-200 Humanoid Phantom and Inside the Two-Meter Box.

Detector Position	Coordinate Positions (cm)		
	X-Coordinate	Y-Coordinate	Z-Coordinate
Mid Head	0.0	0.0	177.15
Left Chest (r)	-10.82	-5.88	149.06
Left Chest (m)	-10.82	-7.49	149.06
Left Chest (l)	-10.82	-9.10	149.06
Front Belt (r)	-10.82	1.61	116.04
Front Belt (m)	-10.82	0.0	116.04
Front Belt (l)	-10.82	-1.61	116.04
Back Belt (r)	10.82	1.61	116.04
Back Belt (m)	10.82	0.0	116.04
Back Belt (l)	10.82	-1.61	116.04
Mid-Gut	0.0	0.0	116.04
Right Arm, Front (r)	-2.97	22.34	95.30
Right Arm, Front (l)	-2.97	20.27	95.30
Left Arm, Side (t)	0.0	-24.51	93.71
Left Arm, Side (b)	0.0	-24.51	92.10
Detector on Shelf (m)	-23.00	-60.00	87.46
Center of Box	0.0	0.0	110.16

(b=bottom, l=left, m=middle, r=right, and t=top)

dose response function. The secondary particle production probability was set to 1.0 for all regions and energy groups in the Monte Carlo calculations, and the in-group energy biasing option in MORSE was switched on. Region dependent and energy independent splitting and Russian Roulette parameters were utilized in the two-meter steel box regions to improve the efficiency of the Monte Carlo calculations. This was accomplished by subdividing the 10.16-cm-thickness of steel into two equally thick concentric regions and assigning each of the steel regions different splitting and Russian Roulette parameters which would allow a sufficient number of source particles (and secondary particles) to escape to obtain acceptable

statistics. Only one biasing region was used in the phantom model due to the complexity of segmenting the geometry in a cost efficient manner. The average air and ground moisture conditions for this series of experiments (APRF air for run ss90-130 given in Table 4, and APRF ground with 39 wt% H₂O given in Table 5) were chosen for the adjoint MORSE calculations. The elemental compositions given in Table 5 were mixed to give the MORSE materials listed in Table 7. It should be noted that in this analysis, the MORSE materials and GIFT geometry model materials are equivalent.

Table 7. MASH Geometry Regions and Cross-Section Materials Used in the Analysis of the APRF Spring 1990 Two-Meter Box Test Bed Experiments.

MORSE Material Number	Material Description	MORSE Material Number	Material Description
1	APRF Ground	6	Bone, Skeleton
2	Air	7	Water
3	SAE 1020 Steel	8	Lexan
4	Plastic Lung	9	5% Borated Polyethylene
5	Soft Tissue		

As presently configured, DRC assumes the DORT fluence on the "coupling surface" is dependent on energy and elevation only, and not on azimuth. Consequently, DRC only uses the fluence at the 400 meter radius in the DORT mesh and does not use the radii encompassing the box. This assumption is valid for small objects at a great distance from the source. Since the size of the box and/or phantom is small relative to the distance from the source, it was felt this assumption was valid for this analysis and would produce an uncertainty within the statistical deviations of the calculated results.

For documentation purposes, sample input data streams (decks) for the air-over-ground analysis (GIP, GRTUNCL, DORT, and VISTA), and two-meter box and phantom analyses (MORSE and DRC), along with the GIFT5 geometry models for the two-meter box, the phantom, and the phantom in the two-meter box, are included in the appendices. This will enable future versions of MASH to be "benchmarked" to the analysis reported in this document.

4.0 DISCUSSION OF RESULTS

4.1 Neutron Dose and Reduction Factors

There is a considerable amount of data generated in the MASH analysis of a series of experiments when multiple detector locations, teams of experimentalists, and geometry configurations and orientations are considered. For documentation purposes and completeness, the bulk of this data is included in the appendices along with the majority of the data comparisons to the experimental data. Data averaged over the different experimental parameters (detector location, geometry configuration, and phantom orientation) will be presented in the main text.

Comparisons of the calculated (MASH) and measured (BTI/DREO) neutron Free-in-Air (FIA) tissue dose are given in Tables A-1 and A-2. Table A-1 presents the dose data for the phantom standing in the free-field (facing and right side towards reactor) at 400 meters from the APRF reactor. Likewise, Table A-2 presents the measured and calculated dose data for the phantom standing in the two-meter box (facing and right side towards reactor) at 400 meters. The comparisons of measured and calculated neutron reduction factors (NRFs) for the dose data presented in Tables A-1 and A-2 are presented in Tables A-3 and A-4, respectively. Finally, comparisons of the measured and calculated neutron doses and reduction factors, averaged over internal, external, and all detector locations on or inside the phantom, are presented in Tables 8 and 9. Calculation to experiment (C/E) ratios are included in each table to help quantify the comparisons.

The C/E ratios for the FIA dose to the phantom standing in the free-field (Table A-1) indicate MASH consistently calculates more dose (20% to 30%) for almost all of the detector locations and for both orientations of the phantom. Two notable exceptions to this are the comparisons at the back belt (BB) and right wrist (RW) locations for the phantom facing the reactor where the MASH calculations agree (within 10%) with the dose measured by the BD-100R dosimeters. The C/E ratios for the FIA dose to the phantom standing in the two-meter box (Table A-2) also indicate a consistent overestimation by MASH of the measured dose external and internal to the phantom for most of the detector locations and both phantom orientations. The MASH overestimation of the measured dose typically ranges from a factor of 1.09 to 1.19 for the various detector locations external and internal to the phantom. One exception to the MASH overestimation phenomenon is the mid-gut (MG) location where the C/E indicates MASH underestimates the dose by approximately 0.80 to 0.89. One final result worth mentioning in Tables A-1 and A-2 are the C/E ratios for the free-field (FF) comparisons. As in the case with the Fall 1989 comparisons², MASH calculates 15%-20% more dose than is measured. [The BTI/DREO reported free-field dose of 3.57 mrad/kWh in Table A-2 is significantly differently from all other measurements of this quantity and is believed (by the authors) to be a bad data point.] This indicates a consistency in both the measured and calculated free-field dose between the two sets of experiments and calculated free-field dose between the two sets of experiments (Fall 1989 and Spring 1990).

There is no apparent reason for the discrepancies exhibited in the results shown in Tables A-1 and A-2. Possible causes include modeling differences (MASH combinatorial geometry phantom vs. the RT-200 humanoid phantom), detector placement on/in the MASH model versus actual position on the RT-200 phantom, temperature corrections for the BD-100R dosimeters, insufficient/inaccurate bubble counts, cross sections, Legendre expansion of the cross sections, quadrature, etc. The measured results in Tables A-1 and A-2 indicate the magnitude of the radiation field around the phantom (i.e. total number of neutrons) is less than that calculated using MASH. This would yield the lower measured doses in Tables A-1 and A-2 for both phantom orientations. The mid-head results in Table A-1 appear to indicate a different measured and calculated distribution of the radiation field around the phantom with the MASH calculations yielding considerably more dose. Possibly, the MASH calculations yield a stronger contribution from the top of the head than is measured. The mid-head detector location in the MASH analysis may be closer to the top of the head than the location in the experiment. The MASH calculations exhibit the proper trend when rotating the phantom from front facing to right side facing the reactor. The MASH calculations show an increase in the dose to the mid-head and the corresponding measurements show a decrease. Since the thickness of tissue-equivalent plastic between the detector and source decrease as the head is turned toward right side on, the dose should increase for the predominantly forward directed radiation field present at 400 meters. This inverse relationship between dose and tissue-equivalent plastic thickness is evidenced by both calculated and measured results at the mid-gut (MG) detector location. Consequently, the measured mid-head (MH) dose in Table A-1 could be suspect for the phantom standing in the free-field with the right side toward the reactor. The consistent overestimation of the dose to the phantom standing in the two-meter box by MASH is also unexplainable at this time. The absolute number of neutrons per kWh that reach the 400 meter test site appear to be different between calculation and experiment. This could indicate a modeling problem in the MASH 2-D air-over-ground analysis or a normalization problem present in either the calculations or measurements. There was fairly good agreement between calculation and experiment for the integral dose in the empty two-meter box in the Fall 1989 comparisons.² There were, however, spectral differences which have not been adequately resolved. These differences in conjunction with a further perturbation of the radiation field inside the box due to the presence of the phantom could possibly explain the discrepancies exhibited in Table A-2. Further investigation and spectral data are the only plausible means of determining if this is the case.

The neutron reduction factor (NRF) comparisons presented in Tables A-3 and A-4 minimize the discrepancies noted in Tables A-1 and A-2 and indicate good agreement between the MASH calculations and the measurements. In particular, at the detector locations where MASH overestimates the measured dose (i.e., C/E > 1.0), the C/E for the corresponding neutron reduction factor will be within the acceptable range of 0.80 to 1.20. This is due to the overestimation of the free-field dose by MASH. (See the definition of the reduction factors given in Table 1.) Those few detector locations where the dose C/E ratios (Tables A-1 and A-2) are less than one have large NRF C/E ratios exhibited in Tables A-3 and A-4, ranging from a factor of 1.30 to 1.50. It should be noted that the low free-field dose measurement (3.57 mrad/kWh) for the phantom standing in the two-meter box with the right side toward the reactor (Table-A-2) yields significantly lower measured NRFs than were calculated in MASH (Table A-4) and C/E ratios for the NRFs greater than the $\pm 20\%$ DNA mandate for acceptable agreement. Obviously, these results are a manifestation of a bad free-

field measurement and are not indicative of the overall agreement between MASH and the experimental results (with respect to the NRFs) and should be considered appropriately.

Understanding the difference associated with each individual comparison is important in understanding the physics and/or mechanics of the processes involved. Often, however, the quantity and diversity of the C/E ratios tend to "muddy the picture" as to the overall quality of the comparison. Consequently, averaging the experimental and analytical results over external, internal, and all detector locations on or inside the phantom yields a summary indication of the agreement between MASH and the measurements for the dose comparisons (Table 8), and the reduction factor comparisons (Table 9). The averaged results presented in these tables give a clearer indication of the overall quality of the comparisons. As one would expect, the results and trends discussed above are still prevalent in the summary results presented in Table 8 and 9 do not yield all C/E ratios within $\pm 20\%$.

4.2 Gamma-Ray Dose and Reduction Factors

Comparisons of the calculated (MASH) and measured gamma-ray dose and reduction factors are given in Appendix B for the different organizations participating in the Spring 1990 experiments at APRF. The tables of dose and reduction factor data have been grouped by organization (not all organizations participated in the full series of measurements). Tables B-1 through B-4 present the comparisons to the HDL data, Tables B-5 through B-8 present the comparisons to the APRF data, Tables B-9 through B-12 present the comparisons to the BTI data, Tables B-13 through B-15 present the comparisons to the DREO data, and Table B-16 presents the comparisons to the ETCA data. In each set of data, the gamma-ray dose comparisons are presented first followed by the gamma-ray reduction factor (GRF) comparisons.

Due to the considerable amount of data presented in the tables of Appendix B, the comparisons of the measured and calculated gamma-ray doses and reduction factors, averaged over internal, external, and all detector locations on or inside the phantom, are presented in Tables 10 through 19 for all the different teams of experimentalists. Furthermore, in Tables 20 and 21, the measurement data, again averaged over internal, external, and all detector locations on or inside the phantom, and for all the teams of experimentalists reporting dose in unit of mrad(Tissue), are averaged together and compared to the MASH calculations. Calculation to experiment (C/E) ratios are included in each table of gamma-ray data (Appendix B and Tables 10 through 21) to help quantify the comparisons.

The experimentalists measured the gamma-ray data using calcium fluoride ($\text{CaF}_2:\text{Mn}$) Thermoluminescent Dosimeters (TLDs) of different sizes and shapes and with different types of shields (i.e., Sn, Al, CH_2 , etc.). All experimentalists (except HDL) reported gamma-ray results in units of dose(Tissue), i.e. mrad(Tissue). To obtain results in units of dose(Tissue), the experimentalists had to apply conversion factor(s) to the response function to convert the response from dose($\text{CaF}_2:\text{Mn}$) (referred to as dose(TLD)) to dose(Tissue). The HDL data is reported in units of dose($\text{CaF}_2:\text{Mn}$). HDL supplied ORNL analysts with the $\text{CaF}_2:\text{Mn}$ response function for direct comparisons to the HDL experimental data. None of the experimentalists corrected the data to account for the differences in the gamma-ray spectrum in the APRF radiation field and the radiation field of the calibration facility. Furthermore,

it should be noted that $\text{CaF}_2:\text{Mn}$ is moderately sensitive to thermal neutrons. Again, none of the experimental data were corrected for the contribution due to the thermal neutron source. This should not be a big factor for free-field measurements inside the two-meter box. However, for the free-field measurements outside the two-meter box and all phantom measurements, the thermal neutrons may contribute 5-10% of the total thermoluminescence signal. The MASH results in Appendix B and Tables 10 through 21 are reported in units of dose(Tissue) using the DABL69⁸ Free-In-Air tissue kerma response function or dose($\text{CaF}_2:\text{Mn}$) using the response function provided by HDL. The MASH results do not contain any contribution from thermal neutrons and are not corrected back to the gamma-ray spectrum of the calibration field used for the different TLDs. The composite effect of the differences in the way the measured and calculated data are reported is difficult to ascertain. It is conceivable that the uncertainties associated with these differences are greater than the $\pm 20\%$ mandate of DNA for acceptable comparisons without regard to the actual comparisons of the calculations and measurements themselves.

Analyzing the comparisons of the calculational and experimental gamma-ray dose and reduction factor results presented in Appendix B show the C/E ratios are typically between 0.80 and 1.20. Within the comparisons to any individual organization, there are detector locations and geometry configurations (i.e. phantom in the free-field, phantom in the two-meter box, etc.) which have poor agreement and a corresponding C/E ratio outside the $\pm 20\%$ acceptable range. However, this same detector location may exhibit excellent agreement when the phantom orientation is changed relative to the reactor. Furthermore, that same detector location, when compared to the results for a different organization, may exhibit excellent agreement between MASH and experiment. This situation lends credence to the comparisons of the "averaged" data presented in Tables 10 through 19. Once again, the comparisons of the average values will yield a clear picture of the quality of the overall comparison of MASH to the measurements. It should be noted that as in the case of the Fall 1989 comparison², the calculation to experiment (C/E) ratios are within the range of ratios obtained when two different sets of experimental data (E/E ratios) are compared. Without going into explicit detail on the comparisons between MASH and each set of experimental data, the more significant trends associated with the comparisons presented in Appendix B will be discussed.

The comparisons of the free-field (FF) dose showed differences up to approximately 30% to 45% for dose (Tissue) between the different teams of experimentalists. The APRF and ETCA teams measured gamma-ray doses of approximately 1.75 mrad(Tissue) and the DREO and BTI teams measured gamma-ray doses of approximately 1.33 mrad(Tissue). Although TLDs were not used in the Fall 1989 comparison, these results are approximately 20% to 30% higher for the APRF and ETCA teams and approximately 20% lower for the DREO and BTI teams when compared to the published dose results of the Fall 1989 study. The MASH calculations exhibited an increase of approximately 10% in the reported free-field dose (compared to the Fall 1989 study). With respect to the MASH calculations, the differences between Fall 1989 and Spring 1990 free-field results can be attributed to meteorological conditions, detector energy range, and an updated APRF leakage source. The extended range of measured free-field doses yielded a corresponding range in C/E values from 0.73 to 1.08.

The spread of the dose C/E ratios within a given set of comparisons to a particular team of experimentalists typically included values both greater than and less than unity for any given phantom orientation/geometry configuration. The APRF comparisons, however, exhibited a trend of all dose C/E ratios less than unity for the phantom standing in the free-field and all dose C/E ratios greater than unity (except one TLD location) for the phantom standing in the two-meter box. As a general trend, the MASH calculations calculated more dose than was measured.

The most consistent discrepancies between calculation and measurement occurred at the mid-gut location for the phantom standing in the two-meter box. This detector location usually exhibited the largest dose C/E ratio with MASH calculating more dose than was measured. A second "trouble spot" in the comparisons was at the detector location on the shelf in the two-meter box (DS) when the phantom was standing in the free-field. The MASH results consistently calculated approximately 20% more dose than was measured by the experimentalists who utilized this detector location. This result suggests a possible difference between calculated and measured angular distribution of the gamma-ray fluence spectrum inside the two-meter box.

The comparisons of the calculated and measured reduction factors showed almost all of the C/E ratios to be within $\pm 20\%$. The main exception to this is the comparison with the APRF data for the phantom in the two-meter box. An underestimation of the calculated free-field dose (when compared to experiment) coupled with an overestimation of the calculated dose on or inside the phantom will amplify the differences in the reduction factors and consequently yield C/E ratios which are greater than $\pm 20\%$.

Averaging the calculational and experimental data over external, internal, and overall detector location on or inside the phantom yields a clear indication of how well the MASH calculations compare to the measurements. These results (Tables 10 through 19) indicate fairly good agreement between MASH and the measurements as a function of detector position (external vs. internal), geometry configuration, and phantom orientation. The comparisons to the HDL data Tables 10 and 11) show good agreement in the dose results for the phantom standing in the free-field and a slight discrepancy for the dose to the phantom in the box. The reduction factor comparisons (Table 11) however, show good agreement for both geometry configurations (phantom standing in the free-field and inside the two-meter box). The comparisons to the APRF data (Tables 12 and 13) show good agreement in the dose results (Table 12) but marginal agreement in the reduction factor results (Table 13) for the phantom standing in the two-meter box. The comparisons to the BTI results (Tables 14 and 15), the DREO results (Tables 16 and 17), and ETCA results (Tables 18 and 19) all show good agreement between MASH and experiment for both dose and reduction factor data. With respect to all of the comparisons in Tables 10 through 19), the internal detector locations (predominantly the mid-gut position) yielded the largest discrepancy between calculation and experiment. Differences in calculational model and measured phantom, absolute detector location in relation to the model or phantom, quality of measurement, and convergence of the calculation are the most probable causes for the larger discrepancies associated with the internal detector locations.

To further summarize the quantity of measured gamma-ray data reported in units of dose(Tissue), the measured results from APRF, BTI, DREO, and ETCA were again averaged

over external, internal, and overall detector location on or inside the phantom and compared to the MASH results in Tables 20 and 21. The HDL data was not included in this table due to the differences in reported dose units. In viewing the comparisons in Tables 20 and 21, all of the C/E ratios are within $\pm 20\%$ except the internal detector average gamma-ray reduction factor for the phantom standing in the box and facing the reactor (Table 21). This indicates fairly consistent agreement between MASH and measurement for the gamma-ray data taken in this experiment.

Table 8

Comparisons of Calculated and BTI/DREO Measured Neutron Dose Averaged Over External, Internal, and All Detector Locations On or Inside the RT-200 Humanoid Phantom at the 400 Meter Test Site at the APRF.			
Neutron Dose (mrads(Tissue)/kWh)	MASH	BTI/DREO	C/E
Phantom Free-Field - Front Toward Reactor			
External Detector Average	3.87	3.21	1.21
Internal Detector Average	0.97	0.80	1.21
Overall Detector Average	3.04	2.52	1.21
Phantom Free-Field - Right Side Toward Reactor			
External Detector Average	3.33	2.49	1.34
Internal Detector Average	0.91	0.66	1.38
Overall Detector Average	2.64	1.96	1.35
Phantom Inside Two-Meter Box - Front Toward Reactor			
External Detector Average	2.18	1.98	1.10
Internal Detector Average	0.31	0.29	1.07
Overall Detector Average	1.64	1.49	1.10
Phantom Inside Two-Meter Box - Right Side Toward Reactor			
External Detector Average	2.03	1.90	1.07
Internal Detector Average	0.30	0.31	0.97
Overall Detector Average	1.54	1.45	1.06

Table 9

Comparisons of Calculated and BTI/DREO Measured Neutron Reduction Factors Averaged over External, Internal, and All Detector Locations On or Inside the RT-200 Humanoid Phantom at the 400 Meter Test Site at the APRF.			
Neutron Reduction Factor	MASH	BTI/DREO	C/E
Phantom Free-Field - Front Toward Reactor			
External Detector Average	1.27	1.27	1.00
Internal Detector Average	5.05	5.14	0.98
Overall Detector Average	1.61	1.62	0.99
Phantom Free-Field - Right Side Toward Reactor			
External Detector Average	1.47	1.67	0.88
Internal Detector Average	5.38	6.35	0.85
Overall Detector Average	1.86	2.12	0.88
Phantom Inside Two-Meter Box - Front Toward Reactor			
External Detector Average	2.25	2.16	1.04
Internal Detector Average	16.1	15.0	1.07
Overall Detector Average	2.98	2.86	1.04
Phantom Inside Two-Meter Box - Right Side Toward Reactor			
External Detector Average	2.41	1.87	1.29
Internal Detector Average	16.3	11.7	1.39
Overall Detector Average	3.19	2.47	1.29

Table 10

Comparisons of Calculated and HDL Measured Gamma-Ray Dose Averaged Over External, Internal, and All Detector Locations On or Inside the RT-200 Humanoid Phantom at the 400 Meter Test Site at the APRF.			
Gamma Dose (mrad(CaF ₂ :Mn)/kWh)	MASH	HDL	C/E
Phantom Free-Field - Front Toward Reactor			
External Detector Average	1.76	1.90	0.93
Internal Detector Average	2.05	1.91	1.07
Overall Detector Average	1.84	1.90	0.97
Phantom Free-Field - Right Side Toward Reactor			
External Detector Average	1.64	1.41	1.16
Internal Detector Average	1.97	1.62	1.22
Overall Detector Average	1.73	1.47	1.18
Phantom Inside Two-Meter Box - Front Toward Reactor			
External Detector Average	0.56	0.49	1.14
Internal Detector Average	0.86	0.65	1.32
Overall Detector Average	0.64	0.53	1.21
Phantom Inside Two-Meter Box - Right Side Toward Reactor			
External Detector Average	0.49	0.40	1.23
Internal Detector Average	0.74	0.61	1.21
Overall Detector Average	0.56	0.46	1.22

Table 11

Comparisons of Calculated and HDL Measured Gamma-Ray Reduction Factors Averaged Over External, Internal, and All Detector Locations On or Inside the RT-200 Humanoid Phantom at the 400 Meter Test Site at the APRF			
Gamma Reduction Factor	MASH	HDL	C/E
Phantom Free-Field - Front Toward Reactor			
External Detector Average	0.77	0.70	1.10
Internal Detector Average	0.66	0.70	0.94
Overall Detector Average	0.74	0.70	1.06
Phantom Free-Field - Right Side Toward Reactor			
External Detector Average	0.83	0.93	0.89
Internal Detector Average	0.69	0.81	0.85
Overall Detector Average	0.78	0.89	0.88
Phantom Inside Two-Meter Box - Front Toward Reactor			
External Detector Average	2.40	2.70	0.89
Internal Detector Average	1.57	2.05	0.77
Overall Detector Average	2.09	2.48	0.84
Phantom Inside Two-Meter Box - Right Side Toward Reactor			
External Detector Average	2.74	3.29	0.83
Internal Detector Average	1.82	2.17	0.84
Overall Detector Average	2.39	2.87	0.83

Table 12

Comparisons of Calculated and APRF Measured Gamma-Ray Dose Averaged Over External, Internal, and All Detector Locations On or Inside the RT-200 Humanoid Phantom at the 400 Meter Test Site at APRF			
Gamma Dose (mrad(Tissue)/kWh)	MASH	APRF	C/E
Phantom Free-Field - Front Toward Reactor			
External Detector Average	1.67	1.92	0.87
Internal Detector Average	1.93	2.15	0.90
Overall Detector Average	1.75	1.99	0.88
Phantom Free-Field - Right Side Toward Reactor			
External Detector Average	1.56	1.79	0.87
Internal Detector Average	1.86	2.15	0.87
Overall Detector Average	1.64	1.89	0.87
Phantom Inside Two-Meter Box - Front Toward Reactor			
External Detector Average	0.59	0.55	1.07
Internal Detector Average	0.89	0.85	1.05
Overall Detector Average	0.68	0.64	1.06
Phantom Inside Two-Meter Box - Right Side Toward Reactor			
External Detector Average	0.52	0.46	1.13
Internal Detector Average	0.77	0.73	1.05
Overall Detector Average	0.59	0.54	1.09

Table 13

Comparisons of Calculated and APRF Measured Gamma-Ray Reduction Factors Averaged Over External, Internal, and All Detector Locations On or Inside the RT-200 Humanoid Phantom at the 400 Meter Test Site at the APRF.			
Gamma Reduction Factor (Tissue)	MASH	APRF	C/E
Phantom Free-Field - Front Toward Reactor			
External Detector Average	0.80	0.88	0.91
Internal Detector Average	0.69	0.79	0.87
Overall Detector Average	0.77	0.86	0.90
Phantom Free-Field - Right Side Toward Reactor			
External Detector Average	0.86	0.96	0.90
Internal Detector Average	0.72	0.80	0.90
Overall Detector Average	0.81	0.91	0.89
Phantom Inside Two-Meter Box - Front Toward Reactor			
External Detector Average	2.24	3.05	0.73
Internal Detector Average	1.49	1.99	0.75
Overall Detector Average	1.96	2.65	0.74
Phantom Inside Two-Meter Box - Right Side Toward Reactor			
External Detector Average	2.54	3.69	0.69
Internal Detector Average	1.72	2.34	0.74
Overall Detector Average	2.23	3.17	0.70

Table 14

Comparisons of Calculated and BTI Measured Gamma-Ray Dose Averaged Over External, Internal, and All Detector Locations On or Inside the RT-200 Humanoid Phantom at the 400 Meter Test Site at the APRF.			
Gamma Dose (mrad(Tissue)/kWh)	MASH	BTI	C/E
Phantom Free-Field - Front Toward Reactor			
External Detector Average	1.67	1.56	1.07
Internal Detector Average	1.93	1.68	1.15
Overall Detector Average	1.75	1.59	1.10
Phantom Free-Field - Right Side Toward Reactor			
External Detector Average	1.56	1.57	0.99
Internal Detector Average	1.86	1.53	1.22
Overall Detector Average	1.64	1.56	1.05
Phantom Inside Two-Meter Box - Front Toward Reactor			
External Detector Average	0.59	0.64	0.92
Internal Detector Average	0.89	0.73	1.22
Overall Detector Average	0.68	0.67	1.01
Phantom Inside Two-Meter Box - Right Side Toward Reactor			
External Detector Average	0.52	0.49	1.06
Internal Detector Average	0.77	0.63	1.22
Overall Detector Average	0.59	0.53	1.11

Table 15

Comparisons of Calculated and BTI Measured Gamma-Ray Reduction Factors Averaged Over External, Internal, and All Detector Locations On or Inside the RT-200 Humanoid Phantom at the 400 Meter Test Site at the APRF.			
Gamma Reduction Factor (Tissue)	MASH	BTI	C/E
Phantom Free-Field - Front Toward Reactor			
External Detector Average	0.80	0.80	1.00
Internal Detector Average	0.69	0.75	0.92
Overall Detector Average	0.77	0.78	0.99
Phantom Free-Field - Right Side Toward Reactor			
External Detector Average	0.86	0.87	0.99
Internal Detector Average	0.72	0.90	0.80
Overall Detector Average	0.81	0.88	0.92
Phantom Inside Two-Meter Box - Front Toward Reactor			
External Detector Average	2.24	2.13	1.05
Internal Detector Average	1.49	1.89	0.70
Overall Detector Average	1.96	2.05	0.96
Phantom Inside Two-Meter Box - Right Side Toward Reactor			
External Detector Average	2.54	2.71	0.94
Internal Detector Average	1.72	2.10	0.82
Overall Detector Average	2.23	2.50	0.89

Table 16

Comparisons of Calculated and DREO Measured Gamma-Ray Dose Averaged Over External, Internal, and ALL Detector Locations On or Inside the RT-200 Humanoid Phantom at the 400 Meter Test Site at the APRF.			
Gamma Dose (mrad(Ti)/kWh)	MASH	DREO	C/E
Phantom Free-Field - Front Toward Reactor			
External Detector Average	1.67	1.61	1.04
Internal Detector Average	1.93	1.83	1.05
Overall Detector Average	1.75	1.67	1.05
Phantom Free-Field - Right Side Toward Reactor			
External Detector Average	1.56		
Internal Detector Average	1.86		
Overall Detector Average	1.64		
Phantom Inside Two-Meter Box - Front Toward Reactor			
External Detector Average	0.59		
Internal Detector Average	0.89		
Overall Detector Average	0.68		
Phantom Inside Two-Meter Box - Right Side Toward Reactor			
External Detector Average	0.52	0.49	1.06
Internal Detector Average	0.77	0.68	1.13
Overall Detector Average	0.59	0.54	1.09

Table 17

Comparisons of Calculated and DREO Measured Gamma-Ray Reduction Factors Averaged Over External, Internal, and All Detector Locations On or Inside the RT-200 Humanoid Phantom at the 400 Meter Test Site at the APRF.			
Gamma Reduction Factor (Tissue)	MASH	DREO	C/E
Phantom Free-Field - Front Toward Reactor			
External Detector Average	0.80	0.81	0.99
Internal Detector Average	0.69	0.71	0.97
Overall Detector Average	0.77	0.78	0.99
Phantom Free-Field - Right Side Toward Reactor			
External Detector Average	0.86	0.88	0.98
Internal Detector Average	0.72	0.81	0.89
Overall Detector Average	0.81	0.86	0.94
Phantom Inside Two-Meter Box - Front Toward Reactor			
External Detector Average	2.24	NM*	-
Internal Detector Average	1.49	NM	-
Overall Detector Average	1.96	NM	-
Phantom Inside Two-Meter Box - Right Side Toward Reactor			
External Detector Average	2.54	2.83	0.90
Internal Detector Average	1.72	2.03	0.85
Overall Detector Average	2.23	2.54	0.88

*Not Measured

Table 18

Comparisons of Calculated and ETCA Measured Gamma-Ray Dose Averaged Over External, Internal, and All Detector Locations On or Inside the RT-200 Humanoid Phantom at the 400 Meter Test Site at the APRF.			
Gamma Dose (mrad(Tissue)/kWh)	MASH	ETCA	C/E
Phantom Free-Field - Front Toward Reactor			
External Detector Average	1.67	2.11	0.79
Internal Detector Average	1.93	2.29	0.84
Overall Detector Average	1.75	2.16	0.81
Phantom Free-Field - Right Side Toward Reactor			
External Detector Average	1.56	NM*	-
Internal Detector Average	1.86	NM	-
Overall Detector Average	1.64	NM	-
Phantom Inside Two-Meter Box - Front Toward Reactor			
External Detector Average	0.59	NM	-
Internal Detector Average	0.89	NM	-
Overall Detector Average	0.68	NM	-
Phantom Inside Two-Meter Box - Right Side Toward Reactor			
External Detector Average	0.52	NM	-
Internal Detector Average	0.77	NM	-
Overall Detector Average	0.59	NM	-

*Not Measured

Table 19

Comparisons of Calculated and ETCA Measured Gamma-Ray Reduction Factors Averaged Over External, Internal, and All Detector Locations On or Inside the RT-200 Humanoid Phantom at the 400 Meter Test Site at the APRF.			
Gamma Reduction Factor (Tissue)	MASH	ETCA	C/E
Phantom Free-Field - Front Toward Reactor			
External Detector Average	0.80	0.87	0.92
Internal Detector Average	0.69	0.80	0.86
Overall Detector Average	0.77	0.85	0.91
Phantom Free-Field - Right Side Toward Reactor			
External Detector Average	0.86	NM*	-
Internal Detector Average	0.72	NM	-
Overall Detector Average	0.81	NM	-
Phantom Inside Two-Meter Box - Front Toward Reactor			
External Detector Average	2.24	NM	-
Internal Detector Average	1.49	NM	-
Overall Detector Average	1.96	NM	-
Phantom Inside Two-Meter Box - Right Side Toward Reactor			
External Detector Average	2.54	NM	-
Internal Detector Average	1.72	NM	-
Overall Detector Average	2.23	NM	-

*Not Measured

Table 20

Comparisons of Calculated and Average Experimentally Measured Gamma-Ray Dose(Tissue) Averaged Over External, Internal, and All Detector Locations On or Inside the RT-200 Humanoid Phantom at the 400 Meter Test Site at the APRF.			
Gamma Dose (mrad(Tissue)/kWh)	MASH	Avg. Expt.	C/E
Phantom Free-Field - Front Toward Reactor			
External Detector Average	1.67	1.80	0.93
Internal Detector Average	1.93	1.99	0.97
Overall Detector Average	1.75	1.85	0.95
Phantom Free-Field - Right Side Toward Reactor			
External Detector Average	1.56	1.68	0.93
Internal Detector Average	1.86	1.84	1.01
Overall Detector Average	1.64	1.73	0.95
Phantom Inside Two-Meter Box - Front Toward Reactor			
External Detector Average	0.59	0.60	0.98
Internal Detector Average	0.89	0.79	1.13
Overall Detector Average	0.68	0.66	1.03
Phantom Inside Two-Meter Box - Right Side Toward Reactor			
External Detector Average	0.52	0.48	1.08
Internal Detector Average	0.77	0.68	1.13
Overall Detector Average	0.59	0.54	1.09

Table 21

Comparisons of Calculated and Average Experimentally Measured Gamma-Ray Reduction Factors(Tissue) Averaged Over External, Internal, and All Detector Locations On or Inside the RT-200 Humanoid Phantom at the 400 Meter Test Site at the APRF.			
Gamma Reduction Factor (Tissue)	MASH	Avg. Expt.	C/E
Phantom Free-Field - Front Toward Reactor			
External Detector Average	0.80	0.84	0.95
Internal Detector Average	0.69	0.76	0.91
Overall Detector Average	0.77	0.82	0.94
Phantom Free-Field - Right Side Toward Reactor			
External Detector Average	0.86	0.90	0.96
Internal Detector Average	0.72	0.83	0.87
Overall Detector Average	0.81	0.88	0.92
Phantom Inside Two-Meter Box - Front Toward Reactor			
External Detector Average	2.24	2.51	0.89
Internal Detector Average	1.49	1.94	0.77
Overall Detector Average	1.96	2.31	0.85
Phantom Inside Two-Meter Box - Right Side Toward Reactor			
External Detector Average	2.54	3.02	0.84
Internal Detector Average	1.72	2.15	0.80
Overall Detector Average	2.23	2.70	0.83

5.0 MONTE CARLO STATISTICAL UNCERTAINTY

Analysis of the MORSE escape history tapes in DRC for all of the detector positions on or inside the phantom (except the mid-gut position) and inside the two-meter box test bed yielded statistical uncertainties on the order of $\pm 3\%$ for integral neutron fluence(dose) and $\pm 2\%$ for total gamma-ray fluence(dose). The mid-gut position yielded statistical uncertainties on the order of $\pm 4\%$ to $\pm 8\%$ for integral neutron fluence(dose) and $\pm 2\%$ for total gamma-ray fluence(dose). The statistical uncertainties for the vehicle secondary particle production, i.e. vehicle (n,γ), the direct gamma-ray plus air secondary gamma production, i.e. source γ 's + air (n,γ), and all contributions from the ground secondary particle production, i.e. ground (n,γ), are typically $\pm 2\%$, $\pm 4\%$, and ± 25 to $\pm 35\%$ respectively. It should be noted that the large statistical uncertainties associated with the ground secondary particle production are not critical to the quality of the calculated results since this contribution to the total dose is insignificant. Spectral fluence(dose) results exhibited statistical uncertainties typically between $\pm 5\%$ and $\pm 15\%$ for neutron energies between 10 MeV and thermal, and between $\pm 5\%$ and $\pm 10\%$ for gamma energies between 10 MeV and 100 keV for all detector locations except the mid-gut location and the mid-head location for the phantom standing in the two-meter box. These two locations (mid-head inside box and mid-gut) exhibited spectral fluence(dose) results with statistical uncertainties typically between $\pm 10\%$ and $\pm 30\%$ for neutron energies between 10 MeV and thermal, and between $\pm 7\%$ and $\pm 12\%$ for gamma-ray energies between 10 MeV and 100 keV. These energy ranges contain the energy groups in the DABL69 group structure which make a significant contribution to the response.

Unfortunately, there was limited detailed information on uncertainties reported with the experimental data utilized in this report. Based on uncertainties reported in numerous previous documents, the accuracy of the detector systems used in this set of experiments ranges from approximately $\pm 5\%$ to $\pm 10\%$, and the reproducibility of the detector system results on a day-to-day basis is approximately $\pm 5\%$ to $\pm 10\%$.

As stated earlier, the composite effect of the differences in the way the measured and calculated gamma-ray data are reported is difficult to ascertain and is not considered in this report.

6.0 CONCLUSIONS

The multiple air-over-ground environments yielded an accurate representation of the ground moisture and meteorological data supplied by APRF. Plotting the dose response as a function of hydrogen content in the air, ground moisture, and detector energy range, and correlating the different experimental measurements with the ground moisture and meteorological data, allowed the ORNL analysts to extrapolate between the different air-over-ground environments to obtain results consistent with the environmental data present at the time of a given measurement. This appears to be the most viable option for representing changing environmental data over a series of measurements. Calculating the fluence on the coupling surface for each air-over-ground environment during a series of measurements would be prohibitive.

Analyzing 200,000 to 400,000 adjoint source particles was sufficient to obtain integral data statistics within $\pm 5\%$ for almost all of the detector locations for the phantom standing in the free-field. The mid-head and mid-gut locations for the phantom standing inside the two-meter box possibly could have utilized more adjoint source particles to obtain a statistical convergence within $\pm 5\%$. Ideally, a minimum of 500,000 adjoint source particles should be used for all calculations of integral data involving the phantom. This would assure adequate statistical convergence of the integral data.

Convergence on the spectral data would be marginal for the number of adjoint source particles used in this analysis since most of the neutron group data were only converged to approximately 10% to 15%. Should comparisons of spectral data for this type of experiment become a requirement in the future, the MASH analysis will have to be rerun to obtain acceptable statistical convergence on the spectral data. For spectral data comparisons, 1,000,000 to 1,500,000 adjoint source particles might be required to obtain tight (within $\pm 5\%$ to $\pm 8\%$) statistical convergence on the energy groups (neutron and gamma-ray) contributing to the response of interest.

Analyzing the calculated dose responses over the energy range of the measured results yielded consistent comparisons between the calculated and measured responses in almost all cases. This point almost goes without saying but is important in this work since one of the purposes is to validate the MASH code system.

The differences in the computational combinatorial geometry phantom model used in the MASH analysis and the RT-200 Humanoid Phantom used in the measurements was not deemed a significant contributor to the discrepancies seen in the comparisons of the results. Absolute detector locations (especially mid-head and mid-gut) relative to the phantom geometry could contribute to some of the differences seen in the results at these locations.

In general, the calculational results show mixed agreement with the measured data. The neutron dose results indicate MASH consistently calculates more dose than was measured for both the phantom standing in the free-field and the phantom standing inside

the two-meter box. The calculation/measurement differences were typically 20% to 30% for the phantom standing in the free-field and 10% to 20% for the phantom standing inside the two-meter box. The neutron reduction factors, however, typically agreed within $\pm 20\%$ for both phantom/box geometry configurations and orientations. With respect to the gamma-ray data, there were individual discrepancies between calculations and measurements. However, typical agreement was within $\pm 20\%$. The gamma-ray free-field environment at 400 meters continues to show a discrepancy between calculation and experiment which further manifest itself through the comparisons of the gamma-ray reduction factors.

To determine the overall quality of the comparisons between MASH and the measurements, both calculational and experimental data were averaged over detector position (internal and external), response function (Tissue and CaF₂:Mn), radiation type (neutron and gamma-ray), and phantom orientation (front facing and right side toward reactor). This averaging procedure produced one set of data for the phantom in the free-field, and one set of data for the phantom inside the two-meter box. The results presented in Table 22, show overall that the calculations agreed quite well with most of the measured data supplied by the experimental teams. Generally, the agreement was within the $\pm 20\%$ limit deemed as acceptable by the DNA. Principal "trouble spots" are the internal detector locations (for neutrons) and free-field locations (for gamma-rays).

Table 22. Overall Comparisons of Calculated and Average Experimentally Measured Neutron and Gamma-Ray Dose and Reduction Factors Averaged Over External, Internal, and All Detector Locations On or Inside the RT-200 Humanoid Phantom, and Phantom Orientation Free-Field or Inside the Two-Meter Box, at the 400 Meter Test Site at the APRF.

Response	Phantom Free-Field			Phantom Inside Two-Meter Box		
	MASH	Expt	C/E	MASH	Expt	C/E
Neutron Dose (mrad(Tissue)/kWh)						
External Detector Average	3.60	2.85	1.26	2.11	1.94	1.09
Internal Detector Average	0.94	0.73	1.29	0.31	0.30	1.03
Overall Detector Average	2.84	2.24	1.27	1.59	1.47	1.08
Gamma Dose (mrad(Tissue)/kWh)						
External Detector Average	1.62	1.76	0.92	0.56	0.53	1.06
Internal Detector Average	1.90	1.94	0.98	0.83	0.72	1.15
Overall Detector Average	1.70	1.81	0.94	0.64	0.58	1.10
Gamma Dose (mrad(CaF₂:Mn)/kWh)						
External Detector Average	1.70	1.66	1.02	0.53	0.45	1.18
Internal Detector Average	2.01	1.77	1.14	0.80	0.63	1.27
Overall Detector Average	1.79	1.69	1.06	0.60	0.50	1.20
Neutron Reduction Factor						
External Detector Average	1.36	1.44	0.94	2.33	2.00	1.17
Internal Detector Average	5.21	5.68	0.92	16.2	13.1	1.24
Overall Detector Average	1.73	1.84	0.94	3.08	2.65	1.16
Gamma Reduction Factor (Tissue)						
External Detector Average	0.83	0.86	0.97	2.38	2.79	0.85
Internal Detector Average	0.70	0.79	0.89	1.60	2.06	0.78
Overall Detector Average	0.79	0.84	-	0.94	2.09	2.53
Gamma Reduction Factor (CaF₂:Mn)						
External Detector Average	0.80	0.80	1.00	2.56	2.97	0.86
Internal Detector Average	0.67	0.75	0.89	1.69	2.11	0.80
Overall Detector Average	0.76	0.78	0.97	2.23	2.66	0.84

7.0 RECOMMENDATIONS

This was the second concerted effort aimed at benchmarking the MASH code against experimental measurements and again there were some glitches in the effort. The most significant problem occurred in the reporting of the gamma-ray dose data. The calculational and experimental results must report the same data for a meaningful comparison to be made. For TLD data, all corrections to the data for spectral effects (calibration field versus radiation field), response functions [dose(Tissue) or dose(TLD)], and contributions due to thermal neutrons must be accounted for or removed from both sets of data. This will allow a true "benchmark" comparison of the MASH code system and reduce the possible sources of discrepancy to be considered.

The comparisons indicate multiple teams of experimentalists performing the same set of measurements yield a better indication of the quality of the comparison. By averaging the different sets of experimental data together, the anomalies and inconsistencies associated with any one measurement will not manifest itself in the overall comparison, yet the trends and results consistent in all of the sets of experimental data will remain. Consequently, future efforts in this series of experiments should have as a minimum, two different teams of experimentalists performing the same measurement using the same type detector system. Also, cross checking experimental results with different detector systems is still considered favorable for determining consistency in the experimental results.

The consistent discrepancy associated with the calculated and measured free-field gamma-ray data (from the Fall 1989 and Spring 1990 studies) must be addressed before the overall quality of the gamma-ray data comparisons can be improved. To resolve the discrepancy, the differences in the spectral data (Fall 1989 comparison) must be successfully addressed and reconciled. To resolve discrepancies with the comparisons on or inside the phantom, future experiments should possibly include the use of a simplified phantom model of known dimensions, simple geometric shapes, and known materials, e.g. a cylindrical water-filled lucite phantom.

This series of measurements, however, has been successful in laying the foundation for the next set of measurements which will include some duplicates of the measurements made in this series as well as measurements involving a anthropomorphic phantom standing free-field and inside the two-meter box test bed lined with 5% borated polyethylene. With adequate resolution of the concerns alluded to in this report and the Fall 1989 report, and with better communication and understanding between the analysts and experimentalists as to the needs of the other, agreement is achievable for all comparisons within the DNA mandated acceptance limit of $\pm 20\%$.

8.0 REFERENCES

1. J. O. Johnson, ed., "A User's Manual for MASH 1.0 - A Monte Carlo Adjoint Shielding Code System," ORNL/TM-11778, Oak Ridge National Laboratory, (March 1992).
2. J. O. Johnson, J. D. Drischler, and J. M. Barnes, "Analysis of the Fall-1989 Two-Meter Box Test Bed Experiments Performed at the Army Pulse Radiation Facility (APRF)," ORNL/TM-11777, Oak Ridge National Laboratory, (May 1991).
3. W. A. Rhoades and M. B. Emmett et al., "Vehicle Code System (VCS) User's Manual," ORNL/TM-4648, Oak Ridge National Laboratory, (August 1974).
4. W. A. Rhoades et al., "Development of a Code System for Determining Radiation Protection of Armored Vehicles (The VCS Code)," ORNL/TM-4664, Oak Ridge National Laboratory, (October 1974).
5. W. A. Rhoades and R. L. Childs, "The DORT Two-Dimensional Discrete Ordinates Transport Code," Nuclear Science & Engineering 99, 1, 88-89 (May 1988).
6. M. B. Emmett, "The MORSE Monte Carlo Radiation Transport Code System," ORNL/TM-4972/R2, Oak Ridge National Laboratory, (July 1984).
7. D. C. Kaul and S. D. Egbert, "Radiation Leakage From The Army Pulse Radiation Facility (APRF) Fast Reactor," SAIC-89/1423, Science Applications International Corporation, San Diego, California, (May 1989).
8. D. T. Ingersoll, R. W. Roussin, C. Y. Fu, and J. E. White, "DABL69: A Broad-Group Neutron/Photon Cross-Section Library for Defense Nuclear Applications," ORNL/TM-10568, Oak Ridge National Laboratory, (June 1989).
9. W. S. Snyder, M. R. Ford, and G. G. Warner, "Estimates of Specific Absorbed Fractions for Photon Sources Uniformly Distributed in Various Organs of a Heterogeneous Phantom," MIRD Pamphlet No. 5, New York: Society for Nuclear Medicine, (1978).
10. L. W. Bain, Jr. and M. J. Reisinger, "The GIFT Code Users Manual; Volume I, Introduction and Input Requirements," BRL Report No. 1802, ADB0060371, Ballistic Research Laboratory, (July 1975).
11. G. G. Kuehl, L. W. Bain, Jr., and M. J. Reisinger, "The GIFT Code Users Manual; Volume II, The Output Options," ARBRL-TR-02189, AD A078364, Ballistic Research Laboratory, (September 1979).

APPENDIX A

**Comparisons of the Calculated (MASH) and Measured Neutron
Dose and Reduction Factors for the Spring 1990 Two-Meter
Box Test Bed Experiments Performed at the
Army Pulse Radiation Facility (APRF).**

Table A-1

<u>MASH VS. BTI/DREO</u>						
Detector Position	Phantom Facing Reactor			Phantom Right Side Toward Reactor		
	MASH	BTI/DREO	C/E	MASH	BTI/DREO	C/E
FF ¹	4.90	4.09	1.20	4.90	4.16	1.18
DS ²	3.03 (.017)*	NM ⁺	-	3.03 (.017)	NM	-
FB ³	4.47 (.019)	3.38	1.32	3.39 (.023)	2.45	1.38
BB ⁴	1.62 (.013)	1.57	1.03	3.29 (.022)	2.10	1.57
LC ⁵	4.52 (.018)	3.67	1.23	3.17 (.020)	2.45	1.29
LW ⁶	4.35 (.019)	3.24	1.34	2.34 (.007)	1.84	1.27
RW ⁷	4.40 (.019)	4.17	1.06	4.47 (.019)	3.59	1.25
MH ⁸	1.20 (.020)	0.90	1.33	1.38 (.021)	0.81	1.70
MG ⁹	0.74 (.036)	0.69	1.07	0.44 (.038)	0.50	0.88

*Fractional Standard Deviation

+Not Measured

¹Free-Field

²Detector on Shelf in 2m Box

³Front Belt

⁴Back Belt

⁵Left Chest

⁶Left Wrist

⁷Right Wrist

⁸Mid-Head

⁹Mid-Gut

Table A-2

<u>MASH VS. BTI/DREO</u>						
<u>Phantom In 2m Box Neutron Dose (mrads(Tissue)/kWh)</u>						
Detector Position	Phantom Facing Reactor			Phantom Right Side Toward Reactor		
	MASH	BTI/DREO	C/E	MASH	BTI/DREO	C/E
FF ¹	4.90	4.27	1.15	4.90	3.57	1.37
DS ²	2.82 (.017)*	2.46	1.15	2.82 (.017)	2.52	1.12
FB ³	2.27 (.018)	1.91	1.19	1.90 (.021)	1.73	1.10
BB ⁴	1.47 (.020)	1.24	1.19	1.90 (.020)	1.68	1.13
LC ⁵	2.35 (.021)	2.33	1.01	1.91 (.019)	1.75	1.09
LW ⁶	2.45 (.018)	2.05	1.20	1.97 (.017)	1.81	1.09
RW ⁷	2.36 (.020)	2.35	1.00	2.49 (.018)	2.55	0.98
MH ⁸	0.41 (.032)	0.32	1.28	0.44 (.031)	0.43	1.02
MG ⁹	0.20 (.068)	0.25	0.80	0.16 (.084)	0.18	0.89

*Fractional Standard Deviation

¹Free-Field²Detector on Shelf in 2m Box³Front Belt⁴Back Belt⁵Left Chest⁶Left Wrist⁷Right Wrist⁸Mid-Head⁹Mid-Gut

Table A-3

MASH VS. BTI/DREO						
Detector Position	Phantom Facing Reactor			Phantom Right Side Toward Reactor		
	MASH	BTI/DREO	C/E	MASH	BTI/DREO	C/E
DS ¹	1.62	NM ⁺	-	1.62	-	-
FB ²	1.10	1.21	0.91	1.45	1.70	0.85
BB ³	3.02	2.61	1.16	1.49	1.98	0.75
LC ⁴	1.08	1.11	0.97	1.55	1.70	0.91
LW ⁵	1.13	1.26	0.90	2.09	2.26	0.92
RW ⁶	1.11	0.98	1.13	1.10	1.16	0.95
MH ⁷	4.08	4.54	0.90	3.55	5.14	0.69
MG ⁸	6.62	5.93	1.12	11.14	8.32	1.34

⁺Not Measured

¹Detector on Shelf in 2m Box

²Front Belt

³Back Belt

⁴Left Chest

⁵Left Wrist

⁶Right Wrist

⁷Mid-Head

⁸Mid-Gut

Table A-4

MASH VS. BTI/DREO						
Phantom In 2m Box Neutron Reduction Factors (mrad(Tissue)/kWh)						
Detector Position	Phantom Facing Reactor			Phantom Right Side Toward Reactor		
	MASH	BTI/DREO	C/E	MASH	BTI/DREO	C/E
DS ¹	1.74	1.74	1.00	1.74	1.42	1.23
FB ²	2.16	2.24	0.96	2.58	2.06	1.25
BB ³	3.33	3.44	0.97	2.58	2.13	1.21
LC ⁴	2.09	1.83	1.14	2.57	2.04	1.26
LW ⁵	2.00	2.08	0.96	2.48	1.97	1.26
RW ⁶	2.08	1.82	1.14	1.97	1.40	1.41
MH ⁷	11.95	13.34	0.90	11.14	8.30	1.34
MG ⁸	24.50	17.08	1.43	30.63	19.83	1.54

¹Free-Field - Detector on Shelf in 2m Box²Front Belt³Back Belt⁴Left Chest⁵Left Wrist⁶Right Wrist⁷Mid-Head⁸Mid-Gut

APPENDIX B

**Comparisons of the Calculated (MASH) and Measured Gamma-Ray
Dose and Reduction Factors for the Spring 1990 Two-Meter
Box Test Bed Experiments Performed at the Army Pulse
Radiation Facility (APRF).**

Table B-1

MASH VS. HDL						
Phantom Free-Field Gamma-Ray Dose (mrad(CaF₂:Mn)/kWh)						
Detector Position	Phantom Facing Reactor			Phantom Right Side Toward Reactor		
	MASH	HDL	C/E	MASH	HDL	C/E
FF ¹	1.36	1.33	1.02	1.36	1.31	1.04
DS ²	0.35 (.021)*	0.29	1.21	0.35 (.021)	0.30	1.17
FB ³	2.04 (.015)	2.10	0.97	1.77 (.014)	1.47	1.20
BB ⁴	1.55 (.016)	1.85	0.84	1.79 (.016)	1.44	1.24
LC ⁵	1.93 (.016)	1.90	1.02	1.66 (.014)	1.45	1.14
LW ⁶	1.58 (.013)	1.74	0.91	1.28 (.012)	1.12	1.14
RW ⁷	1.68 (.013)	1.91	0.88	1.70 (.015)	1.56	1.09
MH ⁸	2.01 (.013)	1.90	1.06	2.05 (.013)	1.70	1.21
MG ⁹	2.08 (.012)	1.91	1.09	1.88 (.011)	1.53	1.23

*Fractional Standard Deviation

¹Free-Field²Detector on Shelf in 2m Box³Front Belt⁴Back Belt⁵Left Chest⁶Left Wrist⁷Right Wrist⁸Mid-Head⁹Mid-Gut

Table B-2

MASH VS. HDL						
Phantom In 2m Box Gamma-Ray Dose (mrad(CaF₂:Mn)/kWh)						
Detector Position	Phantom Facing Reactor			Phantom Right Side Toward Reactor		
	MASH	HDL	C/E	MASH	HDL	C/E
FF ¹	1.34	1.32	1.02	1.34	1.31	1.02
DS ²	0.36 (.020)*	0.33	1.09	0.32 (.021)	0.27	1.19
FB ³	0.65 (.022)	0.49	1.33	0.56 (.021)	0.41	1.37
BB ⁴	0.60 (.020)	0.52	1.15	0.55 (.021)	0.40	1.38
LC ⁵	0.62 (.022)	0.53	1.17	0.52 (.021)	0.53	0.98
LW ⁶	0.44 (.022)	0.43	1.02	0.36 (.022)	0.38	0.95
RW ⁷	0.48 (.021)	0.47	1.02	0.46 (.023)	0.27	1.70
MH ⁸	0.88 (.022)	0.66	1.33	0.76 (.023)	0.64	1.19
MG ⁹	0.83 (.019)	0.63	1.32	0.71 (.019)	0.57	1.25

*Fractional Standard Deviation

¹Free-Field

²Detector on Shelf in 2m Box

³Front Belt

⁴Back Belt

⁵Left Chest

⁶Left Wrist

⁷Right Wrist

⁸Mid-Head

⁹Mid-Gut

Table B-3

MASH VS. HDL						
Phantom Free-Field Gamma-Ray Reduction Factors (mrad(CaF ₂ :Mn)/kWh)						
Detector Position	Phantom Facing Reactor			Phantom Right Side Toward Reactor		
	MASH	HDL	C/E	MASH	HDL	C/E
DS ¹	3.89	4.59	0.85	3.89	4.37	0.89
FB ²	0.67	0.63	1.06	0.76	0.89	0.85
BB ³	0.88	0.72	1.22	0.76	0.91	0.84
LC ⁴	0.70	0.70	1.00	0.82	0.90	0.91
LW ⁵	0.86	0.76	1.13	1.06	1.17	0.91
RW ⁶	0.81	0.70	1.16	0.80	0.84	0.95
MH ⁷	0.68	0.70	0.97	0.66	0.77	0.86
MG ⁸	0.65	0.70	0.93	0.72	0.86	0.84

¹Detector on Shelf in 2m Box²Front Belt³Back Belt⁴Left Chest⁵Left Wrist⁶Right Wrist⁷Mid-Head⁸Mid-Gut

Table B-4

<u>MASH VS. HDL</u>						
Phantom In 2m Box Gamma-Ray Reduction Factors (mrad(CaF ₂ :Mn)/kWh)						
Detector Position	Phantom Facing Reactor			Phantom Right Side Toward Reactor		
	MASH	HDL	C/E	MASH	HDL	C/E
DS ¹	3.72	4.00	0.93	4.19	4.85	0.86
FB ²	2.05	2.69	0.76	2.41	3.20	0.75
BB ³	2.24	2.54	0.88	2.44	3.28	0.74
LC ⁴	2.17	2.49	0.87	2.59	2.47	1.05
LW ⁵	3.05	3.07	0.99	3.69	3.45	1.07
RW ⁶	2.77	2.81	0.99	2.92	4.85	0.60
MH ⁷	1.53	2.00	0.77	1.76	2.05	0.86
MG ⁸	1.62	2.10	0.77	1.88	2.30	0.82

¹Detector on Shelf in 2m Box²Front Belt³Back Belt⁴Left Chest⁵Left Wrist⁶Right Wrist⁷Mid-Head⁸Mid-Gut

Table B-5

<u>MASH VS. APRF</u>						
<u>Phantom Free-Field Gamma-Ray Dose (mrad(Tissue)/kWh)</u>						
Detector Position	Phantom Facing Reactor			Phantom Right Side Toward Reactor		
	MASH	APRF	C/E	MASH	APRF	C/E
FF ¹	1.34	1.70	0.79	1.34	1.72	0.78
DS ²	0.38 (.020)*	0.31	1.23	0.38 (.020)	0.32	1.19
FB ³	1.93 (.017)	2.08	0.93	1.68 (.015)	1.90	0.88
BB ⁴	1.48 (.018)	1.68	0.88	1.72 (.017)	1.91	0.90
LC ⁵	1.84 (.018)	2.08	0.88	1.58 (.016)	1.97	0.80
LW ⁶	1.51 (.015)	1.83	0.83	1.19 (.014)	1.31	0.91
RW ⁷	1.61 (.015)	1.95	0.83	1.63 (.017)	1.84	0.89
MH ⁸	1.93 (.015)	2.15	0.90	1.98 (.014)	2.29	0.86
MG ⁹	1.92 (.013)	2.14	0.90	1.73 (.013)	2.00	0.87

*Fractional Standard Deviation

¹Free-Field²Detector on Shelf in 2m Box³Front Belt⁴Back Belt⁵Left Chest⁶Left Wrist⁷Right Wrist⁸Mid-Head⁹Mid-Gut

Table B-6

MASH VS. APRF						
Phantom In 2m Box Gamma-Ray Dose (mrads(Tissue)/kWh)						
Detector Position	Phantom Facing Reactor			Phantom Right Side Toward Reactor		
	MASH	APRF	C/E	MASH	APRF	C/E
FF ¹	1.33	1.69	0.79	1.32	1.71	0.77
DS ²	0.38 (.020)*	0.39	0.97	0.35 (.021)	0.33	1.06
FB ³	0.69 (.022)	0.61	1.13	0.58 (.021)	0.49	1.18
BB ⁴	0.63 (.020)	0.56	1.13	0.58 (.021)	0.52	1.12
LC ⁵	0.66 (.022)	0.59	1.12	0.55 (.021)	0.49	1.12
LW ⁶	0.47 (.022)	0.49	0.96	0.39 (.022)	0.37	1.05
RW ⁷	0.52 (.021)	0.52	1.00	0.49 (.023)	0.45	1.09
MH ⁸	0.93 (.022)	0.91	1.02	0.81 (.023)	0.74	1.09
MG ⁹	0.85 (.020)	0.79	1.08	0.73 (.020)	0.72	1.01

*Fractional Standard Deviation

¹Free-Field

²Detector on Shelf in 2m Box

³Front Belt

⁴Back Belt

⁵Left Chest

⁶Left Wrist

⁷Right Wrist

⁸Mid-Head

⁹Mid-Gut

Table B-7

<u>MASH VS. APRF</u>						
Phantom Free-Field Gamma-Ray Reduction Factors (mrad(Tissue)/kWh)						
Detector Position	Phantom Facing Reactor			Phantom Right Side Toward Reactor		
	MASH	APRF	C/E	MASH	APRF	C/E
DS ¹	3.53	5.48	0.64	3.53	5.38	0.66
FB ²	0.69	0.82	0.84	0.80	0.91	0.88
BB ³	0.91	1.01	0.90	0.78	0.90	0.87
LC ⁴	0.73	0.82	0.89	0.85	0.87	0.98
LW ⁵	0.88	0.93	0.95	1.12	1.31	0.85
RW ⁶	0.83	0.87	0.95	0.82	0.93	0.88
MH ⁷	0.69	0.79	0.87	0.68	0.75	0.91
MG ⁸	0.70	0.79	0.89	0.77	0.86	0.90

¹Detector on Shelf in 2m Box²Front Belt³Back Belt⁴Left Chest⁵Left Wrist⁶Right Wrist⁷Mid-Head⁸Mid-Gut

Table B-8

MASH VS. APRF						
Phantom In 2m Box Gamma-Ray Reduction Factors (mrad(Tissue)/kWh)						
Detector Position	Phantom Facing Reactor			Phantom Right Side Toward Reactor		
	MASH	APRF	C/E	MASH	APRF	C/E
DS ¹	3.50	4.33	0.81	3.77	5.18	0.73
FB ²	1.94	2.77	0.70	2.26	3.49	0.65
BB ³	2.10	3.02	0.70	2.26	3.29	0.69
LC ⁴	2.01	2.86	0.70	2.39	3.49	0.68
LW ⁵	2.81	3.45	0.81	3.38	4.62	0.73
RW ⁶	2.58	3.25	0.79	2.70	3.80	0.71
MH ⁷	1.43	1.86	0.77	1.64	2.31	0.71
MG ⁸	1.56	2.14	0.73	1.80	2.38	0.76

¹Detector on Shelf in 2m Box

²Front Belt

³Back Belt

⁴Left Chest

⁵Left Wrist

⁶Right Wrist

⁷Mid-Head

⁸Mid-Gut

Table B-9

MASH VS. BTI						
Phantom Free-Field Gamma-Ray Dose (mrad(Tissue)/kWh)						
Detector Position	Phantom Facing Reactor			Phantom Right Side Toward Reactor		
	MASH	BTI	C/E	MASH	BTI	C/E
FF ¹	1.34	1.24	1.08	1.34	1.37	0.98
DS ²	0.38 (.020)*	NM ⁺	-	0.38 (.020)	NM	-
FB ³	1.93 (.017)	1.76	1.10	1.68 (.015)	1.55	1.08
BB ⁴	1.48 (.018)	1.29	1.15	1.72 (.017)	1.68	1.02
LC ⁵	1.84 (.018)	1.77	1.04	1.58 (.016)	1.63	0.97
LW ⁶	1.51 (.015)	1.42	1.06	1.19 (.014)	1.40	0.85
RW ⁷	1.61 (.015)	1.54	1.05	1.63 (.017)	1.58	1.03
MH ⁸	1.93 (.015)	1.81	1.07	1.98 (.014)	1.68	1.18
MG ⁹	1.92 (.013)	1.54	1.25	1.73 (.013)	1.37	1.26

^{*}Fractional Standard Deviation[†]Not Measured¹Free-Field²Detector on Shelf in 2m Box³Front Belt⁴Back Belt⁵Left Chest⁶Left Wrist⁷Right Wrist⁸Mid-Head⁹Mid-Gut

Table B-10

<u>MASH VS. BTI</u>						
Phantom In 2m Box Gamma-Ray Dose (mrads(Tissue)/kWh)						
Detector Position	Phantom Facing Reactor			Phantom Right Side Toward Reactor		
	MASH	BTI	C/E	MASH	BTI	C/E
FF ¹	1.33	1.37	0.97	1.32	1.32	1.00
DS ²	0.38 (.020)*	0.42	0.90	0.35 (.021)	0.33	1.06
FB ³	0.69 (.022)	0.64	1.08	0.58 (.021)	0.52	1.12
BB ⁴	0.63 (.020)	0.66	0.95	0.58 (.021)	0.50	1.16
LC ⁵	0.66 (.022)	0.71	0.93	0.55 (.021)	0.59	0.93
LW ⁶	0.47 (.022)	0.72	0.65	0.39 (.022)	0.39	1.00
RW ⁷	0.52 (.021)	0.49	1.06	0.49 (.023)	0.44	1.11
MH ⁸	0.93 (.022)	0.81	1.15	0.81 (.023)	0.70	1.16
MG ⁹	0.85 (.020)	0.64	1.33	0.73 (.020)	0.56	1.30

*Fractional Standard Deviation

¹Free-Field

²Detector on Shelf in 2m Box

³Front Belt

⁴Back Belt

⁵Left Chest

⁶Left Wrist

⁷Right Wrist

⁸Mid-Head

⁹Mid-Gut

Table B-11

MASH VS. BTI						
Phantom Free-Field Gamma-Ray Reduction Factors (mrad(Tissue)/kWh)						
Detector Position	Phantom Facing Reactor			Phantom Right Side Toward Reactor		
	MASH	BTI	C/E	MASH	BTI	C/E
DS ¹	3.53	NM ⁺	-	3.53	NM	-
FB ²	0.69	0.70	0.99	0.80	0.88	0.91
BB ³	0.91	0.96	0.95	0.78	0.82	0.95
LC ⁴	0.73	0.70	1.04	0.85	0.84	1.01
LW ⁵	0.88	0.87	1.01	1.12	0.98	1.14
RW ⁶	0.83	0.81	1.02	0.82	0.87	0.94
MH ⁷	0.69	0.69	1.00	0.68	0.82	0.83
MG ⁸	0.70	0.81	0.86	0.77	1.00	0.77

*Not Measured

¹Detector on Shelf in 2m Box

²Front Belt

³Back Belt

⁴Left Chest

⁵Left Wrist

⁶Right Wrist

⁷Mid-Head

⁸Mid-Gut

Table B-12

MASH VS. BTI						
Phantom In 2m Box Gamma-Ray Reduction Factors (mrad(Tissue)/kWh)						
Detector Position	Phantom Facing Reactor			Phantom Right Side Toward Reactor		
	MASH	BTI	C/E	MASH	BTI	C/E
DS ¹	3.50	3.26	1.07	3.77	4.00	0.94
FB ²	1.94	2.14	0.91	2.26	2.54	0.89
BB ³	2.10	2.08	1.01	2.26	2.64	0.86
LC ⁴	2.01	1.93	1.04	2.39	2.24	1.07
LW ⁵	2.81	1.90	1.48	3.38	3.38	1.00
RW ⁶	2.58	2.80	0.92	2.70	3.00	0.90
MH ⁷	1.43	1.69	0.85	1.64	1.89	0.87
MG ⁸	1.56	2.14	0.73	1.80	2.36	0.76

¹Detector on Shelf in 2m Box

²Front Belt

³Back Belt

⁴Left Chest

⁵Left Wrist

⁶Right Wrist

⁷Mid-Head

⁸Mid-Gut

Table B-13

MASH VS. DREO						
Phantom Gamma-Ray Dose (mrad(Tissue)/kWh)						
Detector Position	Phantom Free-Field Facing Reactor			Phantom In 2m Box Right Side Toward Reactor		
	MASH	DREO	C/E	MASH	DREO	C/E
FF ¹	1.34	1.30	1.03	1.32	1.38	0.96
DS ²	0.38 (.020)*	NM ⁺	-	0.35 (.021)	0.39	0.90
FB ³	1.93 (.017)	1.85	1.04	0.58 (.021)	0.54	1.07
BB ⁴	1.48 (.018)	1.35	1.10	0.58 (.021)	0.52	1.12
LC ⁵	1.84 (.018)	1.74	1.06	0.55 (.021)	0.52	1.06
LW ⁶	1.51 (.015)	1.49	1.01	0.39 (.022)	0.40	0.98
RW ⁷	1.61 (.015)	1.62	0.99	0.49 (.023)	0.46	1.07
MH ⁸	1.93 (.015)	1.91	1.01	0.81 (.023)	0.73	1.11
MG ⁹	1.92 (.013)	1.74	1.10	0.73 (.020)	0.63	1.16

^{*}Fractional Standard Deviation⁺Not Measured¹Free-Field²Detector on Shelf in 2m Box³Front Belt⁴Back Belt⁵Left Chest⁶Left Wrist⁷Right Wrist⁸Mid-Head⁹Mid-Gut

Table B-14

MASH VS. DREO						
Phantom Free-Field Gamma-Ray Reduction Factors (mrad(Tissue)/kWh)						
Detector Position	Phantom Facing Reactor			Phantom Right Side Toward Reactor		
	MASH	DREO	C/E	MASH	DREO	C/E
DS ¹	3.53	NM ⁺	-	3.77	NM	-
FB ²	0.69	0.70	0.99	0.80	0.83	0.96
BB ³	0.91	0.96	0.95	0.78	0.92	0.85
LC ⁴	0.73	0.75	0.97	0.85	0.85	1.00
LW ⁵	0.88	0.87	1.01	1.12	1.06	1.06
RW ⁶	0.83	0.80	1.04	0.82	0.77	1.06
MH ⁷	0.69	0.68	1.01	0.68	0.77	0.88
MG ⁸	0.70	0.75	0.93	0.77	0.85	0.91

⁺Not Measured

¹Detector on Shelf in 2m Box

²Front Belt

³Back Belt

⁴Left Chest

⁵Left Wrist

⁶Right Wrist

⁷Mid-Head

⁸Mid-Gut

Table B-15

MASH VS. DREO						
Phantom In 2m Box Gamma-Ray Reduction Factors (mrad(Tissue)/kWh)						
Detector Position	Phantom Facing Reactor			Phantom Right Side Toward Reactor		
	MASH	DREO	C/E	MASH	DREO	C/E
DS ¹	3.50	NM ⁺	-	3.77	3.54	1.06
FB ²	1.94	NM	-	2.26	2.56	0.88
BB ³	2.10	NM	-	2.26	2.65	0.85
LC ⁴	2.01	NM	-	2.39	2.65	0.90
LW ⁵	2.81	NM	-	3.38	3.45	0.98
RW ⁶	2.58	NM	-	2.70	3.00	0.90
MH ⁷	1.43	NM	-	1.64	1.89	0.87
MG ⁸	1.56	NM	-	1.80	2.19	0.82

⁺Not Measured

¹Detector on Shelf in 2m Box

²Front Belt

³Back Belt

⁴Left Chest

⁵Left Wrist

⁶Right Wrist

⁷Mid-Head

⁸Mid-Gut

Table B-16

MASH VS. ETCA						
Detector Position	Gamma-Ray Dose Phantom Facing Reactor			Gamma-Ray Reduction Factors Phantom Facing Reactor		
	MASH	ETCA	C/E	MASH	ETCA	C/E
FF ¹	1.34	1.83	0.73	-	-	-
DS ²	0.38 (.020)*	NM ⁺	-	3.53	NM	-
FB ³	1.93 (.017)	2.29	0.84	0.69	0.80	0.86
BB ⁴	1.48 (.018)	1.85	0.80	0.91	0.99	0.92
LC ⁵	1.84 (.018)	2.23	0.83	0.73	0.82	0.89
LW ⁶	1.51 (.015)	2.04	0.74	0.88	0.90	0.98
RW ⁷	1.61 (.015)	2.12	0.76	0.83	0.86	0.97
MH ⁸	1.93 (.015)	3.17	0.61	0.69	0.58	1.19
MG ⁹	1.92 (.013)	2.41	0.80	0.70	0.76	0.92

*Fractional Standard Deviation

+Not Measured

¹Free-Field

²Detector on Shelf in 2m Box

³Front Belt

⁴Back Belt

⁵Left Chest

⁶Left Wrist

⁷Right Wrist

⁸Mid-Head

⁹Mid-Gut

APPENDIX C

Sample Input Decks for GIP, GRTUNCL, DORT, VISTA, XCHEKER,
MORSE, and DRC Used in the MASH Analysis of the Spring 1990
Two-Meter Box Test Bed Experiments Performed at the Army
Pulse Radiation Facility (APRF).

```

gip mixtures for the 5/90 two meter box experiments -- p5 forward

1$$ 69 3 4 72 612 /igm,iht,ihm,ms
    0 144 210 0 5 /mcr,mtp,mtm,ith,isct
    1 2 2 120 /iprt,iout,idot,nbuf
e t

10$$ 4i145 150 19q6 4i151 156 10q6 4i157 162 3q6 4i163 168 5q6
/     aprf ground borated concrete      air          1020 steel

        4i169 174 19q6 4i175 180 19q6 4i181 186 3q6 4i187 192 3q6
/     aprf ground     aprf ground      air          air

        4i193 198 3q6 4i199 204 3q6 4i205 210 4q6
/     air           air           hydraulic oil

11$$  58i1 60 10i67 78 40i85 126 4i139 144 / aprf ground

16i1 18 4i31 36 16i43 60 4i91 96
4i103 108 10i127 138 / borated concrete

4i1 6 10i25 36 4i79 84 / air

4i19 24 16i55 72 10i97 108 / 1020 steel

58i1 60 10i67 78 40i85 126 4i139 144 / aprf ground

58i1 60 10i67 78 40i85 126 4i139 144 / aprf ground

4i1 6 10i25 36 4i79 84 / air

4i1 6 4i19 24 4i31 36 4i61 66 4i73 78 / hydraulic oil

12** /number densities (atoms/b-cm)
6r4.802-02 6r8.860-09 6r3.244-08 6r3.489-04
6r4.392-05 6r4.304-02 6r1.319-04 6r8.435-05
6r1.272-03 6r8.794-03 6r3.337-06 6r3.269-06
6r1.893-04 6r2.403-05 6r6.654-06 6r2.970-04
6r2.572-07 6r2.582-07 6r4.490-07 6r6.761-08 /aprft ground-39% h2o

```

Figure C-1. Sample GIP Input for the MASH Analysis of the APRF Spring 1990 Two-Meter Box Test Bed Experiments.

6r7.020-03	6r2.887-04	6rl.168-03	6r5.908-02	
6rl.659-03	6r4.656-03	6rl.080-02	6r3.436-03	
6rl.431-03	6r7.667-04	6r6.709-04		/borated concrete
6r7.011-07	6r3.833-05	6rl.063-05	6r2.292-07	/air-ss90-130 051490
6r8.078-04	6r4.213-04	6r6.113-05	6r7.381-05	
6r3.877-04	6r8.391-02			/1020 steel
6r4.010-02	6r9.877-09	6r3.616-08	6r3.889-04	
6r4.896-05	6r4.127-02	6rl.470-04	6r9.403-05	
6rl.418-03	6r9.803-03	6r3.720-06	6r3.645-06	
6r2.110-04	6r2.678-05	6r7.418-06	6r3.310-04	
6r2.867-07	6r2.878-07	6r5.006-07	6r7.537-08	/apr ground-32% h2o
6r5.480-02	6r7.989-09	6r2.925-08	6r3.146-04	
6r3.960-05	6r4.456-02	6rl.189-04	6r7.605-05	
6rl.147-03	6r7.929-03	6r3.009-06	6r2.948-06	
6rl.706-04	6r2.166-05	6r6.000-06	6r2.677-04	
6r2.319-07	6r2.328-07	6r4.049-07	6r6.096-08	/apr ground-45% h2o
6r3.560-07	6r3.952-05	6rl.078-05	6r2.364-07	/air-ss90-127 051190
6r6.033-07	6r3.804-05	6rl.051-05	6r2.275-07	/air-ss90-118 050890
6r8.511-07	6r3.798-05	6rl.062-05	6r2.272-07	/air-ss90-124 050990
6rl.081-06	6r3.804-05	6rl.075-05	6r2.275-07	/air-ss90-136 051690
6r2.145-02	6r2.600-02	6r2.600-03	6r6.499-04	
6r3.901-03				/hydraulic oil
13\$	1 2 3 4 5 6 43 44 45 46 47 48 49 50 51 52 53 54 55 56 57 58 59 60 61 62 63 64 65 66 67 68 69 70 71 72 79 80 81 82 83 84 85 86 87 88 89 90 91 92 93 94 95 96 97 98 99 100 101 102 103 104 105 106 107 108 109 110 111 112 113 114 115 116 117 118 119 120 121 122 123 124 125 126 127 128 129 130 131 132 133 134 135 136 137 138 157 158 159 160 161 162 163 164 165 166 167 168 169 170 171 172 173 174 175 176 177 178 179 180 181 182 183 184 185 186 199 200 201 202 203 204 205 206 207 208 209 210 223 224 225 226 227 228 / h,b10,b11,c,n,o,na,mg,al,si,p,s,cl,ar,k,ca,mn,fe,co,ni,cu,zr,nb,sn			

t

Figure C-1. (continued)

```

' grtuncl - aprf aog, 5/90 2m box expt., saic 1990 leakage source
' 16.143m source height, simple topography out to 1080m test site
' 32% ground moisture, ss90-127 5/14/90 air parameters, s90e5.

1$$ 0 5 8 123 146 / ith,isct,izm,im,jm
   69 3 4 72 0 / igm,iht,ihm,ms
   0 66 66 2 0 / mcr,mtp,mt,idatl,noa
   4 1 0 23 2 / imode,iprte,nflsv,npso,iprtf
   0 40 0 2000 0 / iprts,iz3,idfac,nbuf,ntnpr

2** 0 1614.3 0 / xnf,zpt,rpt
t
1** f0 /fission spectrum

2** /axii (jm+1)
-80 -75 -70 -65 -60 -55 -50 -45 -40 -35 -30 -25 -20 -15 -10 -5 -2.5
-1 0 50 150 250 350 450 550 700 950 1100 1220 1311 1381 1435 1476
1508 1532 1551 1566 1577 1585 1592 1597 1601 1604 1607 1608.5 1610
1614.3 1619 1620.5 1622 1624 1627 1631 1636 1643 1651 1662 1677 1696
1720 1752 1793 1847 1917 2008 2126 2279 2479 2739 3076 3514 4085 4826
5789 7042 8670 10787 13000 15500 18000 20500 23000 25500 28000 30500
33000 35500 38000 40500 43000 45500 48000 50500 53000 55500 58000
60500 63000 65500 68000 70500 73000 75500 78000 80500 83000 85500
88000 90500 93000 95500 98000 100500 103000 106000 109000 112000
115000 118000 121000 124000 127000 130000 133000 136000 139000 142000
145000 148000 151000 154000 157000 160000 163000 166000 169000 172000
175000 178000 181000 184000 187000 190000 193000 196000 199000 201000

4** /radii (im+1)
0 4.6 6 7.8 10 13 17 22 29 37 48 63 82 106 138 179 233 303 394 512 665
865 1125 1462 1900 2471 3212 4175 5428 7056 9000 11000 13000 15000
16500 17500 19000 21000 23000 25000 27000 28500 29500 30500 31500
33000 35000 37000 38500 39500 40500 41500 43000 45000 47000 49000
51000 53000 55000 57000 59000 61000 63000 65000 67000 69000 71000
73000 75000 77000 79000 81000 83000 85000 87000 89000 91000 93000
95000 97000 99000 101000 103000 105000 106500 107500 108500 109500
111000 113000 115000 117000 119000 121000 123000 125000 127000 129000
131000 133000 135000 137000 139000 142000 145000 148000 151000 154000
157000 160000 163000 166000 169000 172000 175000 178000 181000 184000
187000 190000 193000 196000 199000 201000

8$$ / zone numbers by interval
' zones 1, 2, & 3-aprf ground, 4 & 5-borated concrete, 6, 7, & 8-air
123rl 8ql23 /j-ints 1-9
19r5 104rl 2ql23 /j-ints 10-12
19r4 3r3 10rl 3 3r2 3 3rl 3 3r2 3 2rl 3 3r2 3 3lrl
   3 3r2 3 35rl 5ql23 /j-ints 13-18

```

Figure C-2. Sample GRTUNCL Input for the MASH Analysis of the APRF Spring 1990 Two-Meter Box Test Bed Experiments.

```

33r7 3r6 5r7 3r6 4r7 3r6 33r7 3r6 5r7 31r8 4q123 /j-ints 19-23
92r7 31r8 51q123 /j-ints 24-75
123r8 70q123 /j-ints 76-146

```

```

9$$ 3r-25 2r-7 3r-37 / mat by zone

```

```

13** / angular directions of source (-1. is down +1. is up)
-.99794 -.98973 -.97337 -.94900 -.91680 -.88117 -.84355 -.80122
-.75441 -.70316 -.64809 -.58978 -.52822 -.46383 -.39684 -.32761
-.25670 -.18443 -.11105 -.03705+.03705+.11105+.18443+.25670
+.32761+.39684+.46383+.52822+.58978+.64809+.70316+.75441
+.80122+.84355+.88117+.91680+.94900+.97337+.98973+.99794

```

```

14**

```

```

' aprf angular leakage source (includes 1 hour delayed gamma source)
' s(angle,energy) 40 angles given in 13** card 69 energies are dab169
' units are 4*pi*particles/steradian per leaking neutron (7-1-90)
1.45e-06 1.48e-06 1.69e-06 1.91e-06 2.09e-06 2.45e-06 2.55e-06 2.66e-06
2.73e-06 2.80e-06 2.77e-06 2.82e-06 2.88e-06 2.91e-06 2.95e-06 3.05e-06
3.07e-06 3.11e-06 3.11e-06 3.11e-06 3.11e-06 3.09e-06 3.09e-06 3.05e-06
3.04e-06 2.96e-06 2.95e-06 2.93e-06 2.89e-06 2.88e-06 2.93e-06 2.86e-06
2.71e-06 2.41e-06 2.04e-06 1.48e-06 1.50e-06 1.63e-06 1.80e-06 1.91e-06
5.32e-06 5.36e-06 6.22e-06 7.11e-06 7.84e-06 9.34e-06 9.86e-06 1.03e-05
1.06e-05 1.09e-05 1.08e-05 1.11e-05 1.13e-05 1.15e-05 1.17e-05 1.21e-05
1.22e-05 1.23e-05 1.23e-05 1.23e-05 1.23e-05 1.23e-05 1.22e-05 1.21e-05
1.20e-05 1.17e-05 1.16e-05 1.15e-05 1.14e-05 1.13e-05 1.15e-05 1.12e-05
1.05e-05 9.23e-06 7.64e-06 5.36e-06 5.45e-06 5.95e-06 6.66e-06 7.11e-06
6.32e-06 6.41e-06 7.41e-06 8.39e-06 9.23e-06 1.09e-05 1.15e-05 1.20e-05
1.23e-05 1.27e-05 1.25e-05 1.28e-05 1.30e-05 1.32e-05 1.34e-05 1.38e-05
1.40e-05 1.41e-05 1.41e-05 1.41e-05 1.41e-05 1.41e-05 1.40e-05 1.39e-05
1.38e-05 1.34e-05 1.34e-05 1.33e-05 1.32e-05 1.31e-05 1.33e-05 1.30e-05
1.22e-05 1.07e-05 8.97e-06 6.36e-06 6.50e-06 7.09e-06 7.91e-06 8.39e-06
4.61e-06 4.66e-06 5.39e-06 6.13e-06 6.73e-06 7.97e-06 8.39e-06 8.73e-06
9.02e-06 9.25e-06 9.14e-06 9.32e-06 9.50e-06 9.66e-06 9.79e-06 1.01e-05
1.02e-05 1.03e-05 1.03e-05 1.03e-05 1.03e-05 1.03e-05 1.02e-05 1.01e-05
1.01e-05 9.82e-06 9.75e-06 9.70e-06 9.63e-06 9.56e-06 9.68e-06 9.47e-06
8.89e-06 7.84e-06 6.52e-06 4.61e-06 4.72e-06 5.16e-06 5.75e-06 6.11e-06
3.55e-05 3.59e-05 4.16e-05 4.72e-05 5.20e-05 6.14e-05 6.48e-05 6.75e-05
6.97e-05 7.14e-05 7.07e-05 7.22e-05 7.34e-05 7.47e-05 7.57e-05 7.82e-05
7.89e-05 7.95e-05 7.98e-05 7.98e-05 7.97e-05 7.95e-05 7.91e-05 7.86e-05
7.79e-05 7.61e-05 7.55e-05 7.50e-05 7.43e-05 7.38e-05 7.48e-05 7.30e-05
6.86e-05 6.04e-05 5.02e-05 3.54e-05 3.63e-05 3.95e-05 4.41e-05 4.70e-05
1.38e-05 1.38e-05 1.61e-05 1.84e-05 2.04e-05 2.43e-05 2.57e-05 2.70e-05
2.79e-05 2.86e-05 2.84e-05 2.89e-05 2.95e-05 3.00e-05 3.05e-05 3.14e-05
3.18e-05 3.21e-05 3.21e-05 3.23e-05 3.21e-05 3.21e-05 3.20e-05 3.18e-05
3.14e-05 3.07e-05 3.04e-05 3.02e-05 3.00e-05 2.96e-05 3.02e-05 2.93e-05
2.75e-05 2.41e-05 1.98e-05 1.36e-05 1.40e-05 1.54e-05 1.74e-05 1.86e-05
1.03e-04 1.04e-04 1.21e-04 1.39e-04 1.53e-04 1.84e-04 1.93e-04 2.02e-04

```

Figure C-2. (continued)

2.09e-04	2.14e-04	2.13e-04	2.16e-04	2.21e-04	2.25e-04	2.29e-04	2.36e-04
2.38e-04	2.39e-04	2.41e-04	2.41e-04	2.41e-04	2.39e-04	2.39e-04	2.38e-04
2.36e-04	2.29e-04	2.27e-04	2.27e-04	2.25e-04	2.23e-04	2.25e-04	2.20e-04
2.05e-04	1.80e-04	1.48e-04	1.02e-04	1.05e-04	1.16e-04	1.31e-04	1.39e-04
2.20e-04	2.20e-04	2.57e-04	2.95e-04	3.27e-04	3.93e-04	4.16e-04	4.34e-04
4.50e-04	4.63e-04	4.57e-04	4.68e-04	4.77e-04	4.84e-04	4.91e-04	5.07e-04
5.13e-04	5.16e-04	5.20e-04	5.20e-04	5.18e-04	5.16e-04	5.14e-04	5.11e-04
5.07e-04	4.95e-04	4.91e-04	4.88e-04	4.84e-04	4.80e-04	4.88e-04	4.75e-04
4.43e-04	3.86e-04	3.16e-04	2.14e-04	2.21e-04	2.46e-04	2.77e-04	2.96e-04
4.16e-04	4.16e-04	4.88e-04	5.63e-04	6.25e-04	7.54e-04	8.00e-04	8.36e-04
8.66e-04	8.91e-04	8.82e-04	9.02e-04	9.20e-04	9.36e-04	9.50e-04	9.82e-04
9.91e-04	9.98e-04	1.00e-03	1.00e-03	1.00e-03	1.00e-03	9.95e-04	9.88e-04
9.81e-04	9.56e-04	9.48e-04	9.43e-04	9.36e-04	9.29e-04	9.41e-04	9.16e-04
8.55e-04	7.41e-04	6.02e-04	4.05e-04	4.20e-04	4.66e-04	5.27e-04	5.63e-04
7.30e-04	7.30e-04	8.59e-04	9.93e-04	1.11e-03	1.34e-03	1.42e-03	1.49e-03
1.54e-03	1.59e-03	1.58e-03	1.61e-03	1.64e-03	1.67e-03	1.70e-03	1.76e-03
1.77e-03	1.79e-03	1.79e-03	1.80e-03	1.79e-03	1.79e-03	1.78e-03	1.77e-03
1.75e-03	1.71e-03	1.70e-03	1.69e-03	1.68e-03	1.66e-03	1.68e-03	1.64e-03
1.52e-03	1.32e-03	1.06e-03	7.09e-04	7.36e-04	8.18e-04	9.23e-04	9.89e-04
1.18e-03	1.18e-03	1.38e-03	1.60e-03	1.80e-03	2.18e-03	2.32e-03	2.43e-03
2.54e-03	2.61e-03	2.59e-03	2.64e-03	2.70e-03	2.75e-03	2.80e-03	2.89e-03
2.91e-03	2.95e-03	2.95e-03	2.96e-03	2.95e-03	2.95e-03	2.93e-03	2.91e-03
2.89e-03	2.82e-03	2.80e-03	2.77e-03	2.75e-03	2.73e-03	2.77e-03	2.68e-03
2.48e-03	2.14e-03	1.72e-03	1.13e-03	1.18e-03	1.31e-03	1.48e-03	1.59e-03
2.91e-03	2.89e-03	3.43e-03	4.00e-03	4.50e-03	5.52e-03	5.88e-03	6.18e-03
6.45e-03	6.66e-03	6.61e-03	6.77e-03	6.91e-03	7.04e-03	7.16e-03	7.41e-03
7.48e-03	7.54e-03	7.57e-03	7.57e-03	7.57e-03	7.55e-03	7.50e-03	7.45e-03
7.39e-03	7.22e-03	7.16e-03	7.11e-03	7.05e-03	6.98e-03	7.04e-03	6.82e-03
6.30e-03	5.39e-03	4.32e-03	2.79e-03	2.89e-03	3.23e-03	3.64e-03	3.91e-03
8.79e-03	8.79e-03	1.04e-02	1.22e-02	1.38e-02	1.70e-02	1.82e-02	1.93e-02
2.02e-02	2.09e-02	2.07e-02	2.13e-02	2.18e-02	2.21e-02	2.25e-02	2.34e-02
2.36e-02	2.38e-02	2.39e-02	2.39e-02	2.39e-02	2.38e-02	2.38e-02	2.36e-02
2.34e-02	2.27e-02	2.25e-02	2.23e-02	2.21e-02	2.20e-02	2.20e-02	2.13e-02
1.96e-02	1.67e-02	1.32e-02	8.43e-03	8.73e-03	9.70e-03	1.09e-02	1.17e-02
2.46e-03	2.46e-03	2.93e-03	3.43e-03	3.91e-03	4.82e-03	5.18e-03	5.47e-03
5.72e-03	5.93e-03	5.91e-03	6.07e-03	6.22e-03	6.34e-03	6.45e-03	6.68e-03
6.75e-03	6.79e-03	6.82e-03	6.82e-03	6.82e-03	6.80e-03	6.77e-03	6.73e-03
6.68e-03	6.50e-03	6.45e-03	6.39e-03	6.34e-03	6.25e-03	6.29e-03	6.07e-03
5.57e-03	4.72e-03	3.73e-03	2.36e-03	2.43e-03	2.70e-03	3.04e-03	3.25e-03
9.02e-03	9.00e-03	1.07e-02	1.26e-02	1.43e-02	1.76e-02	1.89e-02	2.00e-02
2.11e-02	2.18e-02	2.18e-02	2.23e-02	2.29e-02	2.34e-02	2.38e-02	2.46e-02
2.50e-02	2.52e-02	2.52e-02	2.52e-02	2.52e-02	2.52e-02	2.50e-02	2.48e-02
2.46e-02	2.41e-02	2.38e-02	2.36e-02	2.34e-02	2.30e-02	2.30e-02	2.23e-02
2.04e-02	1.72e-02	1.36e-02	8.55e-03	8.82e-03	9.75e-03	1.10e-02	1.18e-02
2.64e-02	2.64e-02	3.13e-02	3.66e-02	4.16e-02	5.11e-02	5.48e-02	5.80e-02
6.07e-02	6.30e-02	6.30e-02	6.48e-02	6.64e-02	6.79e-02	6.89e-02	7.13e-02
7.22e-02	7.25e-02	7.29e-02	7.29e-02	7.27e-02	7.27e-02	7.23e-02	7.18e-02
7.13e-02	6.95e-02	6.89e-02	6.82e-02	6.73e-02	6.63e-02	6.64e-02	6.39e-02

Figure C-2. (continued)

5.86e-02	4.97e-02	3.95e-02	2.50e-02	2.55e-02	2.80e-02	3.13e-02	3.34e-02
2.84e-02	2.86e-02	3.36e-02	3.91e-02	4.41e-02	5.39e-02	5.79e-02	6.11e-02
6.39e-02	6.64e-02	6.64e-02	6.82e-02	6.98e-02	7.13e-02	7.23e-02	7.47e-02
7.54e-02	7.59e-02	7.61e-02	7.59e-02	7.59e-02	7.57e-02	7.55e-02	7.52e-02
7.47e-02	7.29e-02	7.22e-02	7.14e-02	7.05e-02	6.97e-02	6.97e-02	6.70e-02
6.13e-02	5.18e-02	4.14e-02	2.64e-02	2.70e-02	2.93e-02	3.23e-02	3.46e-02
4.79e-03	4.86e-03	5.64e-03	6.52e-03	7.30e-03	8.80e-03	9.41e-03	9.91e-03
1.03e-02	1.07e-02	1.07e-02	1.09e-02	1.12e-02	1.14e-02	1.15e-02	1.19e-02
1.20e-02	1.21e-02	1.21e-02	1.21e-02	1.20e-02	1.20e-02	1.20e-02	1.19e-02
1.19e-02	1.16e-02	1.15e-02	1.14e-02	1.13e-02	1.11e-02	1.12e-02	1.08e-02
9.89e-03	8.45e-03	6.88e-03	4.55e-03	4.63e-03	4.95e-03	5.41e-03	5.75e-03
3.54e-02	3.59e-02	4.18e-02	4.80e-02	5.39e-02	6.48e-02	6.91e-02	7.29e-02
7.59e-02	7.86e-02	7.86e-02	8.05e-02	8.22e-02	8.36e-02	8.48e-02	8.75e-02
8.82e-02	8.86e-02	8.88e-02	8.84e-02	8.84e-02	8.84e-02	8.82e-02	8.77e-02
8.73e-02	8.52e-02	8.47e-02	8.38e-02	8.29e-02	8.16e-02	8.18e-02	7.89e-02
7.23e-02	6.18e-02	5.04e-02	3.34e-02	3.38e-02	3.61e-02	3.93e-02	4.16e-02
4.27e-02	4.36e-02	5.02e-02	5.75e-02	6.41e-02	7.68e-02	8.18e-02	8.61e-02
8.95e-02	9.25e-02	9.25e-02	9.48e-02	9.68e-02	9.84e-02	9.98e-02	1.03e-01
1.04e-01	1.04e-01	1.04e-01	1.04e-01	1.04e-01	1.04e-01	1.03e-01	1.03e-01
1.03e-01	1.00e-01	9.93e-02	9.84e-02	9.72e-02	9.57e-02	9.57e-02	9.23e-02
8.48e-02	7.25e-02	5.93e-02	3.98e-02	4.02e-02	4.25e-02	4.61e-02	4.86e-02
4.82e-02	4.93e-02	5.63e-02	6.38e-02	7.07e-02	8.36e-02	8.86e-02	9.29e-02
9.66e-02	9.97e-02	9.95e-02	1.02e-01	1.04e-01	1.05e-01	1.07e-01	1.10e-01
1.11e-01	1.11e-01	1.11e-01	1.10e-01	1.10e-01	1.10e-01	1.10e-01	1.10e-01
1.09e-01	1.07e-01	1.06e-01	1.05e-01	1.04e-01	1.02e-01	1.02e-01	9.86e-02
9.09e-02	7.82e-02	6.48e-02	4.46e-02	4.48e-02	4.70e-02	5.05e-02	5.30e-02
2.68e-02	2.73e-02	3.13e-02	3.52e-02	3.91e-02	4.61e-02	4.89e-02	5.13e-02
5.32e-02	5.50e-02	5.50e-02	5.63e-02	5.73e-02	5.84e-02	5.91e-02	6.07e-02
6.11e-02	6.13e-02	6.13e-02	6.09e-02	6.07e-02	6.09e-02	6.09e-02	6.07e-02
6.05e-02	5.91e-02	5.88e-02	5.82e-02	5.75e-02	5.66e-02	5.66e-02	5.47e-02
5.04e-02	4.34e-02	3.61e-02	2.52e-02	2.52e-02	2.63e-02	2.82e-02	2.95e-02
3.04e-02	3.13e-02	3.54e-02	3.98e-02	4.39e-02	5.16e-02	5.47e-02	5.72e-02
5.93e-02	6.11e-02	6.11e-02	6.23e-02	6.34e-02	6.43e-02	6.52e-02	6.68e-02
6.72e-02	6.73e-02	6.72e-02	6.68e-02	6.66e-02	6.68e-02	6.68e-02	6.66e-02
6.64e-02	6.50e-02	6.47e-02	6.41e-02	6.34e-02	6.25e-02	6.27e-02	6.05e-02
5.61e-02	4.86e-02	4.09e-02	2.91e-02	2.93e-02	3.02e-02	3.21e-02	3.34e-02
1.54e-02	1.57e-02	1.80e-02	2.09e-02	2.36e-02	2.86e-02	3.05e-02	3.25e-02
3.39e-02	3.54e-02	3.55e-02	3.66e-02	3.75e-02	3.82e-02	3.88e-02	4.00e-02
4.02e-02	4.04e-02	4.04e-02	4.02e-02	4.00e-02	4.02e-02	4.00e-02	4.00e-02
3.96e-02	3.88e-02	3.84e-02	3.79e-02	3.73e-02	3.66e-02	3.63e-02	3.46e-02
3.14e-02	2.63e-02	2.11e-02	1.34e-02	1.34e-02	1.42e-02	1.53e-02	1.62e-02
2.71e-02	2.79e-02	3.14e-02	3.54e-02	3.91e-02	4.59e-02	4.88e-02	5.11e-02
5.30e-02	5.47e-02	5.48e-02	5.61e-02	5.72e-02	5.79e-02	5.86e-02	6.02e-02
6.04e-02	6.05e-02	6.02e-02	5.98e-02	5.97e-02	5.98e-02	5.98e-02	5.98e-02
5.97e-02	5.82e-02	5.79e-02	5.73e-02	5.66e-02	5.57e-02	5.55e-02	5.36e-02
4.91e-02	4.23e-02	3.54e-02	2.48e-02	2.48e-02	2.57e-02	2.71e-02	2.84e-02
2.54e-02	2.61e-02	2.95e-02	3.32e-02	3.68e-02	4.30e-02	4.57e-02	4.79e-02
4.98e-02	5.13e-02	5.13e-02	5.25e-02	5.34e-02	5.41e-02	5.48e-02	5.63e-02

Figure C-2. (continued)

5.64e-02	5.66e-02	5.64e-02	5.59e-02	5.59e-02	5.61e-02	5.61e-02	5.61e-02
5.59e-02	5.47e-02	5.45e-02	5.39e-02	5.34e-02	5.27e-02	5.27e-02	5.09e-02
4.68e-02	4.05e-02	3.39e-02	2.43e-02	2.43e-02	2.52e-02	2.66e-02	2.75e-02
4.68e-02	4.79e-02	5.47e-02	6.27e-02	7.07e-02	8.54e-02	9.16e-02	9.70e-02
1.02e-01	1.06e-01	1.06e-01	1.10e-01	1.12e-01	1.15e-01	1.16e-01	1.20e-01
1.21e-01	1.21e-01	1.21e-01	1.20e-01	1.20e-01	1.20e-01	1.20e-01	1.20e-01
1.19e-01	1.16e-01	1.15e-01	1.13e-01	1.11e-01	1.09e-01	1.08e-01	1.03e-01
9.32e-02	7.79e-02	6.29e-02	4.05e-02	4.05e-02	4.25e-02	4.54e-02	4.79e-02
3.48e-02	3.61e-02	4.07e-02	4.63e-02	5.16e-02	6.13e-02	6.54e-02	6.89e-02
7.20e-02	7.45e-02	7.48e-02	7.68e-02	7.86e-02	7.98e-02	8.09e-02	8.34e-02
8.38e-02	8.39e-02	8.38e-02	8.30e-02	8.29e-02	8.32e-02	8.32e-02	8.32e-02
8.29e-02	8.09e-02	8.04e-02	7.95e-02	7.82e-02	7.68e-02	7.64e-02	7.34e-02
6.68e-02	5.66e-02	4.68e-02	3.20e-02	3.21e-02	3.32e-02	3.50e-02	3.64e-02
2.07e-02	2.13e-02	2.43e-02	2.80e-02	3.18e-02	3.86e-02	4.16e-02	4.43e-02
4.66e-02	4.86e-02	4.91e-02	5.07e-02	5.20e-02	5.30e-02	5.39e-02	5.57e-02
5.61e-02	5.63e-02	5.61e-02	5.55e-02	5.55e-02	5.55e-02	5.55e-02	5.54e-02
5.50e-02	5.36e-02	5.29e-02	5.22e-02	5.11e-02	4.98e-02	4.93e-02	4.66e-02
4.16e-02	3.45e-02	2.77e-02	1.72e-02	1.71e-02	1.78e-02	1.89e-02	1.98e-02
9.81e-03	1.00e-02	1.14e-02	1.31e-02	1.48e-02	1.79e-02	1.93e-02	2.05e-02
2.16e-02	2.25e-02	2.27e-02	2.34e-02	2.39e-02	2.45e-02	2.48e-02	2.55e-02
2.57e-02	2.57e-02	2.57e-02	2.54e-02	2.54e-02	2.54e-02	2.54e-02	2.54e-02
2.52e-02	2.45e-02	2.43e-02	2.39e-02	2.34e-02	2.29e-02	2.25e-02	2.13e-02
1.89e-02	1.56e-02	1.25e-02	7.84e-03	7.75e-03	8.09e-03	8.52e-03	8.89e-03
7.80e-03	7.91e-03	9.06e-03	1.05e-02	1.20e-02	1.48e-02	1.61e-02	1.72e-02
1.82e-02	1.91e-02	1.93e-02	2.00e-02	2.05e-02	2.11e-02	2.14e-02	2.21e-02
2.23e-02	2.23e-02	2.23e-02	2.21e-02	2.21e-02	2.21e-02	2.21e-02	2.20e-02
2.18e-02	2.13e-02	2.09e-02	2.05e-02	2.02e-02	1.95e-02	1.91e-02	1.80e-02
1.59e-02	1.29e-02	1.02e-02	6.07e-03	5.97e-03	6.29e-03	6.64e-03	6.97e-03
1.91e-03	1.93e-03	2.18e-03	2.52e-03	2.88e-03	3.52e-03	3.80e-03	4.07e-03
4.29e-03	4.46e-03	4.54e-03	4.70e-03	4.82e-03	4.91e-03	5.00e-03	5.16e-03
5.18e-03	5.18e-03	5.16e-03	5.11e-03	5.09e-03	5.09e-03	5.07e-03	5.04e-03
5.00e-03	4.84e-03	4.77e-03	4.66e-03	4.55e-03	4.41e-03	4.30e-03	4.05e-03
3.55e-03	2.91e-03	2.34e-03	1.41e-03	1.35e-03	1.40e-03	1.46e-03	1.52e-03
6.18e-04	6.29e-04	7.20e-04	8.39e-04	9.81e-04	1.20e-03	1.32e-03	1.43e-03
1.53e-03	1.62e-03	1.66e-03	1.73e-03	1.79e-03	1.84e-03	1.88e-03	1.95e-03
1.96e-03	1.98e-03	1.96e-03	1.95e-03	1.95e-03	1.93e-03	1.91e-03	1.89e-03
1.88e-03	1.78e-03	1.73e-03	1.67e-03	1.60e-03	1.51e-03	1.43e-03	1.30e-03
1.12e-03	9.27e-04	7.80e-04	4.68e-04	3.88e-04	3.84e-04	3.91e-04	3.93e-04
2.66e-04	2.73e-04	3.00e-04	3.30e-04	3.61e-04	4.14e-04	4.36e-04	4.52e-04
4.66e-04	4.75e-04	4.75e-04	4.84e-04	4.91e-04	4.97e-04	4.98e-04	5.09e-04
5.07e-04	5.04e-04	4.98e-04	4.89e-04	4.88e-04	4.91e-04	4.95e-04	4.97e-04
4.97e-04	4.89e-04	4.88e-04	4.86e-04	4.82e-04	4.77e-04	4.77e-04	4.63e-04
4.29e-04	3.71e-04	3.25e-04	2.54e-04	2.61e-04	2.64e-04	2.70e-04	2.75e-04
4.14e-04	4.16e-04	4.68e-04	5.34e-04	6.11e-04	7.47e-04	8.13e-04	8.68e-04
9.18e-04	9.57e-04	9.72e-04	1.01e-03	1.03e-03	1.05e-03	1.07e-03	1.10e-03
1.11e-03	1.11e-03	1.10e-03	1.09e-03	1.09e-03	1.09e-03	1.09e-03	1.09e-03
1.09e-03	1.06e-03	1.05e-03	1.03e-03	1.01e-03	9.81e-04	9.63e-04	9.06e-04
7.97e-04	6.43e-04	5.22e-04	3.29e-04	3.21e-04	3.36e-04	3.50e-04	3.63e-04

Figure C-2. (continued)

1.26e-04	1.22e-04	1.36e-04	1.53e-04	1.74e-04	2.09e-04	2.27e-04	2.43e-04
2.57e-04	2.68e-04	2.71e-04	2.80e-04	2.88e-04	2.91e-04	2.95e-04	3.04e-04
3.04e-04	3.02e-04	2.98e-04	2.95e-04	2.93e-04	2.93e-04	2.93e-04	2.91e-04
2.89e-04	2.79e-04	2.75e-04	2.70e-04	2.63e-04	2.52e-04	2.45e-04	2.27e-04
2.00e-04	1.66e-04	1.40e-04	9.31e-05	8.47e-05	8.57e-05	8.75e-05	8.86e-05
2.34e-05	2.21e-05	2.38e-05	2.61e-05	2.91e-05	3.48e-05	3.73e-05	3.93e-05
4.11e-05	4.23e-05	4.25e-05	4.34e-05	4.38e-05	4.39e-05	4.39e-05	4.45e-05
4.39e-05	4.32e-05	4.23e-05	4.13e-05	4.07e-05	4.11e-05	4.13e-05	4.14e-05
4.14e-05	4.07e-05	4.05e-05	4.02e-05	3.96e-05	3.88e-05	3.82e-05	3.63e-05
3.23e-05	2.75e-05	2.41e-05	1.84e-05	1.77e-05	1.80e-05	1.84e-05	1.86e-05
2.86e-06	2.68e-06	2.77e-06	2.93e-06	3.18e-06	3.68e-06	3.86e-06	3.98e-06
4.07e-06	4.13e-06	4.09e-06	4.07e-06	4.04e-06	3.96e-06	3.86e-06	3.80e-06
3.66e-06	3.52e-06	3.36e-06	3.20e-06	3.14e-06	3.20e-06	3.25e-06	3.30e-06
3.38e-06	3.38e-06	3.43e-06	3.48e-06	3.50e-06	3.52e-06	3.54e-06	3.45e-06
3.21e-06	2.95e-06	2.80e-06	2.48e-06	2.45e-06	2.46e-06	2.48e-06	2.48e-06
4.41e-07	4.04e-07	4.05e-07	4.18e-07	4.43e-07	5.11e-07	5.36e-07	5.55e-07
5.68e-07	5.77e-07	5.73e-07	5.70e-07	5.63e-07	5.48e-07	5.32e-07	5.25e-07
5.04e-07	4.80e-07	4.57e-07	4.32e-07	4.25e-07	4.32e-07	4.39e-07	4.50e-07
4.61e-07	4.63e-07	4.73e-07	4.84e-07	4.93e-07	5.00e-07	5.07e-07	5.04e-07
4.88e-07	4.72e-07	4.64e-07	4.36e-07	4.32e-07	4.36e-07	4.41e-07	4.45e-07
1.16e-07	1.07e-07	1.06e-07	1.08e-07	1.15e-07	1.31e-07	1.36e-07	1.39e-07
1.41e-07	1.42e-07	1.40e-07	1.38e-07	1.34e-07	1.29e-07	1.24e-07	1.19e-07
1.11e-07	1.03e-07	9.50e-08	8.70e-08	8.45e-08	8.80e-08	9.22e-08	9.68e-08
1.02e-07	1.06e-07	1.11e-07	1.16e-07	1.21e-07	1.24e-07	1.28e-07	1.30e-07
1.27e-07	1.24e-07	1.24e-07	1.21e-07	1.22e-07	1.23e-07	1.24e-07	1.24e-07
2.05e-08	1.89e-08	1.84e-08	1.88e-08	1.96e-08	2.20e-08	2.25e-08	2.29e-08
2.30e-08	2.30e-08	2.27e-08	2.23e-08	2.16e-08	2.07e-08	1.96e-08	1.88e-08
1.75e-08	1.61e-08	1.47e-08	1.33e-08	1.29e-08	1.37e-08	1.45e-08	1.55e-08
1.65e-08	1.74e-08	1.84e-08	1.95e-08	2.05e-08	2.13e-08	2.21e-08	2.25e-08
2.23e-08	2.21e-08	2.25e-08	2.21e-08	2.25e-08	2.27e-08	2.29e-08	2.30e-08
2.75e-09	2.54e-09	2.45e-09	2.48e-09	2.57e-09	2.86e-09	2.93e-09	2.96e-09
2.96e-09	2.96e-09	2.91e-09	2.84e-09	2.75e-09	2.63e-09	2.48e-09	2.34e-09
2.18e-09	1.98e-09	1.80e-09	1.61e-09	1.56e-09	1.67e-09	1.80e-09	1.93e-09
2.09e-09	2.21e-09	2.38e-09	2.54e-09	2.68e-09	2.80e-09	2.93e-09	3.02e-09
3.00e-09	3.02e-09	3.05e-09	3.04e-09	3.09e-09	3.13e-09	3.16e-09	3.16e-09
5.16e-10	4.77e-10	4.63e-10	4.70e-10	4.88e-10	5.39e-10	5.54e-10	5.61e-10
5.63e-10	5.61e-10	5.54e-10	5.39e-10	5.20e-10	4.97e-10	4.68e-10	4.45e-10
4.11e-10	3.77e-10	3.41e-10	3.05e-10	2.96e-10	3.16e-10	3.39e-10	3.64e-10
3.93e-10	4.16e-10	4.45e-10	4.72e-10	4.98e-10	5.22e-10	5.45e-10	5.57e-10
5.54e-10	5.52e-10	5.61e-10	5.55e-10	5.63e-10	5.68e-10	5.75e-10	5.77e-10
7.39e-11	6.80e-11	6.70e-11	6.84e-11	7.16e-11	8.00e-11	8.25e-11	8.38e-11
8.41e-11	8.39e-11	8.23e-11	8.04e-11	7.75e-11	7.39e-11	6.97e-11	6.61e-11
6.11e-11	5.61e-11	5.11e-11	4.61e-11	4.47e-11	4.73e-11	5.04e-11	5.38e-11
5.75e-11	6.04e-11	6.43e-11	6.79e-11	7.13e-11	7.45e-11	7.72e-11	7.86e-11
7.75e-11	7.66e-11	7.72e-11	7.59e-11	7.68e-11	7.75e-11	7.84e-11	7.86e-11
1.31e-11	1.21e-11	1.18e-11	1.20e-11	1.24e-11	1.37e-11	1.41e-11	1.42e-11
1.43e-11	1.42e-11	1.40e-11	1.37e-11	1.33e-11	1.27e-11	1.20e-11	1.15e-11
1.07e-11	9.88e-12	9.06e-12	8.23e-12	8.02e-12	8.47e-12	8.98e-12	9.56e-12

Figure C-2. (continued)

1.02e-11	1.06e-11	1.13e-11	1.19e-11	1.24e-11	1.29e-11	1.34e-11	1.36e-11
1.33e-11	1.31e-11	1.32e-11	1.29e-11	1.30e-11	1.31e-11	1.32e-11	1.33e-11
2.09e-12	1.95e-12	1.93e-12	1.98e-12	2.02e-12	2.14e-12	2.18e-12	2.18e-12
2.18e-12	2.16e-12	2.11e-12	2.07e-12	2.02e-12	1.95e-12	1.88e-12	1.82e-12
1.74e-12	1.64e-12	1.55e-12	1.46e-12	1.44e-12	1.50e-12	1.57e-12	1.64e-12
1.71e-12	1.75e-12	1.82e-12	1.89e-12	1.96e-12	2.00e-12	2.05e-12	2.05e-12
1.96e-12	1.91e-12	1.89e-12	1.76e-12	1.74e-12	1.76e-12	1.77e-12	1.78e-12
1.84e-08	1.84e-08	1.82e-08	1.82e-08	1.82e-08	1.80e-08	1.80e-08	1.79e-08
1.78e-08	1.77e-08	1.78e-08	1.77e-08	1.76e-08	1.76e-08	1.76e-08	1.74e-08
1.75e-08	1.75e-08	1.76e-08	1.77e-08	1.77e-08	1.77e-08	1.78e-08	1.80e-08
1.82e-08	1.86e-08	1.89e-08	1.91e-08	1.93e-08	1.93e-08	1.93e-08	1.93e-08
1.89e-08	1.84e-08	1.82e-08	1.82e-08	1.86e-08	1.88e-08	1.88e-08	1.88e-08
8.98e-08	9.09e-08	9.07e-08	9.06e-08	9.06e-08	9.00e-08	8.97e-08	8.95e-08
8.91e-08	8.88e-08	8.91e-08	8.89e-08	8.88e-08	8.84e-08	8.84e-08	8.79e-08
8.79e-08	8.79e-08	8.80e-08	8.82e-08	8.80e-08	8.79e-08	8.79e-08	8.80e-08
8.84e-08	8.91e-08	8.93e-08	8.95e-08	8.97e-08	8.97e-08	8.91e-08	8.89e-08
8.84e-08	8.73e-08	8.70e-08	8.54e-08	8.50e-08	8.50e-08	8.43e-08	8.43e-08
3.39e-06	3.63e-06	3.71e-06	3.82e-06	3.98e-06	4.25e-06	4.34e-06	4.41e-06
4.47e-06	4.48e-06	4.45e-06	4.43e-06	4.39e-06	4.36e-06	4.30e-06	4.25e-06
4.18e-06	4.07e-06	3.95e-06	3.80e-06	3.77e-06	3.80e-06	3.86e-06	3.91e-06
3.93e-06	3.91e-06	3.91e-06	3.89e-06	3.88e-06	3.86e-06	3.86e-06	3.75e-06
3.52e-06	3.20e-06	2.98e-06	2.50e-06	2.46e-06	2.39e-06	2.29e-06	2.23e-06
1.09e-04	1.17e-04	1.19e-04	1.22e-04	1.28e-04	1.36e-04	1.39e-04	1.42e-04
1.43e-04	1.44e-04	1.42e-04	1.41e-04	1.40e-04	1.39e-04	1.37e-04	1.35e-04
1.32e-04	1.28e-04	1.23e-04	1.18e-04	1.16e-04	1.18e-04	1.20e-04	1.22e-04
1.24e-04	1.23e-04	1.24e-04	1.24e-04	1.24e-04	1.23e-04	1.24e-04	1.21e-04
1.14e-04	1.03e-04	9.66e-05	8.25e-05	8.18e-05	8.02e-05	7.70e-05	7.48e-05
1.17e-04	1.25e-04	1.34e-04	1.45e-04	1.57e-04	1.75e-04	1.83e-04	1.90e-04
1.95e-04	2.00e-04	1.98e-04	2.00e-04	2.01e-04	2.01e-04	2.02e-04	2.04e-04
2.03e-04	1.99e-04	1.96e-04	1.91e-04	1.89e-04	1.91e-04	1.92e-04	1.94e-04
1.95e-04	1.92e-04	1.92e-04	1.91e-04	1.90e-04	1.88e-04	1.89e-04	1.82e-04
1.68e-04	1.46e-04	1.30e-04	1.01e-04	1.01e-04	9.94e-05	9.86e-05	9.92e-05
2.00e-04	2.09e-04	2.44e-04	2.83e-04	3.22e-04	3.84e-04	4.12e-04	4.35e-04
4.57e-04	4.74e-04	4.74e-04	4.86e-04	4.97e-04	5.04e-04	5.11e-04	5.25e-04
5.27e-04	5.28e-04	5.24e-04	5.21e-04	5.19e-04	5.21e-04	5.21e-04	5.21e-04
5.21e-04	5.08e-04	5.06e-04	5.01e-04	4.95e-04	4.89e-04	4.89e-04	4.67e-04
4.22e-04	3.57e-04	3.01e-04	2.05e-04	2.05e-04	2.05e-04	2.12e-04	2.21e-04
6.41e-04	6.62e-04	8.10e-04	9.83e-04	1.14e-03	1.41e-03	1.53e-03	1.63e-03
1.73e-03	1.81e-03	1.81e-03	1.87e-03	1.92e-03	1.96e-03	1.99e-03	2.06e-03
2.08e-03	2.09e-03	2.09e-03	2.07e-03	2.07e-03	2.08e-03	2.08e-03	2.07e-03
2.06e-03	2.01e-03	2.00e-03	1.98e-03	1.96e-03	1.92e-03	1.92e-03	1.83e-03
1.64e-03	1.37e-03	1.12e-03	7.21e-04	7.18e-04	7.29e-04	7.64e-04	8.13e-04
1.57e-03	1.61e-03	2.00e-03	2.45e-03	2.87e-03	3.56e-03	3.89e-03	4.15e-03
4.40e-03	4.61e-03	4.62e-03	4.78e-03	4.90e-03	5.02e-03	5.10e-03	5.30e-03
5.34e-03	5.37e-03	5.38e-03	5.36e-03	5.36e-03	5.37e-03	5.36e-03	5.34e-03
5.32e-03	5.18e-03	5.16e-03	5.11e-03	5.05e-03	4.95e-03	4.97e-03	4.72e-03
4.24e-03	3.51e-03	2.85e-03	1.80e-03	1.80e-03	1.85e-03	1.95e-03	2.09e-03
5.11e-03	5.25e-03	6.47e-03	7.89e-03	9.23e-03	1.15e-02	1.25e-02	1.34e-02

Figure C-2. (continued)

1.41e-02	1.48e-02	1.48e-02	1.54e-02	1.58e-02	1.61e-02	1.64e-02	1.70e-02
1.72e-02	1.72e-02	1.73e-02	1.72e-02	1.72e-02	1.72e-02	1.72e-02	1.71e-02
1.71e-02	1.66e-02	1.65e-02	1.64e-02	1.62e-02	1.60e-02	1.60e-02	1.52e-02
1.36e-02	1.13e-02	9.12e-03	5.66e-03	5.73e-03	5.93e-03	6.31e-03	6.74e-03
5.11e-03	5.20e-03	6.47e-03	8.01e-03	9.45e-03	1.19e-02	1.30e-02	1.40e-02
1.48e-02	1.56e-02	1.57e-02	1.62e-02	1.67e-02	1.71e-02	1.74e-02	1.81e-02
1.83e-02	1.84e-02	1.84e-02	1.84e-02	1.84e-02	1.84e-02	1.84e-02	1.83e-02
1.82e-02	1.77e-02	1.76e-02	1.75e-02	1.73e-02	1.69e-02	1.69e-02	1.61e-02
1.43e-02	1.17e-02	9.39e-03	5.64e-03	5.72e-03	6.03e-03	6.48e-03	6.97e-03
8.46e-03	8.58e-03	1.07e-02	1.33e-02	1.57e-02	1.99e-02	2.18e-02	2.35e-02
2.50e-02	2.62e-02	2.63e-02	2.73e-02	2.81e-02	2.87e-02	2.92e-02	3.05e-02
3.08e-02	3.10e-02	3.12e-02	3.10e-02	3.10e-02	3.10e-02	3.10e-02	3.08e-02
3.08e-02	2.99e-02	2.99e-02	2.94e-02	2.92e-02	2.87e-02	2.87e-02	2.71e-02
2.41e-02	1.96e-02	1.56e-02	9.17e-03	9.40e-03	1.00e-02	1.08e-02	1.17e-02
1.38e-02	1.39e-02	1.73e-02	2.16e-02	2.58e-02	3.29e-02	3.63e-02	3.91e-02
4.16e-02	4.39e-02	4.40e-02	4.56e-02	4.69e-02	4.82e-02	4.90e-02	5.09e-02
5.15e-02	5.20e-02	5.21e-02	5.20e-02	5.20e-02	5.20e-02	5.19e-02	5.17e-02
5.15e-02	5.03e-02	4.99e-02	4.95e-02	4.89e-02	4.80e-02	4.79e-02	4.53e-02
4.00e-02	3.23e-02	2.53e-02	1.45e-02	1.49e-02	1.61e-02	1.75e-02	1.89e-02
2.37e-02	2.40e-02	2.98e-02	3.74e-02	4.49e-02	5.82e-02	6.44e-02	6.97e-02
7.45e-02	7.87e-02	7.93e-02	8.23e-02	8.50e-02	8.69e-02	8.86e-02	9.23e-02
9.32e-02	9.39e-02	9.42e-02	9.40e-02	9.39e-02	9.42e-02	9.41e-02	9.40e-02
9.37e-02	9.15e-02	9.10e-02	9.03e-02	8.91e-02	8.75e-02	8.70e-02	8.18e-02
7.17e-02	5.70e-02	4.41e-02	2.42e-02	2.51e-02	2.73e-02	2.96e-02	3.17e-02
2.40e-02	2.52e-02	3.00e-02	3.66e-02	4.33e-02	5.48e-02	6.02e-02	6.50e-02
6.94e-02	7.30e-02	7.36e-02	7.62e-02	7.84e-02	8.01e-02	8.13e-02	8.42e-02
8.49e-02	8.51e-02	8.51e-02	8.47e-02	8.46e-02	8.51e-02	8.52e-02	8.56e-02
8.57e-02	8.41e-02	8.38e-02	8.33e-02	8.25e-02	8.10e-02	8.04e-02	7.54e-02
6.57e-02	5.22e-02	4.15e-02	2.32e-02	2.34e-02	2.48e-02	2.60e-02	2.73e-02
1.86e-02	2.03e-02	2.47e-02	3.02e-02	3.63e-02	4.61e-02	5.13e-02	5.58e-02
6.01e-02	6.39e-02	6.48e-02	6.78e-02	7.02e-02	7.23e-02	7.41e-02	7.70e-02
7.82e-02	7.88e-02	7.89e-02	7.86e-02	7.86e-02	7.90e-02	7.92e-02	7.95e-02
7.96e-02	7.78e-02	7.74e-02	7.66e-02	7.54e-02	7.36e-02	7.25e-02	6.76e-02
5.83e-02	4.56e-02	3.65e-02	1.92e-02	1.85e-02	1.93e-02	1.99e-02	2.07e-02
1.07e-02	1.17e-02	1.37e-02	1.61e-02	1.88e-02	2.26e-02	2.49e-02	2.69e-02
2.89e-02	3.07e-02	3.12e-02	3.27e-02	3.40e-02	3.50e-02	3.58e-02	3.74e-02
3.77e-02	3.77e-02	3.75e-02	3.70e-02	3.69e-02	3.73e-02	3.74e-02	3.73e-02
3.73e-02	3.60e-02	3.55e-02	3.49e-02	3.40e-02	3.30e-02	3.25e-02	3.01e-02
2.62e-02	2.18e-02	1.86e-02	1.05e-02	9.33e-03	9.20e-03	9.14e-03	9.19e-03
1.68e-02	1.80e-02	2.00e-02	2.20e-02	2.38e-02	2.52e-02	2.62e-02	2.69e-02
2.74e-02	2.76e-02	2.69e-02	2.69e-02	2.66e-02	2.64e-02	2.61e-02	2.63e-02
2.58e-02	2.51e-02	2.46e-02	2.39e-02	2.38e-02	2.41e-02	2.46e-02	2.49e-02
2.55e-02	2.51e-02	2.54e-02	2.57e-02	2.57e-02	2.55e-02	2.55e-02	2.43e-02
2.15e-02	1.88e-02	1.72e-02	1.12e-02	9.02e-03	8.73e-03	8.66e-03	8.67e-03
2.80e-03	2.90e-03	3.21e-03	3.58e-03	3.92e-03	4.23e-03	4.43e-03	4.63e-03
4.77e-03	4.87e-03	4.78e-03	4.83e-03	4.88e-03	4.88e-03	4.87e-03	4.99e-03
4.94e-03	4.87e-03	4.78e-03	4.68e-03	4.63e-03	4.66e-03	4.70e-03	4.75e-03
4.77e-03	4.64e-03	4.63e-03	4.58e-03	4.52e-03	4.40e-03	4.39e-03	4.14e-03

Figure C-2. (continued)

3.71e-03	3.37e-03	3.07e-03	2.06e-03	1.77e-03	1.76e-03	1.78e-03	1.79e-03
3.51e-04	3.49e-04	3.81e-04	4.20e-04	4.60e-04	5.02e-04	5.29e-04	5.53e-04
5.72e-04	5.91e-04	5.83e-04	5.95e-04	6.04e-04	6.09e-04	6.13e-04	6.30e-04
6.28e-04	6.23e-04	6.16e-04	6.09e-04	6.02e-04	5.99e-04	5.94e-04	5.90e-04
5.83e-04	5.57e-04	5.42e-04	5.24e-04	5.01e-04	4.73e-04	4.55e-04	4.28e-04
4.06e-04	3.81e-04	3.50e-04	2.51e-04	2.15e-04	2.13e-04	2.15e-04	2.16e-04
1.71e-05	1.63e-05	1.63e-05	1.67e-05	1.81e-05	2.09e-05	2.20e-05	2.30e-05
2.38e-05	2.44e-05	2.46e-05	2.52e-05	2.57e-05	2.61e-05	2.64e-05	2.74e-05
2.73e-05	2.71e-05	2.69e-05	2.64e-05	2.58e-05	2.51e-05	2.44e-05	2.36e-05
2.27e-05	2.12e-05	2.04e-05	1.97e-05	1.91e-05	1.86e-05	1.84e-05	1.78e-05
1.72e-05	1.65e-05	1.58e-05	1.31e-05	1.26e-05	1.25e-05	1.25e-05	1.26e-05
4.16e-07	4.09e-07	4.22e-07	4.42e-07	4.70e-07	5.57e-07	6.05e-07	6.39e-07
6.77e-07	7.05e-07	7.12e-07	7.30e-07	7.44e-07	7.55e-07	7.59e-07	7.76e-07
7.74e-07	7.67e-07	7.49e-07	7.26e-07	6.95e-07	6.77e-07	6.64e-07	6.53e-07
6.39e-07	6.10e-07	5.94e-07	5.76e-07	5.57e-07	5.34e-07	5.25e-07	5.01e-07
4.76e-07	4.42e-07	4.08e-07	3.45e-07	3.27e-07	3.14e-07	3.03e-07	3.03e-07
3.84e-08	4.05e-08	4.41e-08	5.02e-08	5.76e-08	6.84e-08	7.43e-08	7.84e-08
8.39e-08	8.71e-08	8.64e-08	8.87e-08	9.07e-08	9.14e-08	9.12e-08	9.16e-08
9.03e-08	8.80e-08	8.48e-08	8.23e-08	8.03e-08	7.82e-08	7.73e-08	7.57e-08
7.39e-08	7.01e-08	6.84e-08	6.50e-08	6.18e-08	5.86e-08	6.02e-08	5.69e-08
5.32e-08	4.71e-08	4.19e-08	3.19e-08	2.66e-08	2.35e-08	1.98e-08	1.81e-08
1.45e-07	1.84e-07	2.21e-07	2.50e-07	2.75e-07	3.05e-07	3.21e-07	3.30e-07
3.32e-07	3.21e-07	3.18e-07	3.29e-07	3.30e-07	3.14e-07	3.02e-07	2.93e-07
2.82e-07	2.70e-07	2.41e-07	2.09e-07	1.91e-07	1.95e-07	1.95e-07	1.96e-07
2.00e-07	1.96e-07	1.96e-07	1.98e-07	1.96e-07	1.95e-07	1.93e-07	2.00e-07
2.02e-07	2.04e-07	1.96e-07	1.29e-07	9.07e-08	8.13e-08	6.48e-08	5.64e-08

15** / source multiplier for each energy group

69rl.0

t

Figure C-2. (continued)

```

' dort - aprf aog, 5/90 2m box expt., saic 1990 leakage source, mm = 240
' 16.143m source height, simple topography out to 1080m test site
' 32% ground moisture, ss90-127 5/14/90 air parameters, s90e5.

61$$ 0 21 4 0 23 / ntflx,ntfog,ntsig,ntbsi,ntdsi
 0 0 0 0 22 / ntfci,ntibi,ntibo,ntnpr,ntdir
 0 e / ntdso

62$$ 0 5 8 123 146 / iadj,isctm,izm,im,jm
 69 3 4 72 0 / igm,iht,ihb,ihm,mixl
 0 66 66 0 240 / mcr,mtp,mtm,idfac,mm
 1 1 0 0 0 / ingeom,ibl,ibr,ibb,ibt
 1 -4 0 4 0 / isrmx,ifxmi,ifxmf,mode,ktype
 2 0 0 0 0 / iacc,kalf,igtype,inpxfm,inpsrm
 0 0 0 0 / njntsr,nintsr,njntfx,nintfx,iact
 8 0 1 1 2 / ired,ipdb2,ifxpri,icsprt,idirf
 13 27 120 11 1 / jdirf,jdirl,nbuf,iepsbz,minblk
 1 1 1 1 1 / maxblk,isbt,msbt,msdm,ibfscl
 4 50 2 0 0 / intsc1,itmscl,nofig,ifdb2z,iswp
 19 28 0 0 0 / keyjn,keyin,nsigtp,norpos,format
 0 0 1500 0 -40 / mstmax,negfix,locobj,lcmobj,nkeyfx
 4 46 0 0 0 / ncndin,neut,italy,isp1,isp2
 e

63** 240 0.0 1-4 1-2 0.0 / tmax,xnf,eps,epp,epv
 1-3 1.0 0.2 1.5 10.0 /epf,ekobj,evth,evchm,evmax
 1.0 1.0 -1.0 0.3 10.0 /evkmx,evi,devdk1,evdelk,sormin
 1.0 1-4 1-2 0.3 -1.5 /conacc,conscl,conepl,wscloi,wsclii
 1.5 0.6 0.0 1-60 0.0 /wsclcn,orf,fsnacc,flxmin,smooth
 1-2 0.2 0.9 / epo,extrcv,theta
 e t
 t

81**      / wts mm240
 0 2r102900-8 0 2r307825-8 0 2r510200-8 0 2r708425-8 0
 2r901350-8 0 563869-8 316131-8 n2 0 641385-8 359590-8 n2 0
 714976-8 400849-8 n2 0 784547-8 439853-8 n2 0 857529-8
 480771-8 n2 0 642875-8 293289-8 479164-8 n3 0 681415-8
 310872-8 507890-8 n3 0 716550-8 326901-8 534077-8 n3 0
 745915-8 340298-8 555965-8 n3 0 775565-8 353825-8 578064-8
 n3 0 489468-8 386282-8 513536-8 364389-8 n4 0 500102-8
 394674-8 524693-8 372306-8 n4 0 508580-8 401365-8 533587-8
 378617-8 n4 0 515474-8 406806-8 540820-8 383750-8 n4 0
 517107-8 408094-8 542534-8 384965-8 n4 q120

```

Figure C-3. Sample DORT Input for the MASH Analysis of the APRF Spring 1990 Two-Meter Box Test Bed Experiments.

```

82**      / mus mm240
-641230-7 -421582-7 m1 -142963-6 -939923-7 m1 -229252-6
-150724-6 m1 -315291-6 -207291-6 m1 -399349-6 -262555-6 m1
-472796-6 -411087-6 -143488-6 m2 -537046-6 -466952-6
-162988-6 m2 -598374-6 -520275-6 -181600-6 m2 -656401-6
-570729-6 -199211-6 m2 -711034-6 -618231-6 -215791-6 m2
-761567-6 -713133-6 -470428-6 -164201-6 m3 -807567-6
-756207-6 -498843-6 -174119-6 m3 -849108-6 -795106-6
-524503-6 -183075-6 m3 -885925-6 -829582-6 -547246-6
-191013-6 m3 -917890-6 -859514-6 -566991-6 -197905-6 m3
-944812-6 -922954-6 -765692-6 -505099-6 -176303-6 m4
-966490-6 -944130-6 -783260-6 -516688-6 -180348-6 m4
-982847-6 -960108-6 -796516-6 -525433-6 -183400-6 m4
-993815-6 -970823-6 -805405-6 -531297-6 -185447-6 m4
-999313-6 -976194-6 -809860-6 -534236-6 -186473-6 m4 q120

83**      / etas mm240
3r-.997942 3r-.989728 3r-.973367 3r-.948995 3r-.916799
5r-.881172 5r-.843553 5r-.801217 5r-.754412 5r-.703158
7r-.648086 7r-.589776 7r-.528222 7r-.463828 7r-.396835
9r-.327613 9r-.256704 9r-.184425 9r-.111045 9r-.037054 g120

84$$ 1 2 3 4 5 6 7 8   / reg nos by zone
t
1** f0   / fission spectrum

2**  /axii (jm+1)
-80 -75 -70 -65 -60 -55 -50 -45 -40 -35 -30 -25 -20 -15 -10 -5 -2.5
-1 0 50 150 250 350 450 550 700 950 1100 1220 1311 1381 1435 1476
1508 1532 1551 1566 1577 1585 1592 1597 1601 1604 1607 1608.5 1610
1614.3 1619 1620.5 1622 1624 1627 1631 1636 1643 1651 1662 1677 1696
1720 1752 1793 1847 1917 2008 2126 2279 2479 2739 3076 3514 4085 4826
5789 7042 8670 10787 13000 15500 18000 20500 23000 25500 28000 30500
33000 35500 38000 40500 43000 45500 48000 50500 53000 55500 58000
60500 63000 65500 68000 70500 73000 75500 78000 80500 83000 85500
88000 90500 93000 95500 98000 100500 103000 106000 109000 112000
115000 118000 121000 124000 127000 130000 133000 136000 139000 142000
145000 148000 151000 154000 157000 160000 163000 166000 169000 172000
175000 178000 181000 184000 187000 190000 193000 196000 199000 201000

```

Figure C-3. (continued)

```

4** /radii (im+1)
0 4.6 6 7.8 10 13 17 22 29 37 48 63 82 106 138 179 233 303 394 512 665
865 1125 1462 1900 2471 3212 4175 5428 7056 9000 11000 13000 15000
16500 17500 19000 21000 23000 25000 27000 28500 29500 30500 31500
33000 35000 37000 38500 39500 40500 41500 43000 45000 47000 49000
51000 53000 55000 57000 59000 61000 63000 65000 67000 69000 71000
73000 75000 77000 79000 81000 83000 85000 87000 89000 91000 93000
95000 97000 99000 101000 103000 105000 106500 107500 108500 109500
111000 113000 115000 117000 119000 121000 123000 125000 127000 129000
131000 133000 135000 137000 139000 142000 145000 148000 151000 154000
157000 160000 163000 166000 169000 172000 175000 178000 181000 184000
187000 190000 193000 196000 199000 201000

5** f1 / energy group boundaries

8$$ / zone numbers by interval
' zones 1, 2, & 3-aprf ground, 4 & 5-borated concrete, 6, 7, & 8-air
123r1 8q123 /j-ints 1-9
19r5 104r1 2q123 /j-ints 10-12
19r4 3r3 10r1 3 3r2 3 3r1 3 3r2 3 2r1 3 3r2 3 31r1
3 3r2 3 35r1 5q123 /j-ints 13-18
33r7 3r6 5r7 3r6 4r7 3r6 33r7 3r6 5r7 31r8 4q123 /j-ints 19-23
92r7 31r8 51q123 /j-ints 24-75
123r8 70q123 /j-ints 76-146

9$$ 3r25 2r7 3r37 / mat by zone

24** 1.-10 1.0 1.-1 1.-2 1.-10 1.0 1.-1 1.-10 / importance by zone

28$$ 35r8 11r25 23r8 / inners by grp

29$$ 24r19 4r20 4r21 4r22 4r23 / key flx j-pos's

30$$ 31 34 35 36 37 42 43 44 49 50
51 56 61 66 71 76 81 85 86 87
88 93 98 103 35 43 50 86 3q4 / key flx i-pos's
t
```

Figure C-3. (continued)

```
'aprf aog/400m/16.14m sh/32% g.m./ss90-127 air s90e5 5/90 2m box  
1$$ 1 13 27 0 0 /nip,jpl,jpu,ned,norm  
69 21 22 23 24 /isgrp,nflsv,naft,nuncl,ndata  
5 6 13 27 0 /n5,n6,nj1,njm,naftm  
0 46 0 /ntype,neui,ngamx  
e t  
  
2** 1614.3 0 e /sh,hsa  
  
4$$ 50 e /ival  
t
```

Figure C-4. Sample VISTA Input for the MASH Analysis of the APRF Spring 1990 Two-Meter Box Test Bed Experiments.

1	9	46	69	2m box	exp/aprf	aog.	5/90	exp.	ss90-130-39	s90e5,	1020	steel	+ phantom	n.d.
46	46	23	23	69	72	4	9	24	67	6	3	0	3	
0	0	0	0	0	0	0	8	2						
1	2	3	4	5	6	43	44	45	46	47	48	49	50	
51	52	53	54	55	56	57	58	59	60	61	62	63	64	
65	66	67	68	69	70	71	72	79	80	81	82	83	84	
85	86	87	88	89	90	91	92	93	94	95	96	97	98	
99	100	101	102	103	104	105	106	107	108	109	110	111	112	
113	114	115	116	117	118	119	120	121	122	123	124	125	126	
127	128	129	130	131	132	133	134	135	136	137	138	157	158	
159	160	161	162	163	164	165	166	167	168	169	170	171	172	
173	174	175	176	177	178	179	180	181	182	183	184	185	186	
199	200	201	202	203	204	205	206	207	208	209	210	223	224	
225	226	227	228											
1	1	4.8016-2												
1	2	8.8600-9												
1	3	3.2435-8												
1	4	3.4889-4												
1	5	4.3922-5												
1	6	4.3043-2												
1	7	1.3186-4												
1	8	8.4348-5												
1	9	1.2722-3												
1	10	8.7935-3												
1	12	3.3368-6												
1	13	3.2693-6												
1	15	1.8926-4												
1	16	2.4025-5												
1	17	6.6540-6												
1	18	2.9695-4												
1	19	2.5719-7												
1	20	2.5817-7												
1	21	4.4903-7												
1	-24	6.7608-8												
2	1	7.0106-7												
2	5	3.8326-5												
2	6	1.0632-5												
2	-14	2.2922-7												
3	4	8.0783-4												
3	10	4.2132-4												
3	11	6.1126-5												
3	12	7.3810-5												
3	17	3.8771-4												
3	-18	8.3911-2												

Figure C-5. Sample XCHEKER Input for the MASH Analysis of the APRF Spring 1990 Two-Meter Box Test Bed Experiments.

4	1	1.6543-2
4	4	1.1849-2
4	5	1.0228-3
4	6	3.8166-3
4	7	1.7367-9
4	9	1.3057-9
4	-13	7.1279-8
5	1	5.8845-2
5	4	3.3642-2
5	5	1.9850-3
5	6	7.7235-3
5	7	2.3220-7
5	9	2.2899-9
5	-13	2.3527-8
6	1	6.1368-2
6	4	1.7881-2
6	5	1.8400-3
6	6	2.5237-2
6	7	1.1955-4
6	8	3.8839-5
6	10	6.0036-7
6	11	1.3868-3
6	12	4.5488-5
6	13	3.4006-5
6	15	3.2988-5
6	16	2.1435-3
6	-18	1.2077-6
7	1	6.6854-2
7	-6	3.3427-2
8	1	3.9800-2
8	4	4.5400-2
8	-6	8.5200-3
9	1	7.1300-2
9	2	4.8700-4
9	3	1.9700-3
9	4	3.4100-2
9	-6	3.6400-3

Figure C-5. (continued)

```

aprf two meter box calc/4in steel/dabl 46n-23g/detailed geometry model
$$ 1000 1500 1500   1   46   23   46   69   0   1   120   4   0
$$ 0   69   1   0
** 1.0   1.0-05   1.0+04   0.0   2.2+05
** 0.0   0.0   110.16   0.0   0.0   0.0   0.0
** 69r1.0
** 8rl1.0 11lr2.0 8r4.0 3r2.0 16rl1.0 3r3.0 12r6.0 8r3.0
** 1.9640+7 1.6905+7 1.4918+7 1.4191+7 1.3840+7 1.2523+7 1.2214+7
1.1052+7 1.0000+7 9.0484+6 8.1873+6 7.4082+6 6.3763+6 4.9658+6
4.7237+6 4.0657+6 3.0119+6 2.3852+6 2.3069+6 1.8268+6 1.4227+6
1.1080+6 9.6164+5 8.2085+5 7.4274+5 6.3927+5 5.5023+5 3.6883+5
2.4724+5 1.5764+5 1.1109+5 5.2475+4 3.4307+4 2.4788+4 2.1875+4
1.0595+4 3.3546+3 1.2341+3 5.8295+2 2.7536+2 1.0130+2 2.9023+1
1.0677+1 3.0590+0 1.12535+0 4.1399-1 2.0000+7 1.4000+7 1.2000+7
1.0000+7 8.0000+6 7.0000+6 6.0000+6 5.0000+6 4.0000+6 3.0000+6
2.5000+6 2.0000+6 1.5000+6 1.0.00+6 7.0000+5 4.5500+5 3.0000+5
1.5000+5 1.0000+5 7.0000+4 4.5000+4 3.0000+4 2.0000+4
0000343276244615
$$ 1   1   0   0   0   4   69   1
$$ 1   1   69   1   1   1   ** 5.0+00   5.0-02   2.0-01   0.0
$$ 1   1   69   2   1   2   ** 2.0+00   2.0-02   1.0-01   0.0
$$ 1   1   69   3   1   3   ** 2.0+00   2.0-02   1.0-01   0.0
$$ 1   1   69   4   1   4   ** 2.0+00   2.0-02   2.0-01   0.0
$$ -1   9r0
$$ 0   0   0   0
** 23r1.0
** 23r1.0
** 23r1.0
** 23r1.0
0000000000   0.001   0.001   0   0   0
1   1
23
2   6
1   6   9   12   19   20
3   16
2   3   4   5   7   8   10   11   13   14   15   16   17   18
21   22
0   1
24
1   1   1   1   1   1   1   1   1   1   1   1   1   1
1   1   1   1   1   1   1   1   1   1   1   1
2m box exp/aprf ground (34%), borated concrete, 10-24-89(a) air, 1020 steel
$$ 46   46   23   23   69   72   4   4   24   41   6   3   0   3
$$ 7z   -8   3z
two meter box/detailed geometry/46n-23g
** 4rl1.0
$$ 1   2

```

Figure C-6. Sample MORSE Input for the MASH Analysis of the Empty Two-Meter Box Used in the APRF Spring 1990 Two-Meter Box Test Bed Experiments.

cm 2.0 meter cubic box geometry (4 inches of steel)
 49 24
 1rpp -120.0000 120.0000 -120.0000 120.0000 -15.0000 230.0000
 2rpp -115.2398 115.2398 -115.2398 115.2398 0.0000 5.0800
 3rpp -110.1598 110.1598 -110.1598 110.1598 5.0800 10.1600
 4rpp -99.9998 -89.8398 -99.9998 -89.8398 10.1600 15.2400
 5rpp 89.8398 99.9998 -99.9998 -89.8398 10.1600 15.2400
 6rpp 89.8398 99.9998 89.8398 99.9998 10.1600 15.2400
 7rpp -99.9998 -89.8398 89.8398 99.9998 10.1600 15.2400
 8rpp -105.0798 105.0798 -105.0798 105.0798 10.1600 215.2396
 9rpp -99.9998 99.9998 -99.9998 99.9998 10.1600 210.1596
 10rpp -79.6798 -69.5198 -112.0598 -110.1598 5.0800 15.2400
 11rpp 69.5198 79.6798 -112.0598 -110.1598 5.0800 15.2400
 12rpp 110.1598 112.0598 -79.6798 -69.5298 5.0800 15.2400
 13rpp 110.1598 112.0598 69.5298 79.6798 5.0800 15.2400
 14rpp 69.5198 79.6798 110.1598 112.0598 5.0800 15.2400
 15rpp -79.6798 -69.5198 110.1598 112.0598 5.0800 15.2400
 16rpp -112.0598 -110.1598 69.5198 79.6798 5.0800 15.2400
 17rpp -112.0598 -110.1598 -79.6798 -69.5198 5.0800 15.2400
 18rpp -99.9998 -89.8398 -117.1398 -115.2398 0.0000 15.2400
 19rpp 89.8398 99.9998 -117.1398 -115.2398 0.0000 15.2400
 20rpp 89.8398 99.9998 115.2398 117.1398 0.0000 15.2400
 21rpp -99.9998 -89.8398 115.2398 117.1398 0.0000 15.2400
 22rcc -94.9198 -117.1398 10.1600 0.0000 1.9000 0.0000
 2.5400
 23rcc 94.9198 -117.1398 10.1600 0.0000 1.9000 0.0000
 2.5400
 24rcc 94.9198 115.2398 10.1600 0.0000 1.9000 0.0000
 2.5400
 25rcc -94.9198 115.2398 10.1600 0.0000 1.9000 0.0000
 2.5400
 26rcc 0.0000 0.0000 210.1596 0.0000 0.0000 5.0800
 25.4000
 27rcc 99.9998 0.0000 110.1598 5.0800 0.0000 0.0000
 25.4000
 28rcc 99.9998 -49.1998 10.1600 10.1600 0.0000 0.0000
 5.0800
 29rpp -110.1598 110.1598 -110.1598 -105.0798 10.1600 215.2396
 30rpp 105.0798 110.1598 -105.0798 105.0798 10.1600 215.2396
 31rpp -110.1598 110.1598 105.0798 110.1598 10.1600 215.2396
 32rpp -110.1598 -105.0798 -105.0798 105.0798 10.1600 215.2396
 33rpp -110.1598 110.1598 -110.1598 110.1598 215.2396 220.3196
 34rcc 0.0000 0.0000 215.2396 0.0000 0.0000 5.0800
 37.4650
 35rcc 105.0798 0.0000 110.1598 5.0800 0.0000 0.0000
 37.4650
 36rpp -5.0800 5.0800 -112.0598 -110.1598 205.1596 228.0196
 37rpp 110.1598 112.0598 -5.0800 5.0800 205.1596 228.0196

Figure C-7. Sample Geometry Input for the MASH Analysis of the Empty Two-Meter Box Used in the APRF Spring 1990 Two-Meter Box Test Bed Experiments.

38rpp	-5.0800	5.0800	110.1598	112.0598	205.1596	228.0196				
39rpp	-112.0598	-110.1598	-5.0800	5.0800	205.1596	228.0196				
40rcc	0.0000	-112.0598	222.9396	0.0000	1.9000	0.0000				
	2.5400									
41rcc	110.1598	0.0000	222.9396	1.9000	0.0000	0.0000				
	2.5400									
42rcc	0.0000	110.1598	222.9396	0.0000	1.9000	0.0000				
	2.5400									
43rcc	-112.0598	0.0000	222.9396	1.9000	0.0000	0.0000				
	2.5400									
44rcc	-85.0000	-110.1598	11.4300	0.0000	10.1600	0.0000				
	1.2700									
45rcc	85.0000	-110.1598	11.4300	0.0000	10.1600	0.0000				
	1.2700									
46rcc	85.0000	99.9998	11.4300	0.0000	10.1600	0.0000				
	1.2700									
47rcc	-85.0000	99.9998	11.4300	0.0000	10.1600	0.0000				
	1.2700									
48rpp	-120.0000	120.0000	-120.0000	120.0000	-15.0000	0.0000				
49rpp	-125.0	125.0000	-125.0	125.0000	-16.00	235.0000				
1	1	-2	-3	-8	-10	-11	-12	-13	-14	z1001
	-15	-16	-17	-18	-19	-20	-21	-22	-23	air
	-24	-25	-28	-29	-30	-31	-32	-33	-34	
	-35	-36	-37	-38	-39	-40	-41	-42	-43	
	-44	-45	-46	-47	-48					
2	2	-3	-10	-11	-12	-13	-14	-15	-16	z1002
	-17	-18	-19	-20	-21					base
3	3	-4	-5	-6	-7	-8	-9	-10	-11	z1003
	-12	-13	-14	-15	-16	-17	-29	-30	-31	base
	-32									
4 or	4or	5or	6or	7						z1004
5	8	-9	-26	-27	-28	-44	-45	-46	-47	z1005
6	9	-4	-5	-6	-7	-26	-27	-28	-44	z1006
	-45	-46	-47							air
7 or	10or	11or	12or	13or	14or	15or	16or	17		z1007
8 or	18	-22or	19	-23or	20	-24or	21	-25		z1008
9 or	22or	23or	24or	25						z1009
10	26									z1010
11	27									z1011
12	28	-3								z1012
13	29	-8	-30	-32	-33	-36	-44	-45		z1013
14	30	-8	-33	-35	-37	-28				z1014
15	31	-8	-30	-32	-33	-38	-46	-47		z1015
16	32	-8	-33	-39						z1016
17	33	-8	-34	-36	-37	-38	-39			z1017

Figure C-7. (continued)

18 or	36	-40or	37	-41or	38	-42or	39	-43	z1018
19 or	40or	41or	42or	43					z1019
20 or	44or	45or	46or	47					z1020
21	34	-26							z1021
22	35	-27							z1022
23	48	-2							z1023
24	49	-1							z1024
-1									
1	1001	0	2	0	/box/z1001/surounding/air				
2	1002	0	3	0	/box/z1002/bottom/base/pad				
3	1003	0	3	0	/box/z1003/upper/base/pad				
4	1004	0	3	0	/box/z1004/inner/alignment/pad				
5	1005	0	3	0	/box/z1005/inner/box				
6	1006	0	2	0	/box/z1006/inner/box/air-void				
7	1007	0	3	0	/box/z1007/outer/wall/alignment/pad				
8	1008	0	3	0	/box/z1008/base/pad/lift/eyelets				
9	1009	0	2	0	/box/z1009/eyelets/voids-air				
10	1010	0	3	0	/box/z1010/inner/box/top/hatch				
11	1011	0	3	0	/box/z1011/inner/box/side/hatch				
12	1012	0	2	0	/box/z1012/inner/outer/cable/run/void-air				
13	1013	0	3	0	/box/z1013/outer/wall/negative/y-axis				
14	1014	0	3	0	/box/z1014/outer/wall/positive/x-axis				
15	1015	0	3	0	/box/z1015/outer/wall/positive/y-axis				
16	1016	0	3	0	/box/z1016/outer/wall/negative/x-axis				
17	1017	0	3	0	/box/z1017/outer/top				
18	1018	0	3	0	/box/z1018/outer/wall/lift/eyelets				
19	1019	0	2	0	/box/z1019/outer/wall/lift/eyelets/void-air				
20	1020	0	2	0	/box/z1020/inner/outer/drain/holes				
21	1021	0	3	0	/box/z1021/outer/top/hatch				
22	1022	0	3	0	/box/z1022/outer/wall/side/hatch				
23	1023	0	1	0	/box/z1023/ground				
24	1024	0	0	0	/box/z1024/external/void				

Figure C-7. (continued)

```

aprf aog/400m/16.14m ss90-130-39 s90e5 5/90 exp. ph+det LAH(t)
$$ 1000 1500 200 1 46 23 46 69 0 1 400 9 0
$$ 0 69 1 0
** 1.0 1.0-05 1.0+04 0.0 2.2+05
** 0.0 -24.5057 93.71 0.0 0.0 0.0 0.0
** 69r1.0
** 8r1.0 11r2.0 8r4.0 3r2.0 16r1.0 3r3.0 12r6.0 8r3.0
** 1.9640+7 1.6905+7 1.4918+7 1.4191+7 1.3840+7 1.2523+7 1.2214+7
1.1052+7 1.0000+7 9.0484+6 8.1873+6 7.4082+6 6.3763+6 4.9658+6
4.7237+6 4.0657+6 3.0119+6 2.3852+6 2.3069+6 1.8268+6 1.4227+6
1.1080+6 9.6164+5 8.2085+5 7.4274+5 6.3927+5 5.5023+5 3.6883+5
2.4724+5 1.5764+5 1.1109+5 5.2475+4 3.4307+4 2.4788+4 2.1875+4
1.0595+4 3.3546+3 1.2341+3 5.8295+2 2.7536+2 1.0130+2 2.9023+1
1.0677+1 3.0590+0 1.12535+0 4.1399-1 2.0000+7 1.4000+7 1.2000+7
1.0000+7 8.0000+6 7.0000+6 6.0000+6 5.0000+6 4.0000+6 3.0000+6
2.5000+6 2.0000+6 1.5000+6 1.0.00+6 7.0000+5 4.5500+5 3.0000+5
1.5000+5 1.0000+5 7.0000+4 4.5000+4 3.0000+4 2.0000+4
0000343277764511
$$ 1 1 0 0 0 1 69 1
$$ 1 1 69 1 1 1 ** 5.0+00 5.0-02 2.0-01 0.0
$$ -1 9r0
$$ 0 0 0 0
** 23r1.0
0000000000 0.001 0.0001 0 0 0
1 1
15
2 1
14
4 2
5 6
5 7
1 2 3 4 16 17 18
6 7
7 8 9 10 11 12 13
7 15
20 21 22 23 24 25 26 27 28 29 30 31 32 33
34
8 1
19
0 1
35
1 1 1 1 1 1 1 1 1 1 1 1 1 1
1 1 1 1 1 1 1 1 1 1 1 1 1 1
1 1 1 1 1 1 1 1 1 1 1 1 1 1
2m box exp/aprf 5/90 exp. ss90-130-39 s90e5, 1020 steel + phantom n.d.
$$ 46 46 23 23 69 72 4 9 24 67 6 3 0 3
$$ 7z -2 3z
2m ph+det LAH(t)
** 1.0
$$ 1 2

```

Figure C-8. Sample MORSE Input for the MASH Analysis of the Combinatorial Geometry Phantom (with BD-100R Detectors) Used in the APRF Spring 1990 Two-Meter Box Test Bed Experiments.

cm 70kg phantom with arms and detectors
 89 35
 1ell .0000 .0000 177.1500 10.000 .0000 .0000
 1 7.5650
 2rec .0000 .0000 164.3000 .0000 .0000 12.8500
 2 10.0000 .0000 .0000 .0000 -8.0000 .0000
 3rec .0000 .0000 90.3000 .0000 .0000 70.0000
 3 .0000 19.2000 .0000 -10.0000 .0000 .0000
 4tec .0000 4.6000 10.3000 .0000 5.0000 80.0000
 4 .0000 4.0000 .0000 -4.0000 .0000 .0000
 4 2.0000
 5tec .0000 -4.6000 10.3000 .0000 -5.0000 80.0000
 5 .0000 4.0000 .0000 -4.0000 .0000 .0000
 5 2.0000
 6rcc .0000 .0000 160.3000 .0000 .0000 4.0000
 6 7.0000
 7arb -10.0000 -10.0000 90.3000 -9.5200 -9.5200 85.5000
 7 -9.5200 9.5200 85.5000 -10.0000 10.0000 90.3000
 7 .0000 9.5200 85.5000 .0000 10.0000 90.3000
 7 .0000 -10.0000 90.3000 .0000 -9.5200 85.5000
 7 1234 4356 6587 7821 7146 2358
 8rpp -50.0000 50.0000 -50.0000 50.0000 -15.0000 230.0000
 9rpp -50.0000 50.0000 -50.0000 50.0000 -15.0000 0.0000
 10ell .0000 8.5000 133.8000 .0000 .0000 24.0000
 10 6.1070
 11rpp -6.1237 1.5000 .0000 5.4000 136.3000 144.3000
 12rec .0000 .0000 91.3000 .0000 .0000 42.5000
 12 .0000 16.4900 .0000 -9.2900 .0000 .0000
 13ell .0000 -8.5000 133.8000 .0000 .0000 24.0000
 13 6.1070
 14rpp -6.1237 1.0000 -8.0000 .0000 133.8000 145.3000
 15ell .0000 .0000 177.1500 9.5000 .0000 .0000
 15 7.0660
 16ell 0.0000 .0000 177.1500 6.0000 .0000 .0000
 16 6.1610
 17rec 5.5000 .0000 112.3000 .0000 .0000 48.0000
 17 -2.5000 .0000 .0000 .0000 2.0000 .0000
 18tec .0000 21.5338 90.3000 .0000 -.7000 69.0000
 18 .0000 2.0000 .0000 -1.0370 .0000 .0000
 18 1.3500
 19tec .0000 -21.5338 90.3000 .0000 .7000 69.0000
 19 .0000 2.0000 .0000 -1.0370 .0000 .0000
 19 1.3500
 20tec .0000 4.6000 10.5000 .0000 5.0000 79.8000
 20 .0000 2.2727 .0000 -2.2727 .0000 .0000
 20 1.1000

Figure C-9. Sample Geometry Input for the MASH Analysis of the Combinatorial Geometry Phantom (with BD-100R Detectors) Used in the APRF Spring 1990 Two-Meter Box Test Bed Experiments.

21tec	.0000	-4.6000	10.5000	.0000	-5.0000	79.8000
21	.0000	2.2727	.0000	-2.2727	.0000	.0000
21	1.1000					
22rec	-3.0000	.0000	90.3000	.0000	.0000	22.0000
22	.0000	12.0000	.0000	-12.0000	.0000	.0000
23rec	-3.8000	.0000	90.3000	.0000	.0000	22.0000
23	.0000	11.3000	.0000	-11.3000	.0000	.0000
24rpp	-15.5000	-3.0000	-12.0000	12.0000	90.3000	112.3000
25rpp	5.0000	10.0000	-10.0000	10.0000	90.3000	104.3000
26rec	.0000	.0000	125.4000	.0000	.0000	32.2000
26	.0000	17.0000	.0000	-9.8000	.0000	.0000
27rec	.0000	.0000	125.4000	.0000	.0000	32.2000
27	.0000	16.5000	.0000	-9.3000	.0000	.0000
28rec	.0000	.0000	126.8000	.0000	.0000	1.4000
28	.0000	17.0000	.0000	-9.8000	.0000	.0000
29rec	.0000	.0000	129.6000	.0000	.0000	1.4000
29	.0000	17.0000	.0000	-9.8000	.0000	.0000
30rec	.0000	.0000	132.4000	.0000	.0000	1.4000
30	.0000	17.0000	.0000	-9.8000	.0000	.0000
31rec	.0000	.0000	135.2000	.0000	.0000	1.4000
31	.0000	17.0000	.0000	-9.8000	.0000	.0000
32rec	.0000	.0000	138.0000	.0000	.0000	1.4000
32	.0000	17.0000	.0000	-9.8000	.0000	.0000
33rec	.0000	.0000	140.8000	.0000	.0000	1.4000
33	.0000	17.0000	.0000	-9.8000	.0000	.0000
34rec	.0000	.0000	143.6000	.0000	.0000	1.4000
34	.0000	17.0000	.0000	-9.8000	.0000	.0000
35rec	.0000	.0000	146.4000	.0000	.0000	1.4000
35	.0000	17.0000	.0000	-9.8000	.0000	.0000
36rec	.0000	.0000	149.2000	.0000	.0000	1.4000
36	.0000	17.0000	.0000	-9.8000	.0000	.0000
37rec	.0000	.0000	152.0000	.0000	.0000	1.4000
37	.0000	17.0000	.0000	-9.8000	.0000	.0000
38rec	.0000	.0000	154.8000	.0000	.0000	1.4000
38	.0000	17.0000	.0000	-9.8000	.0000	.0000
39rec	.0000	.0000	160.3000	.0000	.0000	9.2700
39	-2.5000	.0000	.0000	.0000	2.0000	.0000
40rcc	11.1000	.0000	157.8514	.0000	.0000	1.3972
40	20.6986					
41rcc	11.1000	.0000	157.8514	.0000	.0000	1.3972
41	19.3014					
42raw	-15.7245	-30.0000	157.8514	26.8245	30.0000	.0000
42	-25.2690	22.5943	.0000	.0000	.0000	1.3972
43raw	-15.7245	30.0000	157.8514	26.8245	-30.0000	.0000
43	-25.2690	-22.5943	.0000	.0000	.0000	1.3972
44rec	.0000	.0000	141.2000	.0000	.0000	16.4000
44	.0000	19.0000	.0000	-9.8000	.0000	.0000
45rec	.0000	.0000	141.2000	.0000	.0000	16.4000
45	.0000	17.0000	.0000	-9.8000	.0000	.0000
46sph	.0000	.0000	90.3000	1.0000		

Figure C-9. (continued)

47raw	7.5000	-30.0000	141.2000	-7.5000	30.0000	.0000
47	13.7500	3.4375	.0000	.0000	.0000	16.4000
48sph	.0000	.0000	90.3000	1.0000		
49raw	7.5000	30.0000	141.2000	-7.5000	-30.0000	.0000
49	13.7500	-3.4375	.0000	.0000	.0000	16.4000
50rec	.0000	.0000	164.3000	.0000	.0000	10.7300
50	9.0000	.0000	.0000	.0000	-7.0000	.0000
51rec	.0000	.0000	164.3000	.0000	.0000	10.7300
51	7.6000	.0000	.0000	.0000	-5.6000	.0000
52rpp	-15.0000	.0000	-15.0000	15.0000	164.3000	175.0300
53sph	.0000	10.0000	142.3000	0.3600		
54sph	.0000	-10.0000	142.3000	0.3600		
55rec	.0000	.0000	90.3000	.0000	.0000	70.0000
55	.0000	17.2000	.0000	-10.0000	.0000	.0000
56rpp	.0000	15.0000	-17.2000	17.2000	90.3000	160.3000
57trc	.0000	21.5338	160.3000	.0000	.0000	-70.0000
57	4.3238	2.1619				
58trc	.0000	-21.5338	160.3000	.0000	.0000	-70.0000
58	4.3238	2.1619				
59rcc	-4.0	0.0	177.1500	8.0	0.0	0.0
59	0.8					
60rcc	-3.9843	0.0	177.1500	7.9746	0.0	0.0
60	0.7873					
61rcc	-10.82	-5.88	145.06	0.0	0.0	8.0
61	0.8					
62rcc	-10.82	-5.88	145.0727	0.0	0.0	7.9746
62	0.7873					
63rcc	-10.82	-7.49	145.06	0.0	0.0	8.0
63	0.8					
64rcc	-10.82	-7.49	145.0727	0.0	0.0	7.9746
64	0.7873					
65rcc	-10.82	-9.10	145.06	0.0	0.0	8.0
65	0.8					
66rcc	-10.82	-9.10	145.0727	0.0	0.0	7.9746
66	0.7873					
67rcc	-10.82	1.61	112.04	0.0	0.0	8.0
67	0.8					
68rcc	-10.82	1.61	112.0527	0.0	0.0	7.9746
68	0.7873					
69rcc	-10.82	0.0	112.04	0.0	0.0	8.0
69	0.8					
70rcc	-10.82	0.0	112.0527	0.0	0.0	7.9746
70	0.7873					
71rcc	-10.82	-1.61	112.04	0.0	0.0	8.0
71	0.8					
72rcc	-10.82	-1.61	112.0527	0.0	0.0	7.9746
72	0.7873					
73rcc	10.82	1.61	112.04	0.0	0.0	8.0

Figure C-9. (continued)

73	0.8						
74rcc	10.82	1.61	112.0527	0.0	0.0	7.9746	
74	0.7873						
75rcc	10.82	0.0	112.04	0.0	0.0	8.0	
75	0.8						
76rcc	10.82	0.0	112.0527	0.0	0.0	7.9746	
76	0.7873						
77rcc	10.82	-1.61	112.04	0.0	0.0	8.0	
77	0.8						
78rcc	10.82	-1.61	112.0527	0.0	0.0	7.9746	
78	0.7873						
79rcc	-4.0	0.0	116.04	8.0	0.0	0.0	
79	0.8						
80rcc	-3.9873	0.0	116.04	7.9746	0.0	0.0	
80	0.7873						
81rcc	-2.9719	22.3438	91.3	0.0	0.0	8.0	
81	0.8						
82rcc	-2.9719	22.3438	91.3127	0.0	0.0	7.9746	
82	0.7873						
83rcc	-2.9719	20.7238	91.3	0.0	0.0	8.0	
83	0.8						
84rcc	-2.9719	20.7238	91.3127	0.0	0.0	7.9746	
84	0.7873						
85rcc	-4.0	-24.5057	93.71	8.0	0.0	0.0	
85	0.8						
86rcc	-3.9873	-24.5057	93.71	7.9746	0.0	0.0	
86	0.7873						
87rcc	-4.0	-24.5057	92.1	8.0	0.0	0.0	
87	0.8						
88rcc	-3.9873	-24.5057	92.1	7.9746	0.0	0.0	
88	0.7873						
89rpp	-60.0000	60.0000	-60.0000	60.0000	-16.5000	235.0000	
1 or	1	-15	-39	-50	-59	-60	
or	2	-15	-39	-50	-59	-60	
or	16	-59	-60				
or	2	-15	-39	-52	-59	-60	
or	2	-15	-39	51	-59	-60	
or	6	-39					
2 or	3	-10	-13	-17	-18	-19	-22
	-44	-80	56	-79	-80	-53	-54
or	55	-10	-13	-17	-18	-19	-22
	-44	-79	-80				
or	11	-17	-13				
or	14	-17	-10				
or	12	-22	-17	-79	-80		
or	23	3	56	-79	-80		
or	24	55	-79	-80			
or	25	3	56	-79	-80		

Figure C-9. (continued)

or	23	55								
or	27	-10	-13	-17	or	28	-10	-13	-17	
or	29	-10	-13	-17	or	30	-10	-13	-17	
or	31	-10	-13	-17	or	32	-10	-13	-17	
or	33	-10	-13	-17	or	34	-10	-13	-17	
or	35	-10	-13	-17	or	36	-10	-13	-17	
or	37	-10	-13	-17	or	38	-10	-13	-17	
or	41	-10	-13	-17		-18	-19	3	56	
or	41	-10	-13	-17		-18	-19	55		
or	40	-42	-43	-41		-18	-19	3	56	
or	40	-42	-43	-41		-18	-19	55		
or	44	-47	-49	-26		55				
or	44	-47	-49	-26		56				
3 or	4	-20	or	5	-21					
4	7	-4	-5	-20	-21					
5	10	-11	-12							
6	13	-14	-12							
7 or	15	-16	-59	or	17	-79	or	39	-79	
8 or	18	or	19							
9 or	20	or	21							
10	22	-23	-24	-25	-17					
11	26	-27	-28	-29	-30	-31	-32	-33	-34	
	-35	-36	-37	-38						
12 or	40	-41	42	-20	-21					
	or	40	-41	43	-20	-21				
13 or	44	-26	47	or	44	-26	49			
14 or	8	-1	-2	-3	-4	-5	-7	-53	-54	
	-6	-57	-58	-61	-63	-65	-67	-69	-71	
	-73	-75	-77	-79	-83	-85	-87	-9	-81	
or	8	-1	-2	-55	-4	-5	-7	-53	-54	
	-6	-57	-58	-56	-9	-61	-63	-65	-67	
	-69	-71	-73	-75	-77	-79	-83	-85	-87	
	-81									
15	9									
16	50	52	-51	-15						
17 or	54	-55	or	53	-55					
18 or	57	-18	-81	-83	or	58	-19	-85	-87	
19 or	59	-60	or	61	-62	or	63	-64	or	
	or	67	-68	or	69	-70	or	71	-72	or
	or	75	-76	or	77	-78	or	79	-80	or
	or	83	-84	or	85	-86	or	87	-88	
20	60									
21	62									
22	64									
23	66									
24	68									
25	70									
26	72									

Figure C-9. (continued)

27	74					
28	76					
29	78					
30	80					
31	82					
32	84					
33	86					
34	88					
35	89	-8				
-1						
1	1	0	5	100	/phantom/z1001/flesh/head-neck	
2	1	0	5	100	/phantom/z1002/flesh/torso	
3	2	0	5	100	/phantom/z1003/flesh/legs	
4	2	0	5	100	/phantom/z1004/sex/organ	
5	2	0	4	90	/phantom/z1005/internal/left/lung	
6	2	0	4	90	/phantom/z1006/internal/right/lung	
7	2	0	6	100	/phantom/z1007/skeletal/skull/neck/spinal	
8	2	0	6	100	/phantom/z1008/skeletal/arms	
9	2	0	6	100	/phantom/z1009/skeletal/legs	
10	2	0	6	100	/phantom/z1010/skeletal/hip	
11	2	0	6	100	/phantom/z1011/skeletal/ribs	
12	3	0	6	100	/phantom/z1012/skeletal/pelvis	
13	13	0	6	100	/phantom/z1013/skeletal/shoulder/blades	
14	3	0	2	100	/phantom/z1014/surrounding/air	
15	3	0	1	100	/phantom/z1015/15-cm/ground	
16	13	0	5	100	/phantom/z1016/flesh/throat	
17	3	0	5	100	/phantom/z1017/flesh/breasts	
18	3	0	5	100	/phantom/z1018/flesh/arms	
19	1106	0	8	100	/detectors/z1041/containers	
20	1107	0	7	100	/detector/z1042/mid-head	
21	1109	0	7	100	/detector/z1043/left-chest 1	
22	1111	0	7	100	/detector/z1044/left-chest 2	
23	1113	0	7	100	/detector/z1045/left-chest 3	
24	1115	0	7	100	/detector/z1046/front/mid-gut 1	
25	1117	0	7	100	/detector/z1047/front/mid-gut 2	
26	1119	0	7	100	/detector/z1048/front/mid-gut 3	
27	1121	0	7	100	/detector/z1049/rear/mid-gut 1	
28	1123	0	7	100	/detector/z1050/rear/mid-gut 2	
29	1125	0	7	100	/detector/z1051/rear/mid-gut 3	
30	1127	0	7	100	/detector/z1052/inner/mid-gut	
31	1129	0	7	100	/detector/z1053/rt. arm/outer	
32	1131	0	7	100	/detector/z1054/rt. arm/inner	
33	1133	0	7	100	/detector/z1055/left-arm/top	
34	1135	0	7	100	/detector/z1056/left-arm/bottom	
35	0	0	0	100	/external void	

Figure C-9. (continued)

```

aprf aog/400m/16.14m ss90-124-32 s90e5 5/90 exp. box+ph+det LAH(t)
$$ 1000 1500 500   1   46   23   46   69   0   1   350   9   0
$$ 0   69   1   0
** 1.0   1.0-05   1.0+04   0.0   2.2+05
** 0.0   -24.5057   93.71   0.0   0.0   0.0   0.0
** 69r1.0
** 8r1.0 13r2.0 10r3.0 5r2.0 10r1.0 4r3.0 15r5.0 4r3.0
** 1.9640+7   1.6905+7   1.4918+7   1.4191+7   1.3840+7   1.2523+7   1.2214+7
    1.1052+7   1.0000+7   9.0484+6   8.1873+6   7.4082+6   6.3763+6   4.9658+6
    4.7237+6   4.0657+6   3.0119+6   2.3852+6   2.3069+6   1.8268+6   1.4227+6
    1.1080+6   9.6164+5   8.2085+5   7.4274+5   6.3927+5   5.5023+5   3.6883+5
    2.4724+5   1.5764+5   1.1109+5   5.2475+4   3.4307+4   2.4788+4   2.1875+4
    1.0595+4   3.3546+3   1.2341+3   5.8295+2   2.7536+2   1.0130+2   2.9023+1
    1.0677+1   3.0590+0   1.12535+0   4.1399-1   2.0000+7   1.4000+7   1.2000+7
    1.0000+7   8.0000+6   7.0000+6   6.0000+6   5.0000+6   4.0000+6   3.0000+6
    2.5000+6   2.0000+6   1.5000+6   1.0.00+6   7.0000+5   4.5500+5   3.0000+5
    1.5000+5   1.0000+5   7.0000+4   4.5000+4   3.0000+4   2.0000+4
0000344226777715
$$   1   1   0   0   0   7   69   1
$$   1   1   46   1   1   1   **   5.0+00   5.0-02   5.0-01   0.0
$$   1   1   46   2   1   2   **   5.0+00   5.0-02   5.0-01   0.0
$$   1   1   46   3   1   3   **   5.0+00   5.0-02   5.0-01   0.0
$$   1   1   46   4   1   4   **   4.0+00   4.0-02   4.0-01   0.0
$$   1   1   46   5   1   5   **   3.0+00   3.0-02   3.0-01   0.0
$$   1   1   46   6   1   6   **   4.0+00   4.0-02   4.0-01   0.0
$$   1   1   46   7   1   7   **   4.0+00   4.0-02   4.0-01   0.0
$$   47   1   69   1   1   1   **   5.0+00   5.0-02   5.0-01   0.0
$$   47   1   69   2   1   2   **   5.0+00   5.0-02   5.0-01   0.0
$$   47   1   69   3   1   3   **   5.0+00   5.0-02   5.0-01   0.0
$$   47   1   69   4   1   4   **   4.0+00   4.0-02   4.0-01   0.0
$$   47   1   69   5   1   5   **   3.0+00   3.0-02   3.0-01   0.0
$$   47   1   69   6   1   6   **   4.0+00   4.0-02   4.0-01   0.0
$$   47   1   69   7   1   7   **   4.0+00   4.0-02   4.0-01   0.0
$$   -1   9r0
$$   0   0   0   0
** 23r1.0
0000000000   0.001   0.0001   0   0   0

```

Figure C-10. Sample MORSE Input for the MASH Analysis of the Combinatorial Geometry Phantom (with BD-100R Detectors) Standing in the Two-Meter Box Used in the APRF Spring 1990 Two-Meter Box Test Bed Experiments.

```

1   1
23
2   6
1   6   9   12   19   20
3   16
2   3   4   5   7   8   10   11   13   14   15   16   17   18
21  22
4   2
29  30
5   7
25  26   27   28   38   39   40
6   7
31  32   33   34   35   36   37
7   18
42  43   44   45   46   47   48   49   50   51   52   53   54   55
56  57   58   59
8   1
41
0   1
24
7   5   4   4   3   5   5   7   4   4   7   5   5
5   5   5   5   7   7   5   5   6   7   2   2   2
2   2   2   2   2   2   2   2   2   2   2   1   1
1   1   1   1   1   1   1   1   1   1   1   1   1
1   1   1
2m box exp/aprf 5/90 exp. ss90-124-32 s90e5, 1020 steel + phantom n.d.
$$ 46   46   23   23   69   72   4   9   24   67   6   3   0   3
$$ 7z   -2   3z
2m box+ph+det LAH(t)
** 7r1.0
$$ 1   2

```

Figure C-10 (continued)
95

cm 2.0 m box geom. (4" of steel) with phantom & all detectors
 141 59
 1rpp -120.0000 120.0000 -120.0000 120.0000 -15.0000 230.0000
 2rpp -115.2398 115.2398 -115.2398 115.2398 0.0000 5.0800
 3rpp -110.1598 110.1598 -110.1598 110.1598 5.0800 10.1600
 4rpp -99.9998 -89.8398 -99.9998 -89.8398 10.1600 15.2400
 5rpp 89.8398 99.9998 -99.9998 -89.8398 10.1600 15.2400
 6rpp 89.8398 99.9998 89.8398 99.9998 10.1600 15.2400
 7rpp -99.9998 -89.8398 89.8398 99.9998 10.1600 15.2400
 8rpp -105.0798 105.0798 -105.0798 105.0798 10.1600 215.2396
 9rpp -99.9998 99.9998 -99.9998 99.9998 10.1600 210.1596
 10rpp -79.6798 -69.5198 -112.0598 -110.1598 5.0800 15.2400
 11rpp 69.5198 79.6798 -112.0598 -110.1598 5.0800 15.2400
 12rpp 110.1598 112.0598 -79.6798 -69.5298 5.0800 15.2400
 13rpp 110.1598 112.0598 69.5298 79.6798 5.0800 15.2400
 14rpp 69.5198 79.6798 110.1598 112.0598 5.0800 15.2400
 15rpp -79.6798 -69.5198 110.1598 112.0598 5.0800 15.2400
 16rpp -112.0598 -110.1598 69.5198 79.6798 5.0800 15.2400
 17rpp -112.0598 -110.1598 -79.6798 -69.5198 5.0800 15.2400
 18rpp -99.9998 -89.8398 -117.1398 -115.2398 0.0000 15.2400
 19rpp 89.8398 99.9998 -117.1398 -115.2398 0.0000 15.2400
 20rpp 89.8398 99.9998 115.2398 117.1398 0.0000 15.2400
 21rpp -99.9998 -89.8398 115.2398 117.1398 0.0000 15.2400
 22rcc -94.9198 -117.1398 10.1600 0.0000 1.9000 0.0000
 2.5400
 23rcc 94.9198 -117.1398 10.1600 0.0000 1.9000 0.0000
 2.5400
 24rcc 94.9198 115.2398 10.1600 0.0000 1.9000 0.0000
 2.5400
 25rcc -94.9198 115.2398 10.1600 0.0000 1.9000 0.0000
 2.5400
 26rcc 0.0000 0.0000 210.1596 0.0000 0.0000 5.0800
 25.4000
 27rcc 99.9998 0.0000 110.1598 5.0800 0.0000 0.0000
 25.4000
 28rcc 99.9998 -49.1998 10.1600 10.1600 0.0000 0.0000
 5.0800
 29rpp -110.1598 110.1598 -110.1598 -105.0798 10.1600 215.2396
 30rpp 105.0798 110.1598 -105.0798 105.0798 10.1600 215.2396
 31rpp -110.1598 110.1598 105.0798 110.1598 10.1600 215.2396
 32rpp -110.1598 -105.0798 -105.0798 105.0798 10.1600 215.2396
 33rpp -110.1598 110.1598 -110.1598 110.1598 215.2396 220.3196
 34rcc 0.0000 0.0000 215.2396 0.0000 0.0000 5.0800
 37.4650
 35rcc 105.0798 0.0000 110.1598 5.0800 0.0000 0.0000
 37.4650

Figure C-11. Sample Geometry Input for the MASH Analysis of the
 Combinatorial Geometry Phantom (with BD-100R Detectors)
 Standing in the Two-Meter Box Used in the APRF
 Spring 1990 Two-Meter Box Test Bed Experiments.

36rpp	-5.0800	5.0800	-112.0598	-110.1598	205.1596	228.0196
37rpp	110.1598	112.0598	-5.0800	5.0800	205.1596	228.0196
38rpp	-5.0800	5.0800	110.1598	112.0598	205.1596	228.0196
39rpp	-112.0598	-110.1598	-5.0800	5.0800	205.1596	228.0196
40rcc	0.0000	-112.0598	222.9396	0.0000	1.9000	0.0000
	2.5400					
41rcc	110.1598	0.0000	222.9396	1.9000	0.0000	0.0000
	2.5400					
42rcc	0.0000	110.1598	222.9396	0.0000	1.9000	0.0000
	2.5400					
43rcc	-112.0598	0.0000	222.9396	1.9000	0.0000	0.0000
	2.5400					
44rcc	-85.0000	-110.1598	11.4300	0.0000	10.1600	0.0000
	1.2700					
45rcc	85.0000	-110.1598	11.4300	0.0000	10.1600	0.0000
	1.2700					
46rcc	85.0000	99.9998	11.4300	0.0000	10.1600	0.0000
	1.2700					
47rcc	-85.0000	99.9998	11.4300	0.0000	10.1600	0.0000
	1.2700					
48rpp	-120.0000	120.0000	-120.0000	120.0000	-15.0000	0.0000
49rpp	-125.0	125.0000	-125.0	125.0000	-16.00	235.0000
50ell	.0000	.0000	177.1500	10.000	.0000	.0000
50	7.5650					
51rec	.0000	.0000	164.3000	.0000	.0000	12.8500
51	10.0000	0.0000	.0000	0.0000	-8.0000	.0000
52rec	.0000	.0000	90.3000	.0000	.0000	70.0000
52	.0000	19.2000	.0000	-10.0000	.0000	.0000
53tec	.0000	4.6000	10.3000	.0000	5.0000	80.0000
53	.0000	4.0000	.0000	-4.0000	.0000	.0000
53	2.0000					
54tec	.0000	-4.6000	10.3000	.0000	-5.0000	80.0000
54	.0000	4.0000	.0000	-4.0000	.0000	.0000
54	2.0000					
55rcc	.0000	.0000	160.3000	.0000	.0000	4.0000
55	7.0000					
56arb	-10.0000	-10.0000	90.3000	-9.5200	-9.5200	85.5000
56	-9.5200	9.5200	85.5000	-10.0000	10.0000	90.3000
56	.0000	9.5200	85.5000	.0000	10.0000	90.3000
56	.0000	-10.0000	90.3000	.0000	-9.5200	85.5000
56	1234	4356	6587	7821	7146	2358
57ell	.0000	8.5000	133.8000	.0000	.0000	24.0000
57	6.1070					
58rpp	-6.1237	1.5000	.0000	5.4000	136.3000	144.3000
59rec	.0000	.0000	91.3000	.0000	.0000	42.5000
59	.0000	16.4900	.0000	-9.2900	.0000	.0000
60ell	.0000	-8.5000	133.8000	.0000	.0000	24.0000
60	6.1070					

Figure C-11. (continued)

61rpp	-6.1237	1.0000	-8.0000	.0000	133.8000	145.3000
62ell	.0000	.0000	177.1500	9.5000	.0000	.0000
62	7.0660					
63ell	0.0000	.0000	177.1500	6.0000	.0000	.0000
63	6.1610					
64rec	5.5000	.0000	112.3000	.0000	.0000	48.0000
64	-2.5000	.0000	.0000	.0000	2.0000	.0000
65tec	.0000	21.5338	90.3000	.0000	-.7000	69.0000
65	.0000	2.0000	.0000	-1.0370	.0000	.0000
65	1.3500					
66tec	.0000	-21.5338	90.3000	.0000	.7000	69.0000
66	.0000	2.0000	.0000	-1.0370	.0000	.0000
66	1.3500					
67tec	.0000	4.6000	10.5000	.0000	5.0000	79.8000
67	.0000	2.2727	.0000	-2.2727	.0000	.0000
67	1.1000					
68tec	.0000	-4.6000	10.5000	.0000	-5.0000	79.8000
68	.0000	2.2727	.0000	-2.2727	.0000	.0000
68	1.1000					
69rec	-3.0000	.0000	90.3000	.0000	.0000	22.0000
69	.0000	12.0000	.0000	-12.0000	.0000	.0000
70rec	-3.8000	.0000	90.3000	.0000	.0000	22.0000
70	.0000	11.3000	.0000	-11.3000	.0000	.0000
71rpp	-15.5000	-3.0000	-12.0000	12.0000	90.3000	112.3000
72rpp	5.0000	10.0000	-10.0000	10.0000	90.3000	104.3000
73rec	.0000	.0000	125.4000	.0000	.0000	32.2000
73	.0000	17.0000	.0000	-9.8000	.0000	.0000
74rec	.0000	.0000	125.4000	.0000	.0000	32.2000
74	.0000	16.5000	.0000	-9.3000	.0000	.0000
75rec	.0000	.0000	126.8000	.0000	.0000	1.4000
75	.0000	17.0000	.0000	-9.8000	.0000	.0000
76rec	.0000	.0000	129.6000	.0000	.0000	1.4000
76	.0000	17.0000	.0000	-9.8000	.0000	.0000
77rec	.0000	.0000	132.4000	.0000	.0000	1.4000
77	.0000	17.0000	.0000	-9.8000	.0000	.0000
78rec	.0000	.0000	135.2000	.0000	.0000	1.4000
78	.0000	17.0000	.0000	-9.8000	.0000	.0000
79rec	.0000	.0000	138.0000	.0000	.0000	1.4000
79	.0000	17.0000	.0000	-9.8000	.0000	.0000
80rec	.0000	.0000	140.8000	.0000	.0000	1.4000
80	.0000	17.0000	.0000	-9.8000	.0000	.0000
81rec	.0000	.0000	143.6000	.0000	.0000	1.4000
81	.0000	17.0000	.0000	-9.8000	.0000	.0000
82rec	.0000	.0000	146.4000	.0000	.0000	1.4000
82	.0000	17.0000	.0000	-9.8000	.0000	.0000
83rec	.0000	.0000	149.2000	.0000	.0000	1.4000
83	.0000	17.0000	.0000	-9.8000	.0000	.0000
84rec	.0000	.0000	152.0000	.0000	.0000	1.4000
84	.0000	17.0000	.0000	-9.8000	.0000	.0000

Figure C-11. (continued)

85rec	.0000	.0000	154.8000	.0000	.0000	1.4000
85	.0000	17.0000	.0000	-9.8000	.0000	.0000
86rec	.0000	.0000	160.3000	.0000	.0000	9.2700
86	-2.5000	.0000	.0000	.0000	2.0000	.0000
87rcc	11.1000	.0000	157.8514	.0000	.0000	1.3972
87	20.6986					
88rcc	11.1000	.0000	157.8514	.0000	.0000	1.3972
88	19.3014					
89raw	-15.7245	-30.0000	157.8514	26.8245	30.0000	.0000
89	-25.2690	22.5943	.0000	.0000	.0000	1.3972
90raw	-15.7245	30.0000	157.8514	26.8245	-30.0000	.0000
90	-25.2690	-22.5943	.0000	.0000	.0000	1.3972
91rec	.0000	.0000	141.2000	.0000	.0000	16.4000
91	.0000	19.0000	.0000	-9.8000	.0000	.0000
92rec	.0000	.0000	141.2000	.0000	.0000	16.4000
92	.0000	17.0000	.0000	-9.8000	.0000	.0000
93sph	.0000	.0000	90.3000	1.0000		
94raw	7.5000	-30.0000	141.2000	-7.5000	30.0000	.0000
94	13.7500	3.4375	.0000	.0000	.0000	16.4000
95sph	.0000	.0000	90.3000	1.0000		
96raw	7.5000	30.0000	141.2000	-7.5000	-30.0000	.0000
96	13.7500	-3.4375	.0000	.0000	.0000	16.4000
97rec	.0000	.0000	164.3000	.0000	.0000	10.7300
97	9.0000	0.0000	.0000	.0000	-7.0000	.0000
98rec	.0000	.0000	164.3000	.0000	.0000	10.7300
98	7.6000	0.0000	.0000	.0000	-5.6000	.0000
99rpp	-15.0000	.0000	-15.0000	15.0000	164.3000	175.0300
100sph	-8.6602	10.0000	142.3000	0.3600		
101sph	-8.6602	-10.0000	142.3000	0.3600		
102rec	.0000	.0000	90.3000	.0000	.0000	70.0000
102	.0000	17.2000	.0000	-10.0000	.0000	.0000
103rpp	.0000	15.0000	-17.2000	17.2000	90.3000	160.3000
104trc	.0000	21.5338	160.3000	.0000	.0000	-70.0000
104	4.3238	2.1619				
105trc	.0000	-21.5338	160.3000	.0000	.0000	-70.0000
105	4.3238	2.1619				
106rcc	-4.0	0.0	177.1500	8.0	0.0	0.0
106	0.8					
107rcc	-3.9843	0.0	177.1500	7.9746	0.0	0.0
107	0.7873					
108rcc	-10.82	-5.88	145.06	0.0	0.0	8.0
108	0.8					
109rcc	-10.82	-5.88	145.0727	0.0	0.0	7.9746
109	0.7873					
110rcc	-10.82	-7.49	145.06	0.0	0.0	8.0
110	0.8					
111rcc	-10.82	-7.49	145.0727	0.0	0.0	7.9746
111	0.7873					

Figure C-11. (continued)

112rcc	-10.82	-9.10	145.06	0.0	0.0	8.0
112	0.8					
113rcc	-10.82	-9.10	145.0727	0.0	0.0	7.9746
113	0.7873					
114rcc	-10.82	1.61	112.04	0.0	0.0	8.0
114	0.8					
115rcc	-10.82	1.61	112.0527	0.0	0.0	7.9746
115	0.7873					
116rcc	-10.82	0.0	112.04	0.0	0.0	8.0
116	0.8					
117rcc	-10.82	0.0	112.0527	0.0	0.0	7.9746
117	0.7873					
118rcc	-10.82	-1.61	112.04	0.0	0.0	8.0
118	0.8					
119rcc	-10.82	-1.61	112.0527	0.0	0.0	7.9746
119	0.7873					
120rcc	10.82	1.61	112.04	0.0	0.0	8.0
120	0.8					
121rcc	10.82	1.61	112.0527	0.0	0.0	7.9746
121	0.7873					
122rcc	10.82	0.0	112.04	0.0	0.0	8.0
122	0.8					
123rcc	10.82	0.0	112.0527	0.0	0.0	7.9746
123	0.7873					
124rcc	10.82	-1.61	112.04	0.0	0.0	8.0
124	0.8					
125rcc	10.82	-1.61	112.0527	0.0	0.0	7.9746
125	0.7873					
126rcc	-4.0	0.0	116.04	8.0	0.0	0.0
126	0.8					
127rcc	-3.9873	0.0	116.04	7.9746	0.0	0.0
127	0.7873					
128rcc	-2.9719	22.3438	91.3	0.0	0.0	8.0
128	0.8					
129rcc	-2.9719	22.3438	91.3127	0.0	0.0	7.9746
129	0.7873					
130rcc	-2.9719	20.7238	91.3	0.0	0.0	8.0
130	0.8					
131rcc	-2.9719	20.7238	91.3127	0.0	0.0	7.9746
131	0.7873					
132rcc	-4.0	-24.5057	93.71	8.0	0.0	0.0
132	0.8					
133rcc	-3.9873	-24.5057	93.71	7.9746	0.0	0.0
133	0.7873					
134rcc	-4.0	-24.5057	92.1	8.0	0.0	0.0
134	0.8					
135rcc	-3.9873	-24.5057	92.1	7.9746	0.0	0.0
135	0.7873					

Figure C-11. (continued)

136rcc	-23.00	-58.3898	83.46	0.0	0.0	8.0				
136	0.8									
137rcc	-23.00	-58.3898	83.4727	0.0	0.0	7.9746				
137	0.7873									
138rcc	-23.00	-59.9998	83.46	0.0	0.0	8.0				
138	0.8									
139rcc	-23.00	-59.9998	83.4727	0.0	0.0	7.9746				
139	0.7873									
140rcc	-23.00	-61.6098	83.46	0.0	0.0	8.0				
140	0.8									
141rcc	-23.00	-61.6098	83.4727	0.0	0.0	7.9746				
141	0.7873									
1	1	-2	-3	-8	-10	-11	-12	-13	-14	
		-15	-16	-17	-18	-19	-20	-21	-22	-23
		-24	-25	-28	-29	-30	-31	-32	-33	-34
		-35	-36	-37	-38	-39	-40	-41	-42	-43
		-44	-45	-46	-47	-48				
2	2	-3	-10	-11	-12	-13	-14	-15	-16	
		-17	-18	-19	-20	-21				
3	3	-4	-5	-6	-7	-8	-9	-10	-11	
		-12	-13	-14	-15	-16	-17	-29	-30	-31
		-32								
4 or	4or	5or	6or	7						
5	8	-9	-26	-27	-28	-44	-45	-46	-47	
6	9	-4	-5	-6	-7	-26	-27	-28	-44	
		-45	-46	-47	-50	-51	-52	-53	-54	-55
		-56	-100	-101	-102	-103	-104	-105	-108	-110
		-112	-114	-116	-118	-120	-122	-124	-128	-130
		-132	-134	-65	-66	-136	-138	-140		
7 or	10or	11or	12or	13or	14or	15or	16or	17		
8 or	18	-22or	19	-23or	20	-24or	21	-25		
9 or	22or	23or	24or	25						
10	26									
11	27									
12	28	-3								
13	29	-8	-30	-32	-33	-36	-44	-45		
14	30	-8	-33	-35	-37	-28				
15	31	-8	-30	-32	-33	-38	-46	-47		
16	32	-8	-33	-39						
17	33	-8	-34	-36	-37	-38	-39			
18 or	36	-40or	37	-41or	38	-42or	39	-43		
19 or	40or	41or	42or	43						
20 or	44or	45or	46or	47						
21	34	-26								
22	35	-27								
23	48	-2								
24	49	-1								

Figure C-11. (continued)

25	or	50	-62	-86	-97	-106	-107			
	or	51	-62	-86	-99	-106	-107			
	or	51	-62	-86	98	-106	-107			
	or	51	-62	-86	-97	-106	-107			
	or	55	-86							
	or	63	-106	-107						
26	or	52	-57	-60	-64	-65	-66	-69	-73	-87
		-91	103	-126	-127	-100	-101			
	or	102	-57	-60	-64	-65	-66	-69	-73	-87
		-91	-126	-127						
	or	58	-64	-60						
	or	61	-64	-57						
	or	59	-69	-64	-126	-127				
	or	70	52	103	-126	-127				
	or	71	102	-126	-127					
	or	72	52	103	-126	-127				
	or	70	102	-126	-127					
	or	74	-57	-60	-64	or 75	-57	-60	-64	
	or	76	-57	-60	-64	or 77	-57	-60	-64	
	or	78	-57	-60	-64	or 79	-57	-60	-64	
	or	80	-57	-60	-64	or 81	-57	-60	-64	
	or	82	-57	-60	-64	or 83	-57	-60	-64	
	or	84	-57	-60	-64	or 85	-57	-60	-64	
	or	88	-57	-60	-64	-65	-66	52	103	
	or	88	-57	-60	-64	-65	-66	102		
	or	87	-89	-90	-88	-65	-66	52	103	
	or	87	-89	-90	-88	-65	-66	102		
	or	91	-94	-96	-73	102				
	or	91	-94	-96	-73	103				
27	or	53	-67	or 54	-68					
28		56	-53	-54	-67	-68				
29		57	-58	-59						
30		60	-61	-59						
31	or	62	-63	-106	or 64	-126	or 86	-126		
32	or	65	or 66							
33	or	67	or 68							
34		69	-70	-71	-72	-64				
35		73	-74	-75	-76	-77	-78	-79	-80	-81
		-82	-83	-84	-85					
36	or	87	-88	89	-67	-68				
	or	87	-88	90	-67	-68				
37	or	91	-73	94	or 91	-73	96			
38		97	99	-98	-62					
39	or	101	-102	or 100	-102					
40	or	104	-65	-128	-130	or 105	-66	-132	-134	
41	or	106	-107	or 108	-109	or 110	-111	or 112	-113	
	or	114	-115	or 116	-117	or 118	-119	or 120	-121	
	or	122	-123	or 124	-125	or 126	-127	or 128	-129	

Figure C-11. (continued)

	or	130	-131	or	132	-133	or	134	-135	or	136	-137
	or	138	-139	or	140	-141						
42		107										
43		109										
44		111										
45		113										
46		115										
47		117										
48		119										
49		121										
50		123										
51		125										
52		127										
53		129										
54		131										
55		133										
56		135										
57		137										
58		139										
59		141										
-1												
1	1001	0	2	100	/box/z1001/surrounding/air-void							
2	1002	0	3	100	/box/z1002/bottom/base/pad							
3	1003	0	3	100	/box/z1003/upper/base/pad							
4	1004	0	3	100	/box/z1004/inner/alignment/pads							
5	1005	0	3	100	/box/z1005/inner/box							
6	1006	0	2	100	/box/z1006/inner/box/void-air							
7	1007	0	3	100	/box/z1007/outer/wall/alignment/pads							
8	1008	0	3	100	/box/z1008/base/pad/lift/eyelets							
9	1009	0	2	100	/box/z1009/eyelets/voids-air							
10	1010	0	3	100	/box/z1010/inner/box/top/hatch							
11	1011	0	3	100	/box/z1011/inner/box/side/hatch							
12	1012	0	2	100	/box/z1012/inner/outer/cable/run/void-air							
13	1013	0	3	100	/box/z1013/outer/wall/negative/y-axis							
14	1014	0	3	100	/box/z1014/outer/wall/positive/x-axis							
15	1015	0	3	100	/box/z1015/outer/wall/positive/y-axis							
16	1016	0	3	100	/box/z1016/outer/wall/negative/x-axis							
17	1017	0	3	100	/box/z1017/outer/top							
18	1018	0	3	100	/box/z1018/outer/wall/lift/eyelets							
19	1019	0	2	100	/box/z1019/outer/wall/lift/eyelets/void-air							
20	1020	0	2	100	/box/z1020/inner/outer/drain/holes							
21	1021	0	3	100	/box/z1021/outer/top/hatch							
22	1022	0	3	100	/box/z1022/outer/wall/side/hatch							
23	1023	0	1	100	/box/z1023/ground							
24	1024	0	0	0	/box/z1024/external/void							
25	1025	0	5	100	/phantom/z1025/flesh/head-neck							
26	1025	0	5	100	/phantom/z1026/flesh/torso							
27	1025	0	5	90	/phantom/z1027/flesh/legs							
28	1028	0	5	90	/phantom/z1028/pelvis-region							

Figure C-11. (continued)

29	1029	0	4	90	/phantom/z1029/internal/left/lung
30	1029	0	4	90	/phantom/z1030/internal/right/lung
31	1031	0	6	90	/phantom/z1031/skeletal/skull-neck-spinal
32	1031	0	6	90	/phantom/z1032/skeletal/arms
33	1031	0	6	90	/phantom/z1033/skeletal/legs
34	1031	0	6	90	/phantom/z1034/skeletal/hip
35	1031	0	6	90	/phantom/z1035/skeletal/ribs
36	1031	0	6	80	/phantom/z1036/skeletal/pelvis
37	1037	0	6	80	/phantom/z1037/skeletal/shoulder-blade
38	1038	0	5	80	/phantom/z1038/flesh/neck
39	1031	0	5	80	/phantom/z1039/flesh/breasts
40	1025	0	5	80	/phantom/z1040/flesh/arms
41	1106	0	8	100	/detectors/z1041/containers
42	1107	0	7	100	/detector/z1042/mid-head
43	1109	0	7	100	/detector/z1043/left-chest 1
44	1111	0	7	100	/detector/z1044/left-chest 2
45	1113	0	7	100	/detector/z1045/left-chest 3
46	1115	0	7	100	/detector/z1046/front/mid-gut 1
47	1117	0	7	100	/detector/z1047/front/mid-gut 2
48	1119	0	7	100	/detector/z1048/front/mid-gut 3
49	1121	0	7	100	/detector/z1049/rear/mid-gut 1
50	1123	0	7	100	/detector/z1050/rear/mid-gut 2
51	1125	0	7	100	/detector/z1051/rear/mid-gut 3
52	1127	0	7	100	/detector/z1052/inner/mid-gut
53	1129	0	7	100	/detector/z1053/rt. arm/outer
54	1131	0	7	100	/detector/z1054/rt. arm/inner
55	1133	0	7	100	/detector/z1055/left-arm/top
56	1135	0	7	100	/detector/z1056/left-arm/bottom
57	1137	0	7	100	/detector/z1057/shelf/inner
58	1139	0	7	100	/detector/z1058/shelf/middle
59	1141	0	7	100	/detector/z1059/shelf/outer

Figure C-11. (continued)
104

```

aprf 400m/16.14m ss90-124-32 s90e5 2m b+p+d LAH(t), rotated 0 degrees
** 40000.0 0.0 -15.0 230.0 0.0 93.71 62 0 0.0
46 neutron - 23 gamma kerma responses input
-- 1=neut 2=veh n-g 3=grd n-g 4=photons
mash 46n/23g group flat response
** 69r1.0
mash 46n/23g group free-in-air tissue kerma response (gy.cm2/n,g)
**
736532-16 704584-16 685894-16 674499-16 661555-16 638136-16 633529-16
598822-16 57632-15 551514-16 546431-16 512651-16 470858-16 457805-16
44359-15 419381-16 357307-16 332494-16 321126-16 291193-16 263438-16
252468-16 222507-16 205934-16 193682-16 179065-16 163746-16 130075-16
102563-16 806538-17 563405-17 359169-17 25917-16 213032-17 147572-17
628401-18 219938-18 925902-19 448136-19 20734-18 103718-19 932428-20
135874-19 228494-19 372646-19 129126-18 401109-16 317559-16 27612-15
23517-15 205102-16 185083-16 164356-16 143343-16 121273-16 1036-14
902669-17 755621-17 585321-17 42722-16 296381-17 192968-17 105409-17
529629-18 348187-18 313231-18 484629-18 10497-16 339599-17
CaF2:Mn TLD Photon Energy Response Function 1 g/cm2 of al, air ss90-130
** 46r0.0
0.0000e+00 0.0000e+00 0.0000e+00 0.0000e+00 2.0498e-11 1.9292e-11
1.6653e-11 1.3828e-11 1.1251e-11 9.3633e-12 8.0459e-12 6.6419e-12
5.0880e-12 3.7033e-12 2.5835e-12 1.7058e-12 1.0321e-12 8.0302e-13
1.0490e-12 1.7457e-12 3.0827e-12 2.9619e-12 3.2699e-13
CaF2:Mn TLD Photon Energy Response Function 0.004" of al, air ss90-130
** 46r0.0
0.0000e+00 0.0000e+00 0.0000e+00 0.0000e+00 2.0837e-11 1.9614e-11
1.6938e-11 1.4076e-11 1.1465e-11 9.5513e-12 8.2177e-12 6.7945e-12
5.2156e-12 3.8046e-12 2.6574e-12 1.7550e-12 1.0612e-12 8.2702e-13
1.0986e-12 1.9548e-12 4.2825e-12 8.1380e-12 1.0711e-11
CaF2:Mn Dose/unit particle fluence - 0.004" of al
** 46r0.0
0.0000e+00 0.0000e+00 0.0000e+00 0.0000e+00 2.1345e-11 2.1283e-11
1.8242e-11 1.4839e-11 1.2013e-11 1.0231e-11 8.6656e-12 7.1425e-12
5.6545e-12 4.0729e-12 2.9564e-12 1.9856e-12 1.2146e-12 9.2596e-13
1.1973e-12 2.1957e-12 4.5231e-12 7.7644e-12 8.1948e-12
CaF2:Mn Dose/unit particle fluence - 1 g/cm2 of al
** 46r0.0
0.0000e+00 0.0000e+00 0.0000e+00 0.0000e+00 2.0998e-11 2.0934e-11
1.7936e-11 1.4578e-11 1.1788e-11 1.0030e-11 8.4851e-12 6.9825e-12
5.5165e-12 3.9646e-12 2.8747e-12 1.9303e-12 1.1813e-12 8.9930e-13
1.1443e-12 1.9588e-12 3.1548e-12 2.5930e-12 1.8842e-13
energy group totals
aprf 400m/16.14m ss90-124-32 s90e5 2m b+p+d LAH(t), rotated 90 degrees
** 40000.0 0.0 -15.0 230.0 90.0 93.71 00 0 0.0
aprf 400m/16.14m ss90-124-32 s90e5 2m b+p+d LAH(t), rotated 180 degrees
** 40000.0 0.0 -15.0 230.0 180.0 93.71 00 0 0.0
aprf 400m/16.14m ss90-124-32 s90e5 2m b+p+d LAH(t), rotated 270 degrees
** 40000.0 0.0 -15.0 230.0 270.0 93.71 00 0 0.0

```

Figure C-12. Sample DRC Input for the MASH Analysis of the APRF Spring 1990 Two-Meter Box Test Bed Experiments.

INTERNAL DISTRIBUTION

- 1. B. R. Appleton
- 2-6. J. M. Barnes
- 7. T. J. Burns
- 8-12. J. D. Drischler
- 13. C. M. Haaland
- 14. D. T. Ingersoll
- 15-19. J. O. Johnson
- 20. J. V. Pace
- 21. W. A. Rhoades
- 22. R. W. Roussin
- 23. R. T. Santoro
- 24. R. C. Ward
- 25-26. EPMD Reports Office
- 27-28. Laboratory Records Department
- 29. Laboratory Records ORNL-RC
- 30. Document Reference Section
- 31. Central Research Library
- 32. ORNL Patent Section

EXTERNAL DISTRIBUTION

- 33. Director, Defense Nuclear Agency
ATTN: RARP (Dr. D. L. Auton)
6801 Telegraph Road
Alexandria, VA 22310-3398
- 34. Dr. Roger W. Brockett
Wang Professor of Electrical Engineering
and Computer Science
Division of Applied Science
Harvard University
Cambridge, Massachusetts 02138
- 35. Dr. N. Ricky Byrn
Nicholes Research Corp.
4040 So. Memorial Parkway
Huntsville, AL 35802
- 36. Director, Harry Diamond Laboratory
ATTN: SLCHD-NW-P (Mr. John Corrigan)
2800 Powder Mill Road
Adelphi, MD 20783-1197

37. Electronics Division, NES
ATTN: Dr. Tom Cousins
Defence Research Establishment Ottawa
Ottawa, Ontario, Canada, K1A 0Z4
38. Commander
U.S. Army Nuclear & Chemical Agency
ATTN: MONA-ZB (Dr. David Bash)
7500 Backlick Rd., Bldg. 2073
Springfield, VA 22150-3198
39. Establisment Technique Central de l' Armement
ATTN: Dr. Joel Dhermain
Centre d'Etudes du Boucher
16 bis Avenue Prieur de la Cote d'or
94114 Arcueil-Cedex, France
40. Dr. John J. Dorning
Department of Nuclear Engineering & Engineering Physics
Thronton Hall, McCormick Road
University of Virginia
Chrlottesville, Va 22901
41. Science Applications International Corporation
ATTN: Dr. Stephen Egbert
10260 Campus Point Drive
San Diego, CA 92121
42. Commander, U.S. Army Combat Systems Test Activity
ATTN: STECS-NE (Mr. John Gerdes)
Aberdeen Proving Ground, MD 21005-5059
43. Ministry of Defence, Atomic Weapons Establishment
ATTN: Dr. Kevin G. Harrison
Building A72, Aldermaston,
Reading, Berkshire, United Kingdom, RG7 4PR
44. Commander, U.S. Army Combat Systems Test Activity
ATTN: STECS-NE (Dr. C. Heimbach)
Aberdeen Proving Ground, MD 21005-5059
45. Director, Bubble Technology Industries, Inc.
ATTN: Dr. Harry Ing
Highway 17
Chalk River, Ontario, Canada, KOJ 1JO
46. Science Applications International Corporation
ATTN: Mr. Dean C. Kaul
10260 Campus Point Drive
San Diego, CA 92121

47. Commander, U.S. Army Combat Systems Test Activity
ATTN: STECS-NE (Dr. A. Halim Kazi)
Aberdeen Proving Ground, MD 21005-5059
48. Director, Armed Forces Radiobiology Research Institute
ATTN: MRAD (CDR Kearsly)
Bethesda, MD 20814-5145
49. Director, Defense Nuclear Agency
ATTN: RARP (MAJ Robert Kehlet)
6801 Telegraph Road
Alexandria, VA 22310-3398
50. Director, Harry Diamond Laboratory
ATTN: SLCHD-NW-P (Mr. Klaus Kerris)
2800 Powder Mill Road
Adelphi, MD 20783-1197
51. US Army Center for EQ/RSTA
ATTN: AMSEL-RSK (Dr. Stanley Kronenberg)
Fort Monmouth, NY 07703
52. Establisment Technique Central de l' Armement
ATTN: Dr. Jacques Laugier
Centre d'Etudes du Boucher
16 bis Avenue Prieur de la Cote d'or
94114 Arcueil-Cedex, France
53. Dr. James E. Leiss
Route 2, Box 142C
Broadway, VA 22815
54. Dr. Neville Moray
Department of Mechanical and Industrial Engineering
University of Illinois
1206 West Green Street
Urbana, IL 61801
55. Director, Defense Nuclear Agency
ATTN: RARP (Ms. Joan Ma Pierre)
6801 Telegraph Road
Alexandria, VA 22310-3398
56. Naval Surface Warfare Center
ATTN: CODE R41 (Mr. Gordon Reil)
New Hampshire Road
White Oak, MD 20903-5000

57. Commander, U.S. Army Foreign Science & Technology Center
ATTN: UVA (Dr. Roger Rydin)
220 7th Street NE
Charlottesville, VA 22901-5396
58. HEAD, Nuclear Radiation Effects
ATTN: Dr. Ludwig Schaenzler
Wehrwissenschaftliche Dienststelle
Postfach 1320
3042 Munster
Federal Republic of Germany
59. David L. Tilson
U.S. Army SDC
ATTN: CSSD-SA-EV
P.O. BOx 1500
Huntsville, AL 35807
60. Commander, U.S. Army Foreign Science & Technology Center
ATTN: AIFRTA (Mr. Charles Ward)
220 7th Street NE
Charlottesville, VA 22901-5396
61. Dr. Mary F. Wheeler
Department of Mathematical Sciences
Rice University
P. O. Box 1892
Houston, Tx 77204-3476
62. Commander, U.S. Army Tank Automotive Command
ATTN: AMSTA-RSK (Mr. Greg Wolfe)
Bldg. 200
Warren, MI 48317-5000
63. Director, Defense Nuclear Agency
ATTN: RARP (Dr. Robert Young)
6801 Telegraph Road
Alexandria, VA 22310-3398
64. Office of the Assistant Manager for Energy
Research and Development
Department of Energy, Oak Ridge Operations
P.O. Box 2001
Oak Ridge, TN 37831
- 65-74. Office of Scientific and Technical Information
P.O. Box 62
Oak Ridge, TN 37830